Scuola Normale Superiore

di Pisa

Characterization of FATZ-3 protein and its interaction with PDZ containing proteins

Thesis submitted for the Degree of Doctor Philosophiae

(Perfezionamento in Genetica Molecolare e Biotechnologie)

Academic Year 2007-2008

Candidate**: Mohamed Soliman Ismail**

Supervisor: **Dr. Georgine Potter Faulkner**

To my beloved Father and Mother

Table of Contents

ACKNOWLEDGMENTS 1

SUMMARY 2

ABBREVIATIONS 4

Chapter 1: INTRODUCTION 7

1 Muscle 7
1.2 The sarcomere 12
1.2.1 The structure of the sarcomere 12
1.2.2 Actin 15
1.3 The Z-disk 16
1.3.1 The structure of the Z-disk 16
1.3.2 Z-disk proteins 18
1.3.2.1 Titin 19
1.3.2.2 MLP 21
1.3.2.3 MURFs 21
1.3.2.4 Calpain 3 22
1.3.2.5 Nebulin and Nebulette 22
1.4 Alpha-actinin 23
1.5 NF-AT3 25
1.6 Filamins 25
1.7 Telethonin 27
1.8 The MARP family 29
1.8.1 Ankrd1 (also known as CARP) 30

1.8.2 Ankrd2 (ANKyrin Repeat Domain 2, also known as ARPP) 30
1.9. Myotilin, Palladin and myopalladin family 32
1.9.1 Myotilin 32
1.9.2 Palladin 33
1.9.3 Myopalladin 34
1.10 The FATZ family 35
1.10.1 FATZ-1 (calsarcin-2, myozenin-1) 37
1.10.2 FATZ-2 (calsarcin-1, myozenin-2) 39
1.10.3 FATZ-3 (myozenin-3/calsarcin-3) 41
1.11 The Enigma family 42
1.11.1 Enigma 44
1.11.2 Enigma homologue protein (ENH) 44
1.11.3 ALP (Actinin associated LIM protein) 45
1.11.4 RIL (Reversion induced protein) 46
1.11.5 CLP-36 (hCLIM1, Elfin) 47
1.11.6 ZASP/Cypher/Oracle 49
1.12 PDZ domains 51
1.12.1 Structure and binding characteristics of PDZ domains 52
1.12.2 Why do PDZ domains bind specifically to the C-terminal of proteins? 53
1.12.3 Classification of PDZ domains 56
1.12.4 The effect of phosphorylation on C-terminus binding 58
1.12.5 The multiplicity and function of PDZ domains 59

Chapter 2: MATERIAL AND METHODS 64

2.1 AlphaScreen 64
2.1.1 AlphaScreen Experiments 65
2.2 Antibodies 67
2.2.1 Primary Antibodies 67
2.2.2 Secondary antibodies 68

2.3 Bacterial strains and growth media 68
2.4 Baculovirus expression system 69
2.5 Cell culture 71
2.5.1 C2C12 cells 71
2.5.2 COS-7 cell line 71
2.5.3 Sf9 cell line 71
2.6 Gene amplification and cloning 72
2.6.1 Amplification and cloning of full length FATZ-3 72
2.6.2 Amplification and cloning of regions of FATZ-3 73
2.6.3 Myotilin 75
2.6.4 Amplification and cloning of FATZ-1, -2, -3 and myotilin lacking last 15 bp 75
2.6.6 PDZ-ZASP pPROEXHTa 76
2.6.7 PDZ-ZM-ALP pGEX-6P 76
2.7 In vitro binding 76
2.8 In vitro transcription and translation 77
2.9 PDZ Array 77
2.10 Peptides 78
2.11 Protein Production 79
2.11.1 Production and purification of native 6His-tagged proteins 79
2.11.2 Production and purification of GST recombinant proteins 80
2.12. Structural Biology Protocols 83
2.12.1 Production and purification of the C-terminal FATZ-3 (81-251aa) for protein 83
12.2.2 Large scale production and purification of C-terminal FATZ-3 protein 85
2.12.3 Dynamic light scattering (DLS) 87
2.12.4 Circular dichroism (CD) 89
2.12.5 Stura Footprint screens 89
2.12.6 Protein crystallization 90
2.13 Transfections and co-immunoprecipitations 90

2.14 Western blotting 91
2.15 Primers used for this study 92

Chapter 3 Results 95

3.1 Amplification, cloning and expression of FATZ-3 95
3.2 The FATZ family, myotilin, palladin and myopalladin share high similarity at their extreme C-termini (last 5 amino acids) 97
3.3 Preparation of native protein for use in AlphaScreen Experiments 101
3.4 The C-terminal (last 5 amino acids) of the FATZ family and myotilin bind the PDZ domains of ZASP, ALP and CLP-36 proteins 103
3.5 The PDZ domain of ZASP binds the IVTT full-length FATZ-3 but not truncated FATZ-3 (minus C-terminal 5 aa's) 106
3.6 Peptides of the C-terminal amino acids of the FATZ family, myotilin, palladin and myopalladin bind to the PDZ domains of ZASP, ALP and CLP proteins 108
3.7 Phosphorylation affects the binding activity of the C-terminal amino acid peptides to the PDZ domains of ZASP, CLP-36 and ALP 110
3.8 The C-terminal FATZ-1 (CD2) competes with the binding between the phosphorylated and non phosphorylated peptides of FATZ-3/myotilin and the ZASP-1 protein 114
3.9 The ACTN2 protein competes with the binding between the phosphorylated and non-phosphorylated peptides of FATZ-3/myotilin and the ZASP-1 protein 116
3.10 PDZ array experiments 119
3.10.1 FATZ-1 peptides bind to the PDZ domain of hCLIMI (CLP-36) and RIL 119
3.10.2 FATZ-2/palladin peptides bind to the PDZ domain of hCLIMI (CLP-36) and RIL 120
3.10.3 FATZ-3/myotilin peptides bind to the PDZ domain of CLP and RIL 121
3.10.4 Myopalladin peptides bind to the PDZ domain of CLP and RIL 122

3.10.5 The mutated peptides do not bind to the PDZ domains of hCLIM1 (CLP-36) and RIL 123
3.10.6 The C-terminal FATZ-3 protein behaves as the non-phosphorylated FATZ-3/myotilin peptide 124
3.11 FATZ-3 interacts with Ankrd2 127
3.11.1 The N-terminal FATZ-3 binds Ankrd2 128
3.12 Expression and purification of FATZ-3 protein 130
3.12.1 Expression and purification of His tagged FATZ-3 full-length protein in Bacteria 131
3.12.2 Protein expression and purification of recombinant GST-FATZ-3 full length protein in Bacteria 132
3.12.3 Protein expression and production of full-length His tagged FATZ-3 protein using the Baculovirus expression system 133
3.12.3.1 Dose efficiency experiment for the P2 virus expressing His-FATZ-3 full-length protein 134
3.12.3.2 Time course experiment for the P2 virus expressing full-length His-FATZ-3 protein 135
3.12.3.3 Purification of native FATZ-3 protein expressed by baculovirus in Sf9 cells 136
3.13 Expression and purification of C-terminal FATZ-3 protein in bacteria 138
3.13.1 Comparison of the expression and purification of GST and His tagged C-terminal FATZ-3 138
3.13.2 Optimization of the purification of C-terminal FATZ-3 protein 140
3.14 Medium scale production and purification of C-terminal FATZ-3 protein 143
3.15 Large scale production and purification of C-terminal FATZ-3 protein 145
3.16 Circular Dichroism (CD) shows high percentage of random coil for the C-terminal FATZ-3 (81-251aa) protein 147
3.17 Dynamic light scattering (DLS) shows a low percentage of protein polydispersity 148
3.18 Stura footprint screen experiment 149
3.19 Crystallization trials 150

Chapter 4 DISCUSSION 152

Chapter 5 CONCLUSIONS 166

Chapter 6 References 168

ACKNOWLEDGEMENTS

This thesis is the harvest of four years full of resisting and insisting to overcome many hard circumstances, I managed to learn many things working in the Muscle Molecular Biology (MMB) laboratory at ICGEB under the supervision of Dr. Georgine Faulkner. I would first like to thank Dr. Georgine Faulkner for her help to me on the professional level by guiding me through my PhD project and teaching me many useful things from her wide experience and helping me to become independent student. I would also like to thank her for her great help on my personal level and supporting me through my hard time (Georgine I thank you very much for all the help you gave to me in the last four years and until this very moment).

This work has been done in collaboration with three different groups and I would like to take the chance to thank all of them, Dr. Olli Carpen, University of Helsinki, Finland, Professor Kristina Carugo, University of Vienna, Austria and especially Professor Giorgio Valle, University of Padua, Italy and the members of his lab for their help in particular Dr. Ivano Zara and Chiara Gardin. Special thanks as well to my colleague and friend Laura Muzzolini for spending with me a lot of time and effort to help me in the protein purification work.

I would also like to thank my colleagues in the MMB lab Anna Belgrano, Snezana Miocić, Valentina Martinelli and my previous colleagues Elisa and Helena.

In my four years at ICGEB I managed to meet great people and friends and I would like to thank them all for giving me the chance to know them and for their great help and support.

I would like to gift this thesis to my great family brothers and sisters and especially to my beloved mother that she will always be in my mind and heart, and to my great father Dr. Soliman Ismail; he is to me not only a father but a brother and a very special friend (father, I thank you very much for your great support and help, you were and still are my guiding light in this life, I wish you a great long happy life).

Last not the least, I would like to thank my tutor Professor Francisco Baralle, for his kind support and precious advice and for ICGEB for giving me the chance to do my PhD in the Muscle Molecular Biology Group.

SUMMARY

The FATZ/calsarcin/myozenin family of proteins has three members FATZ-1 (calsarcin-2/myozenin-1), FATZ-2 (calsarcin-1/myozenin-2) and FATZ-3 (calsarcin-3/myozenin-3) all localized in the Z-disk and with have high homology to each other at their N- and C-terminals. The FATZ family has been shown to interact with γ-filamin, α-actinin, telethonin, ZASP (Cypher/Oracle) and calcineurin. Together with Prof. O. Carpen we noted that all three members of the FATZ family share high homology with myotilin, palladin and myopalladin at their extreme C-terminal. In fact the final 5 amino acids of FATZ-3 and myotilin are identical (ESEEL), as are those of FATZ-2 and palladin (ESEDL). Computer analysis of the sequences of these proteins indicated that the last four amino acids were considered a probable class III PDZ binding motif (X[DE]X[IVL]). Searches of protein sequence databases revealed that the C-terminal E[ST][DE][DE]L motif is present almost exclusively in the FATZ family of proteins, myotilin, palladin and myopalladin and is evolutionary conserved in these proteins from zebrafish to humans indicating its importance for their biological function.

A main object of this study was to determine if the proteins with this new type of Class III PDZ binding motif at their C-terminal could indeed bind PDZ domains. Since both the FATZ family and myotilin bind ZASP-1 which is a PDZ domain protein we wanted to discover if these interactions occurred via the PDZ domain of ZASP. To do this we collaborated with Prof. G Valle whose group use the AlphaScreen technique to study protein-protein interactions. Biotinylated phosphorylated and non-phosphorylated peptides were designed based on the final C-terminal 5 amino acids of the FATZ family, myotilin, palladin and myopalladin as well as a control peptide ESEEE having E

instead of L as its last amino acid. Native protein was also produced for use in AlphaScreen experiments, both to full length proteins and proteins lacking the terminal 5 amino acids. Since ZASP belongs to the Enigma family of proteins the PDZ domains of other members such as ALP and CLP-36 were also checked for their interactions. The results presented here show that the terminal amino acids were responsible and crucial for the interaction with the PDZ domain and that phosphorylation modulated this interaction. These results were further confirmed by *in vitro* binding experiments such as GST pull-down and PDZ Array. Another Enigma family member RIL was found to bind to this new motif based on PDZ array experiments. The results presented in this thesis demonstrate that proteins of the FATZ family, myotilin, palladin and myopalladin interact with the PDZ domains of Enigma family members via their final C-terminal amino acids. Therefore these final 5 amino acids may represent a new type of class III PDZ binding motif specific for the PDZ domain of Enigma proteins.

I found another binding partner for FATZ-3, namely the I-band protein Ankrd2 whose binding I mapped to the N-terminal of FATZ-3.

The second object of this thesis was to study the tertiary structure FATZ-3 by using protein crystallography. I faced a lot of difficulties expressing and producing native full-length FATZ-3 protein first in bacteria and then using the Baculovirus expression system. It was challenging to obtain enough native purified protein for crystallization studies. I was able to do so using the C-terminal region of FATZ-3 protein (171 amino acids) and undertook crystallization studies at the laboratory of Prof. Kristina Carugo. I tried about 300 crystallization conditions and started to obtain crystals after 1 month. However none of the crystals gave a good diffraction pattern when checked by X-ray.

ABBREVIATIONS

A-band	Anisotropic in polarised light
ABD	Actin-binding domain
ADP	Adenine di-phosphate
ALP	Actinin-associated LIM protein
AlphaScreen	Amplified Luminescent Proximity Homogeneous Assay
Ankrd2	Ankyrin repeat domain 2 protein
AP	Alkaline phosphatase
AR LGMD	Autosomal recessive Limb-Girdle Muscular Dystrophy
ATP	Adenine tri-phosphate
BCIP	5-bromo-4-chloro-3-indolyl phosphate
BSA	Bovine serum albumin
Calsarcin	denotes calcineurin associated sarcomeric protein
CD	Circular dichroism
CH	calponin homology
CHO	Chinese hamster overy
CnA	Calcineurin subunit A
CLP	C-terminal LIM domain protein
COS-7	monkey, African green, kidney
Co-IP	Co-immunoprecipitation
DARP	Diabetes-related Ankyrin Repeat Protein
DCM	Dilated cardiomyopathy
DHPLC	Performance liquid chromatography
Dlg	Discs large protein
DLS	Dynamic light scattering

DMD	Duchenne Muscular Dystrophy
EBP50	Ezrin-radixin-moesin binding phosphoprotein-50
ECL	Enhanced chemiluminescence
ENH	Enigma homologue protein
FATZ	γ-filamin, Alpha-actinin and Telethonin binding protein
FL	Full lenght
GFP	Green fluorescent protein
GST	Glutathione S-transferase
HA	Hemagglutinin
HCM	Hypertrophic cardiomyopathy
hCLIM1	carboxyl terminal LIM domain protein
HMERF	Hereditary myopathy with early respiration failure
HRP	Horseradish peroxidise
Ig	Immunoglobulin
IKEPP	Intestinal and kidney enriched PDZ protein
IPTG	Isopropyl-β-D-thiogalactoside
IVTT	*In vitro* transcribed and translated
kDa	Kilo Dalton
LB	Luria Broth
LGMD	Limb girdle muscular dystrophy
LIMK	LIM domain kinase
LIM domains	Designated LIM for the first three proteins in which it was discovered in, Lin11, Isl-1 & Mec-3
MARP	Muscle ankyrin repeat protein
M-band	Mittel, meaning middle in German
MDM2	Mouse double minute 2
MHC	Myosin heavy chain
MFM	myofibrillar myopathy

MLP	Muscle LIM protein
MRF	Myogenic regulatory factor
MURFs	Muscle Specific RING-finger proteins
NBT	Nitro blue tetrazolium
NFAT	Nuclear factor of activated T-cells
Ni-NTA	Nitrilo-tri-acetic acid
OD_{600}	Optical density at 600 nm
ORF	Open reading frame
PAGE	PolyAcrylamide gel electrophoresis
PBS	Phosphate buffered saline
PDVF	Polyvinyldifluoride
PDZ domains	The name comes from the first three proteins that has been discovered in, PSD-95 , Dlg and ZO-1
PEG	Poly ethylene glycol
PKC	Protein kinase C
PML	Promyelocytic leukemia protein
PSD-95	Post-synaptic density 95 kDa
RIL	Reversion induced protein
SDS	Sodium dodecyl-sulphate
Sf9	Spodoptera frugiperda
SLRs	spectrin-like repeats
TB	Terrific broth
TEV	Tobacco Etch Virus
TID	Telethonin interacting domain
UV	Ultraviolat light
ZASP	Z-band alternatively spliced PDZ domain protein
Z-disk	Zwischen, meaning between in German
ZO-1	Zonula occludens 1 protein

Chapter 1 INTRODUCTION

1 Muscle

The function of muscle in the body is to produce force and cause motion, either locomotion or movement within internal organs. Most muscle contraction occurs without conscious thought and is necessary for survival. Our hearts contract without us thinking about it, our intestines contract while digesting food and we breathe all without conscious thought. Although movements such as walking, running, writing or even turning our head require conscious thought they are so automatic that usually we are unaware that they result from signals sent to the brain to tell our body parts to move.

Muscle is the contractile tissue of the body and is derived from the mesodermal layer of embryonic germ cells. Muscle fibres are bound together by perimysium into bundles which group together to form a muscle which is enclosed in a sheath of epimysium (Fig 1). Muscle spindles are distributed throughout the muscles and provide sensory feedback information to the central nervous system. Individual muscle fibres are surrounded by endomysium. The muscle myofibre is composed of several nuclei and myofibrils. Myobrils are made up of sarcomeres, the basic contractile unit of muscle that are composed of fibres of actin and myosin.

Muscle can be classified into three types: 1) Skeletal muscle (striated, voluntary muscle) is anchored by tendons to bone and enables movement of the skeleton. These muscles are highly specialised for rapid force production. An average adult male has 40-50% of skeletal muscle whereas an average adult female has 30-40%. 2) Cardiac muscle

(striated, involuntary muscle) is an intermittently contracting muscle that maintains the blood supply to the organs of the body. 3) Smooth muscle (non-striated, involuntary muscle) is found within the walls of organs and structures such as the oesophagus, stomach, intestines, bronchi, uterus, urethra, bladder, and blood vessels, and unlike skeletal muscle, smooth muscle is not under conscious control. Smooth muscles are involuntary muscles. Skeletal muscles can be divided into two main types; Type I, slow oxidative, slow twitch, or "red" muscle is dense with capillaries and is rich in mitochondria and myoglobin, giving the muscle tissue its characteristic red colyes our. It can carry oxygen and sustain aerobic activity. Type II which is less dense in mitochondria and myoglobin it is the fastest muscle type in humans. It can contract more quickly and with a greater amount of force than oxidative muscle, but can sustain only short, anaerobic bursts of activity before muscle contraction becomes painful.

Cardiac and skeletal muscles are "striated" in that they contain sarcomeres and are packed into highly-regular arrangements of bundles; smooth muscle has neither. While skeletal muscles are arranged in regular, parallel bundles, cardiac muscle connects at branching, irregular angles. Striated muscle contracts and relaxes in short, intense bursts, whereas smooth muscle sustains longer or even near-permanent contractions.

Although the three (skeletal, cardiac and smooth) types of muscle have significant differences all three use the movement of actin against myosin to create contraction. In skeletal muscle, contraction is stimulated by electrical impulses transmitted by nerves, the motor nerves and motoneurons in particular. Cardiac and smooth muscle contractions are stimulated by internal pacemaker cells which regularly contract, and propagate contractions to other muscle cells with which they are in contact. All skeletal

muscle and many smooth muscle contractions are facilitated by the neurotransmitter acetylcholine.

Muscular activity accounts for much of the body's energy consumption. All muscle cells produce adenosine triphosphate (ATP) molecules which are used to power the movement of the myosin heads. Muscles contain ATP in the form of creatine phosphate which is generated from ATP and can regenerate ATP when needed by the action of creatine kinase. Muscles also store glucose in the form of glycogen. Glycogen can be rapidly converted to glucose when energy is required for sustained, powerful contractions. Within the voluntary skeletal muscles, the glucose molecule is metabolized in a process called glycolysis, the oxidation of glucose. Glucose is oxidized to either lactate or pyruvate. Under aerobic conditions, the dominant product in most tissues is pyruvate and the pathway is known as aerobic glycolysis. Aerobic glycolysis of glucose to pyruvate, requires two equivalents of ATP to activate the process, with the subsequent production of four equivalents of ATP and two equivalents of NADH. One mole of glucose is oxidised to two moles of pyruvate accompanied by the net production of two moles each of ATP and NADH. Muscle cells also contain globules of fat, which are used for energy during aerobic exercise. The aerobic energy systems take longer to produce the ATP and reach peak efficiency, and require many more biochemical steps, but produce significantly more ATP than anaerobic glycolysis

When oxygen is depleted, as for instance during prolonged vigorous exercise, the dominant glycolytic product in many tissues is lactate and the process is known as anaerobic glycolysis. Under anaerobic conditions and in erythrocytes under aerobic conditions, pyruvate is converted to lactate by the enzyme lactate dehydrogenase (LDH), and the lactate is transported out of the cell into the circulation. The conversion

of pyruvate to lactate, under anaerobic conditions, provides the cell with a mechanism for the oxidation of NADH (produced during the G3PDH reaction) to NAD^+; which occurs during the LDH catalyzed reaction. This reduction is required since NAD^+ is a necessary substrate for G3PDH, without which glycolysis will cease. Normally, during aerobic glycolysis the electrons of cytoplasmic NADH are transferred to mitochondrial carriers of the oxidative phosphorylation pathway generating a continuous pool of cytoplasmic NAD^+. Aerobic glycolysis generates substantially more ATP per mole of glucose oxidized than does anaerobic glycolysis. The utility of anaerobic glycolysis, to a muscle cell when it needs large amounts of energy, stems from the fact that the rate of ATP production from glycolysis is approximately 100X faster than from oxidative phosphorylation. During exertion muscle cells do not need to energize anabolic reaction pathways. The requirement is to generate the maximum amount of ATP, for muscle contraction, in the shortest time frame. This is why muscle cells derive almost all of the ATP consumed during exertion from anaerobic glycolysis.

Cardiac muscle can readily consume any of the three macronutrients (protein, glucose and fat) without a 'warm up' period and always extracts the maximum ATP yield from any molecule involved. The heart and liver will also consume the lactic acid produced and excreted by skeletal muscles during exercise.

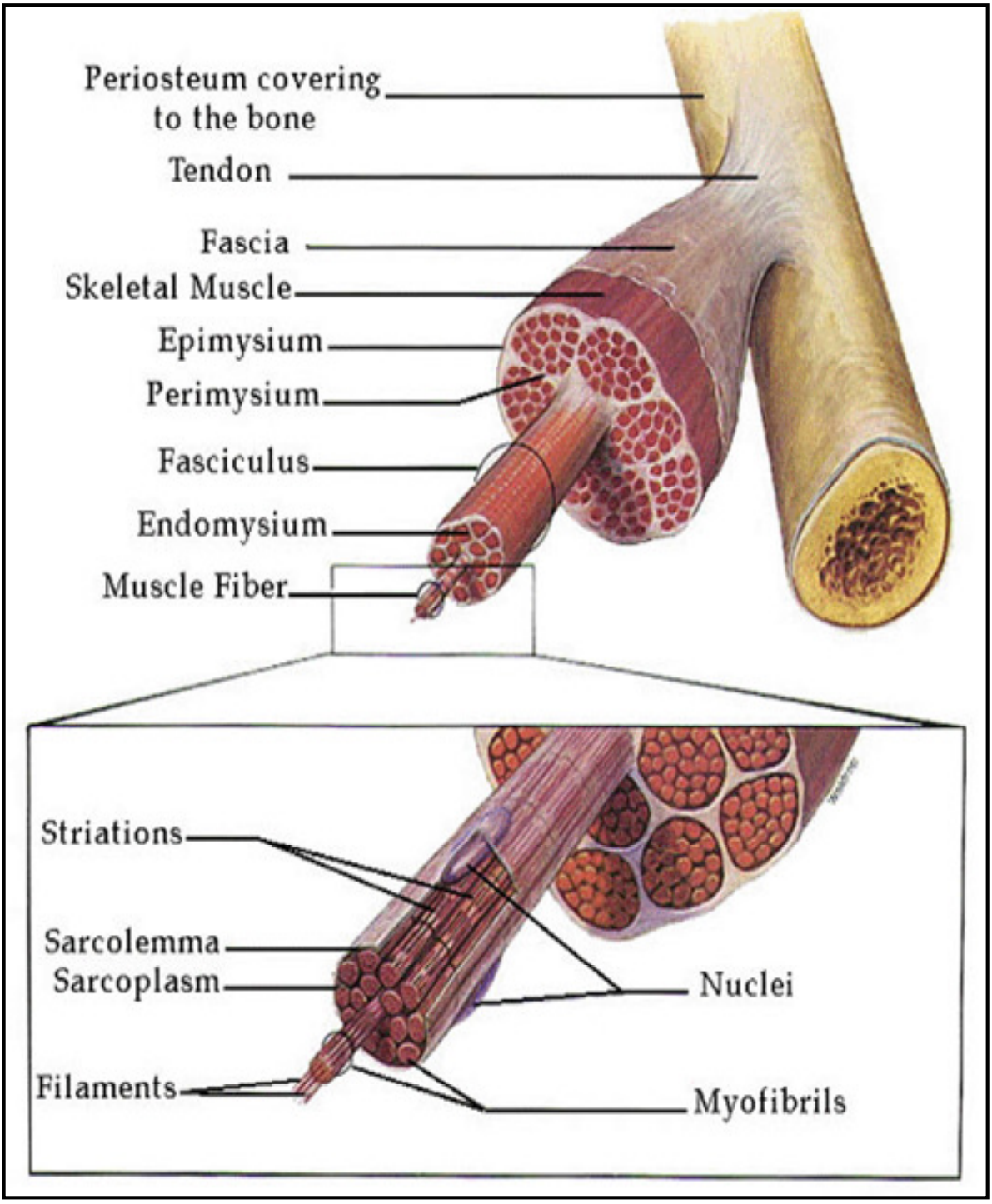

Figure 1. The relationship between muscle fibres and the connective tissues of the tendon, epimysium, perimysium and endomysium. Enlargement shows an expanded view of a single muscle fibre containing several nuclei, myofibrils and filaments. (the Figure is taken from Fox, S.I. Human Physiology, 4th Ed.)

2 The sarcomere

2.1 The structure of the sarcomere

All striated muscles are built of subunits known as sarcomeres. These sarcomeres are approximately 2-3 µm long and 1-2 µm in diameter and link end to end to form thin strands known as myofibrils (Craig and Padron, 2004). The striation pattern in muscle results from alternating ordered arrays of myofilaments, *i.e.* myosin and actin filaments (Cooke, 1995). Figure 2 is a schematic diagram of the sarcomere depicting the following features; thick and thin filaments, A band, M-band, I –band and Z-disk. Thick filaments are composed of mainly of myosin whereas thin filaments are composed of actin filaments associated with tropomyosin and troponin. The bands in the sarcomere were originally named according to their features under a polarized light microscope. The central **A-band** (Anisotropic in polarised light) is the region where thick and thin filaments interdigitate and is composed of a hexagonal array of aligned, bipolar myosin filaments and adjacent filaments that are cross-linked at their centres by proteins of the **M-band** (Mittel, meaning middle in German). Electron microscopy images of the A-band showed that there are six thin filaments surrounding one thick filament in a hexagonally arrangement and myosin heads extend to interact with actin forming crossbridges. The region of the A-band without any actinomyosin overlap is called the **H-zone** (Heller, meaning bright in German). The regions containing only actin filaments are termed **I-bands** (Isotropic in polarised light) and this surrounds the Z-disk. Actin overlaps partly with myosin and extends to the **Z-disk** (Zwischen, meaning between in German) at both ends of the sarcomere therefore the Z-disk is the border between each sarcomere. The actin filaments are polar structures, and Z-disc proteins

serve to provide a mechanical link between actin arrays of opposite polarity from adjacent sarcomeres (Huxley and Niedergerke, 1954; Huxley and Hanson, 1954).

The thick and thin filaments represent the main contractile units of the sarcomere. The myosin heads slides along the actin (thin filaments) through a binding interaction which is stimulated by ATP, ADP and inorganic phosphate (Pi). The contraction starts with myosin binding to actin, and the binding of ATP to myosin reduces the affinity of this interaction resulting in the separation of the myosin head from the actin protein, then the myosin head hydrolyses ATP and producing ADP; this reaction generates the power needed to move the myosin head along the actin filament. The replacement of ADP with ATP increases the affinity of binding of the myosin head towards actin. This cycle of ATP hydrolyses and addition of ADP represents the main force generation that is required for filament movement which results in the contraction of the sarcomere which turns the whole muscle to contract.

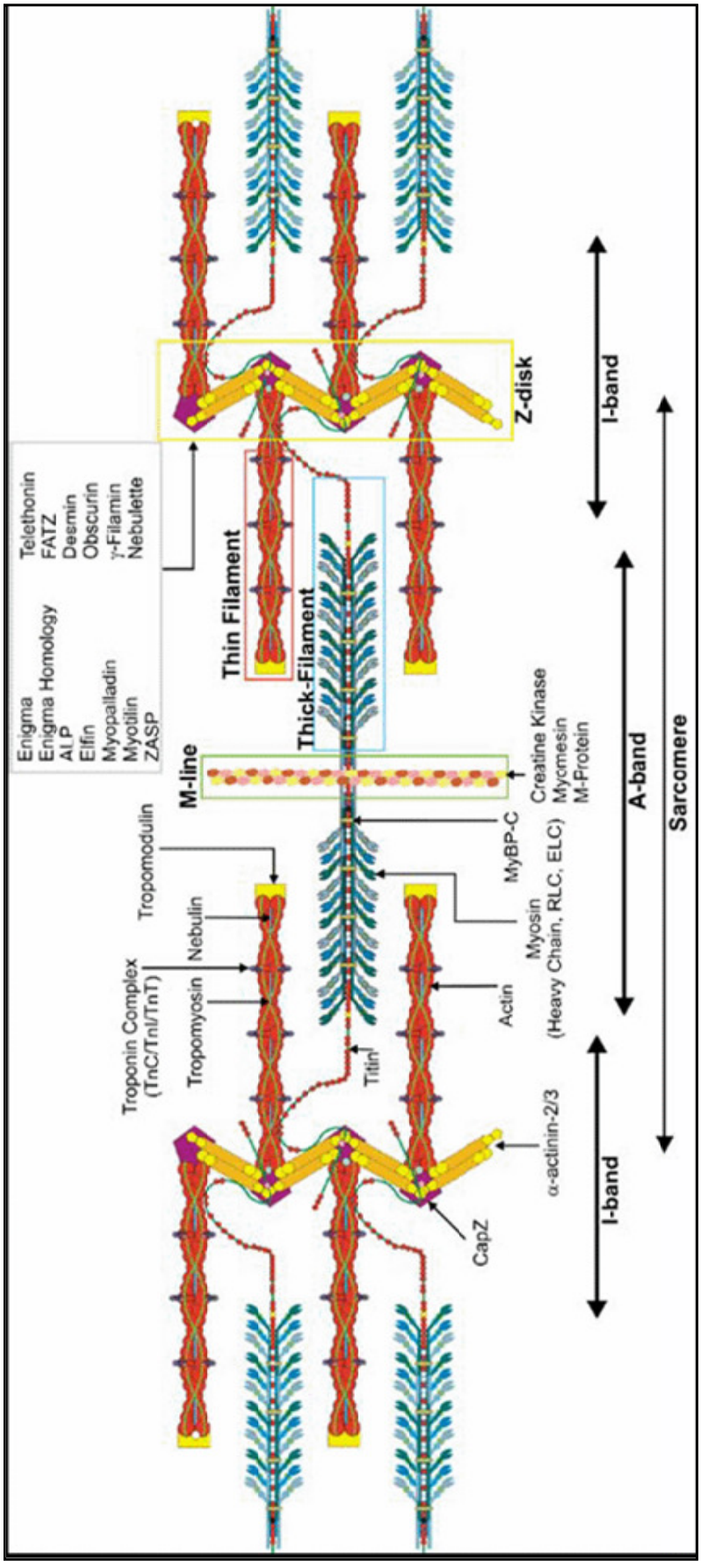

Figure 2: A schematic representation of the sarcomere. The thick filaments (blue), thin filaments (red), I-band, Z-disk (yellow), A-band and M-lines are indicated (Au, 2004).

1.2.1 Actin

Thin filaments are mainly composed of **Actin.** This protein is responsible for diverse cellular functions such as motility, cytokinesis and contraction. Actin filaments form two twisted α-helices that associate with the regulatory proteins tropomyosin and troponin. CapZ stabilizes and prevents depolymerization of actin filaments by binding their plus (+) ends. Moreover it attaches actin filaments to the Z-disk and also binds α-actinin-2 (Casella et al., 1987; Papa et al., 1999). Early in myofibril assembly, thin filament components associate with nascent Z-lines to form the first identifiable structures called I-Z-I complexes (Holtzer et al., 1997). Several Actin isoforms exist, each encoded by separate genes whose expression patterns are regulated developmentally and in a tissue specific manner. Their sequences and molecular structures are very similar. Two muscle-specific isoforms, cardiac and skeletal actins, are co-expressed at varying levels depending on the species, muscle fibre and developmental stage. Vascular and visceral actins are expressed in smooth muscle and also in striated muscle fibres transiently during development. Two non-muscle actins, the cytoplasmic isoforms, are co-expressed with other actin isoforms in many tissues.

Mutations in actin can lead to different diseases such as actin myopathy and nemaline myopathy characterized by myofibrillar structural abnormalities and muscle weakness (Ilkovski et al., 2001; Nowak et al., 1999) and also familial dilated cardiomyopathy (DCM) and heart failure, characterized by impaired force transmission and hypertrophic cardiomyopathy (HCM) (Olson et al., 2000; Olson et al., 1998)**.** Thus single amino acid substitutions in actin can result in distinct clinical manifestations, depending on the particular functional domain affected.

1.3 The Z-disk

1.3.1 The structure of the Z-disk

At the beginning of myofibrillogenesis α-actinin rich Z bodies are formed that are the precursors of the Z-disk (Rhee et al., 1994; Sanger et al., 2000). These Z-bodies are just below the plasma membrane and are connected with stress fibre-like structure made up of actin and non-muscle myosin resembling adhesion junctions found in non-muscle cells. The Z-body matures to a striated structure of three filament components; thin filament made up of actin and actin-binding proteins and thick filament consisting of oligomerized myosin (muscle) and titin (Clark et al., 2002; Granzier and Labeit, 2004) as well as intermediate filaments mainly composed of desmin that surround the myofilaments at the Z disk in cardiomyocytes (Clark et al., 2002) and link it to desmosomes, focal adhesion junctions, and the nucleus.

Sarcomeres are separated from one another by the Z-disk, the borderline between sarcomeres. The Z-disk keeps the structure of the sarcomere in register by tethering actin and transmits tension during muscle contraction. Filaments from neighbouring sarcomeres overlap at the Z-disk and are cross-linked by tight interaction with α-actinin-2 which is a major component of the Z-disk (Hoshijima, 2006). Alpha-actinin-2 is assembled in the Z-disk as homodimers and aligned in an antiparallel fashion, cross-linking actin and organizing its polarized orientation (Frank et al., 2006) (fig 3). The width of the Z-disk varies depending on the type of muscle. The Z-disc in skeletal muscle fast-twitch fibres has a width of about 30-50 nm (Luther, 1991; Luther, 2000), while in cardiac muscle and skeletal slow-twitch fibres its width is about 100-140 nm (Luther et al., 2002; Yamaguchi et al., 1985).

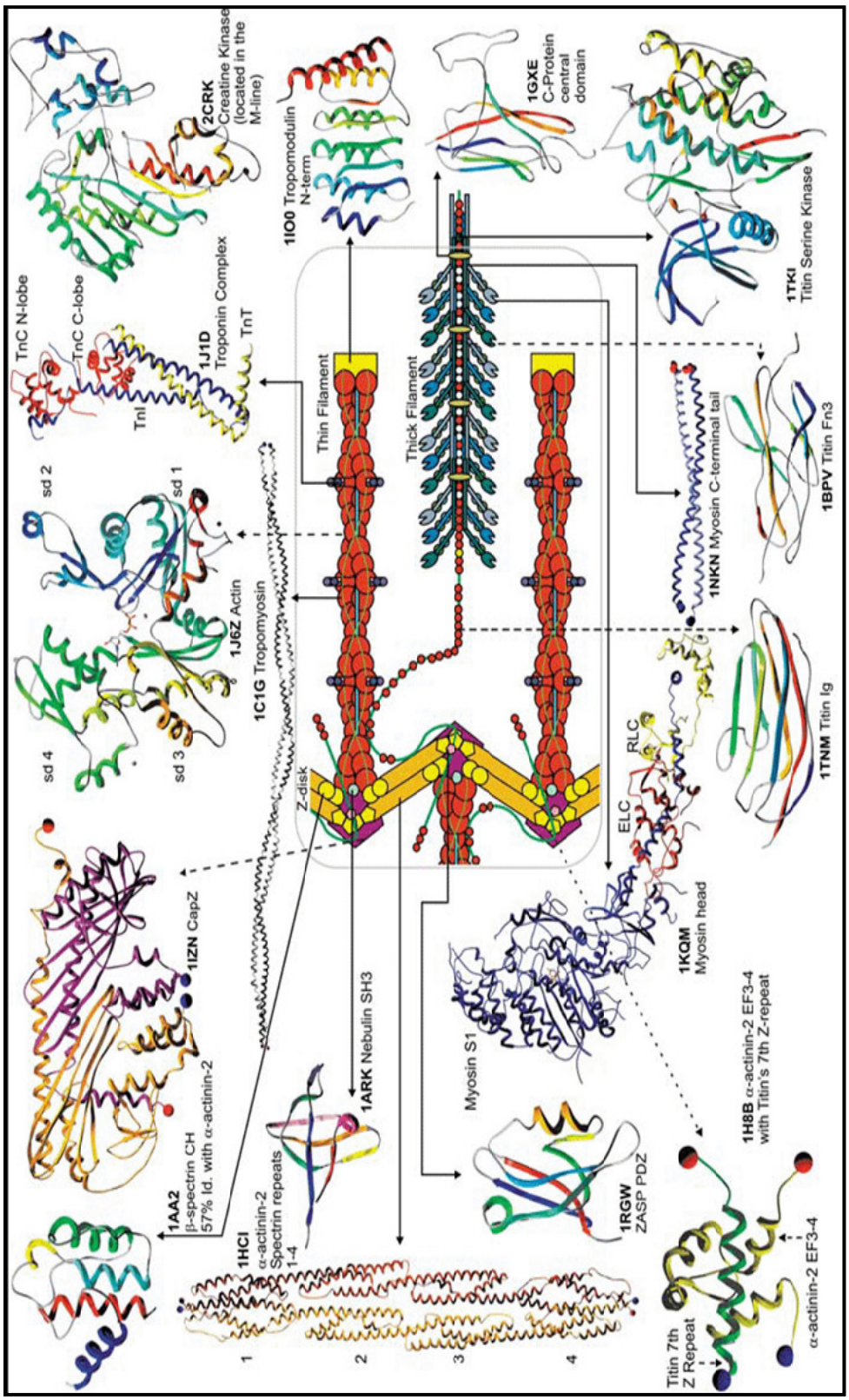

Figure 3 A schematic diagram depicting the structural components of a section of the sarcomere. All structures are displayed using a ribbon representation and are labelled with their PDB accession codes and subdomains or chain name. Monomeric structures are coloured from blue to red, from the N- to C-termini; a single colour per chain has been used for multimeric structures, with blue and red spheres indicating N- and C-termini (except myosin-S1 and the troponin complex) (Au, 2004).

1.3.2 Z-disk proteins

It is now clear that the Z disk is not just a simple mechanical structure but a centre for interactions and signalling in the sarcomere. In recent years the number of proteins localised in the Z-disk has increased dramatically but not as much as their interactions among themselves as well as other proteins not normally localised in the Z-disc such as cytoskeletal proteins, nuclear proteins and kinases to mention just a few.

MLP (CSPR3) is a LIM protein downregulated in the adult skeletal muscle up regulated (Arber et al., 1994). MLP is highly expressed in developing and adult heart. Its importance is demonstrated by the fact that the MLP-null mouse develops severe cardiac dysfunction which resembles human dilated cardiomyopathy (Arber et al., 1997). Muscle PDZ-LIM proteins are thought to act as adapters in transmitting mechanical stress signals from the Z-disk to the nucleus will be dealt with in more detail later in the Introduction. Some PDZ-LIM proteins are also present in heart for example ZASP, ALP, enigma and CLP-36. The Z-disk contains many other proteins such as the FATZ (Calsarcin/Myozenin) family, ZASP (Cypher/Oracle), myotilin, myopalladin, myopodin, enigma homology protein, filamin-C, telethonin, desmin, obscurin and titin to mention just a few. As mentioned before most of these proteins interact with each other as well as signalling proteins; for example the FATZ family interacts with and negatively controls calcineurin which it localises to the Z-disk (Frey and Olson, 2002; Frey et al., 2000). Mutations in several Z-disk proteins has been shown to cause cardiomyopathies and or muscular dystrophies, for instance mutations in ZASP (Vatta et al., 2003), FATZ-2 (Osio et al., 2007) and myotilin (Hauser et al., 2002) have been found in patients suffering from cardiomyopathy. The network of interactions of the Z-disk proteins strengthens the Z-disk and allows it to withstand the force caused by the

contraction of the sarcomere. As noted before this places the Z-disk at the centre of the sarcomeric structure (Hoshijima, 2006). Some Z-disk proteins are discussed below and in other sections however I am aware that this is by no means a fully detailed or comprehensive review of all Z-disk proteins.

1.3.2.1 Titin

Titin spans the entire sarcomere and can be divided in three principal regions: Z-disk Titin, I-line Titin and M-line Titin. The Z-disk Titin represents the N-terminal part of the molecule and contains several Ig-like repeats that bind α-actinin (Ohtsuka et al., 1997) and telethonin (Gregorio et al., 1998). Titin, together with telethonin and MLP constitutes a stretch sensor complex in cardiomyocytes (Knoll et al., 2002). The difference in number of alternatively spliced Ig-like repeats in titin isoforms varies between different muscle types and has been suggested to affect the number of cross-links between α-actinin-2 and actin and hence to cause variations in Z-disk thickness (Gautel and Goulding, 1996). Moreover Z-disk titin interacts with Obscurin and small ankyrin 1 (sAnk1) (Kontrogianni-Konstantopoulos and Bloch, 2003), suggesting the existence of a complex implicated in the organization of the sarcoplasmic reticulum around the myofibril (Bang et al., 2001a). In addition to the structural and elastic properties of titin there is evidence that it is involved in signalling pathways. In fact I-line Titin interacts and forms a complex with Calpain protease 94 (Sorimachi et al., 1995) and all the members of the MARP family (CARP, Ankrd2 and DARP) (Miller et al., 2003). Remarkably, all I-band ligands of Titin are also found in the nucleus where they can participate in transcriptional and cell cycle regulation. It seems likely that this dual localization (I-band and nucleus) is not just a coincidence but reflects a dual

function for these proteins: being part of a Titin-based stretch sensing complex in the I-band and regulating transcription in the nucleus. Furthermore, such dual localization may also provide a communication pathway between the I-band and nucleus that links stretch sensing to gene expression (Granzier and Labeit, 2004).

The C-terminal region of titin is located in the M-line. This region contains a Serine/Threonine kinase activity that phosphorylates telethonin in developing muscle (Mayans et al., 1998). However, the upstream elements controlling the Titin kinase activation, its range of cellular substrates and its role in mature muscle are largely unknown. The elastic properties of the Titin molecule and the mechanical deformation of the M-band during stretch and contraction suggest that the signalling properties of the Titin kinase might be modulated by mechanically induced conformational changes (Lange et al., 2005). Also M-line Titin binds to the RING finger protein MURF-1 (Centner et al., 2001) and nbr-1, which interacts with the MURF-2 binding protein p62 (Lange et al., 2005). Nbr-1 acts as a cytoskeleton-associated kinase scaffolding protein that assembles large sarcomeric "signalosomes" through interactions with multiple elements, linking the Titin kinase to p62 and MURF-1 (Lange et al., 2005).

Titin is involved in muscle disease; in fact mutations in the Titin gene, that affect the binding sites for Telethonin and α-actinin, have been found in patients with dilated cardiomyopathy and are thought to be correlated with the disease (Itoh-Satoh et al., 2002). Mutations in the Titin gene that lead to autosomal dominant tibial muscular dystrophy were found to cause LGMD type 2J (Vainzof and Zatz, 2003) and a point mutation in the kinase domain that disrupts the binding with nbr-1 resulted in hereditary myopathy with early respiration failure (HMERF) (Lange et al., 2005).

1.3.2.2 MLP

The Muscle Lim Protein is localized at the periphery of the Z-disk (Arber et al., 1997) and at the intercalated disc (Ehler et al., 2001). The ultrastructural analysis of MLP -/- murine cardiomyocytes revealed a misalignment of the Z-disk (Arber et al., 1997) and morphological defects at costameres and intercalated discs (Ehler et al., 2001) suggesting that MLP plays a primary role in maintaining the stability of these structures. The genetic ablation of MLP in the mouse results in DCM (Arber et al., 1997) and a point mutation in the human MLP gene has also been associated with this pathological condition. This single nucleotide mutation resulted in a severe charge change at position 4 in the MLP protein (W4R) that lies within the N-terminal telethonin interacting domain (TID) of MLP, thus disrupting the binding between the two proteins and causing telethonin miss-localization and Z-line disruption. Since MLP binds telethonin, it was suggested that, together with titin, they could constitute a stretch sensor (Knoll et al., 2002). MLP is known to interact with MyoD (Kong et al., 1997) and has also been implicated in the communication with the nucleus especially in response to hypertrophic signals (Ecarnot-Laubriet et al., 2000).

1.3.2.3 MURFs

The MURFs (Muscle Specific RING-finger proteins) are a family of RING/B-box proteins expressed in striated muscle. Three MURF genes encode three highly similar proteins that can form homo- and heterodimers: MURF-1, MURF-2 and MURF-3 (Centner et al., 2001). MURF-1 acts as a ubiquitin ligase, thereby controlling proteasome-dependent degradation of muscle proteins. Among its targets there are M-line Titin, Nebulin, Myotilin and Telethonin. MURF-1 is part of the structural scaffold

of the M-line lattice but has also been implicated in the regulation of gene expression and myocardiocytic contractility (Witt et al., 2005). MURF-2 co-localizes both with MURF-1 in the M-line and with MURF-3 in microtubules (McElhinny et al., 2004). MURF-3 is a microtubule associated protein differentially expressed during myogenesis and up-regulated during differentiation, probably to stabilize microtubules (Spencer et al., 2000). This is the isoform of MURF located in the Z-line of skeletal muscle where it is though to act as a link between the sarcomeric and the microtubules compartments since it can bind MURF-1, MURF-2 and Z-disk and M-line proteins such as Titin (Spencer et al., 2000).

1.3.2.4 Calpain 3

Muscle-specific Calpain3/p94 is a Ca^{2+} dependent cysteine protease present both in the M-line and the I-line, where it binds to Titin (Sorimachi et al., 1995). Calpain3/94 is thought to have a regulatory function in the modulation of transcription factors and to be involved in the disassembly of sarcomeric proteins (Vainzof and Zatz, 2003). The importance of its function is suggested by the observation that mutations in the Calpain3/94 gene, with consequent loss of function, lead to LGMD type 2A (Richard et al., 1995).

1.3.2.5 Nebulin and Nebulette

Nebulin is an actin-binding protein which is localized in the I-band of skeletal muscle. It is a large protein (600-900 kDa) that together with Titin forms the third filament system of the myofibril. The C-terminal of the protein is located in the Z-disc, while the rest extends until the end of the thin filaments and its length is proportional to that of the

thin filament. Its binding with actin monomers is sensitive to both calcium and calmodulin (Wright et al., 1993). Nebulin also binds α-actinin (Nave et al., 1990). Mutations in nebulin can cause nemaline myopathy, an autosomal recessive disease. It has been suggested that nebulin acts as a template for the formation of actin filaments (Kruger et al., 1991). Nebulin is found only in skeletal muscle not in heart where a smaller protein called nebulette (109 kDa) that is highly homologous to the C-terminal of nebulin (Millevoi et al., 1998) is found. The C-terminal homology between nebulin and nebulette is thought to be necessary to conserve their binding to the Z-disk (Moncman and Wang, 1995).

1.4 Alpha-actinin

Alpha-Actinin was first discovered in 1964 (Ebashi and Ebashi, 1964). The α-actinin family of proteins plays a very important role in muscle contraction and in the organization of the cytoskeleton. It is a highly conserved family of actin binding proteins, which belong to the spectrin superfamily which includes spectrins, dystrophin and utrophin. Alpha-actinin is an antiparallel homodimer whose structure consists of three major domains; an N-terminal actin-binding domain (ABD) which is a highly conserved region with two calponin homology (CH1 and CH2) domains. The CH1 is responsible for binding actin, while the CH2 increases the binding affinity (Gimona et al., 2002). The central rod domain of α-actinin has tandem spectrin-like repeats (SLRs) which are less conserved than the ABD domain. The number of SLRs in α-actinin has changed during evolution, in vertebrates there are 4 SLRs. Some members of the spectrin super family can contain up to 30 SLRs. In α-actinin the SLRs are involved in

the formation of anti-parallel homodimers and they also bind other interacting proteins (Djinovic-Carugo et al., 2002; MacArthur and North, 2004; Thomas et al., 1997). The C-terminal region which consists of two EF hand (EFh) domains is important for the functional diversities of the α-actinin isoforms.

In humans there are four isoforms of α-actinin, 1, 2, 3, and 4: which are encoded by ACTN1, ACTN2, ACTN3, and ACTN4, respectively. These isoforms share an 80% identity (Beggs et al., 1992; Honda et al., 1998; Millake et al., 1989) and can be characterized according to their biochemical properties, expression patterns and subcellular localisation into two groups; the non-muscle cytoskeletal (calcium sensitive) isoforms alpha-actinin-1 and 4 (Tang et al., 2001) and the muscle sarcomeric (calcium insensitive) isoforms α-actinin-2 and -3 (Blanchard et al., 1989; MacArthur and North, 2004). Alpha-actinin-1 is concentrated at the ends of stress fibres in focal contacts and alpha-actinin-4 is localized in stress fibres and can also be translocated to the nucleus (Honda et al., 1998). The muscle isoforms lack five amino acids at the EFh domain which eliminates their ability to bind calcium. The EFh domain is also responsible for the interaction with titin (Ohtsuka et al., 1997) and ZASP (Faulkner et al., 1999). Alpha-actinin-2 and -3 can be found mainly in the Z-disc, and to a lesser extent in sarcolemma. However α-actinin-3 is absent in cardiac muscles (Beggs et al., 1992; Hance et al., 1999; Lazarides and Granger, 1978) and is not found in 16% of the world population, suggesting that other isoforms can compensate for its absence from the Z-disc of skeletal muscles, especially since there is no phenotypic changes seen when α-actinin-3 is absent (North and Beggs, 1996).

Several studies have shown the importance of α-actinin in muscle function since mice lacking α-actinin die due to degeneration of myofibrils and disruption of the Z-disc

(Fyrberg et al., 1998; Fyrberg et al., 1990; Roulier et al., 1992). It has also been found that over expression of a C-terminal deletion of α-actinin causes Z-disc hypertrophy (Lin et al., 1998; Schultheiss et al., 1992) and a mutation in α-actinin-2 (Q9P) has been found to be associated with dilated cardiomyopathy, this mutation disrupts the binding of α-actinin-2 with MLP (Mohapatra et al., 2003).

1.5 NF-AT3

NF-AT3 is a transcription factor localized both in the Z-disk and in the nucleus. In normal conditions NF-AT3 is tethered to the Z-disk by calcineurin. NF-AT3 resides in the Z-disk because of its interaction with calcineurin. When a signal activates calcineurin, it de-phosphorylates NF-AT3 provoking its translocation into the nucleus. Both NF-AT3 and calcineurin are found in hypertrophy pathways (Olson, 2000).

1.6 Filamins

The Filamins are a family of cytoskeletal proteins which organize filamentous actin in networks and stress fibres. Filamins were first discovered as a family of non-muscle actin-binding proteins (Popowicz et al., 2006; Stossel et al., 2001; van der Flier and Sonnenberg, 2001). The name filamin refers to is filamentous colocalization with actin stress fibres (Wang et al., 1975). There are three main human isoforms of filamin A, B and C encoded respectively by the genes FLNA , FLNB and FLNC (Gorlin et al., 1990). The three isoforms share from 70-80% identity with each other and the exon-intron structure of all the isoforms is highly conserved (Chakarova et al., 2000; Xie et al.,

1998). These isoforms are expressed in most human tissues with some difference in the expression pattern: filamin A is expressed in heart, lung, blood vessels and haematopoietic cells; filamin B is expressed in kidney and pancreas; filamin C is restricted to striated muscle and found predominantly in the Z-disc and in the intercalated disks (Maestrini et al., 1993; Takafuta et al., 1998).

The structure of filamin consists of 24 Ig-like domains (or repeats), each domain is composed of 96 amino acids (Davies et al., 1978). The N-terminal of filamin contains two calponin homology (CH) domains containing 274 amino acids that form the ABD domain (Banuelos et al., 1998). The filamin protein forms a homodimer and electron micrographs showed this homodimer as an extended Y-shaped. The filamin dimer has a molecular weight of 280 kD (Hartwig and Stossel, 1981; Tyler et al., 1980). Himmel and colleagues have shown that the filamin Ig-like domain is sufficient for its dimerisation (Himmel et al., 2003) and serves as a platform for other molecules that participate in the regulation of filamin (Stossel et al., 2001).

Apart from actin cross-linking in cytoskeleton (Hartwig and Stossel, 1981), filamin has many other functions such as linking extra-cellular proteins and the actin cytoskeleton with transmembrane receptors (Meyer et al., 1997). It also plays an important role in signal transduction by serving as a platform for a variety of signalling molecules. A mutation in the filamin C gene (FLNC) can cause myofibrillar myopathy (MFM), this mutation has been mapped to the Ig-like domain 24 (Vorgerd et al., 2005).

1.7 Telethonin

Telethonin (Valle et al., 1997), also known as T-cap (Gregorio et al., 1998) is a small sarcomeric protein with a molecular weight of 19kD. The human telethonin shares around 90% homology with the mouse telethonin (Mason et al., 1999). The N-terminal of telethonin binds to the N-terminal of titin at the Z1 and Z2 Ig-like domains and both these domains and telethonin are localized in the Z-disk (Gregorio et al., 1998; Mues et al., 1998). The binding of telethonin to the N-terminal of titin is very important for Z-disk stability since it has been shown in primary cultures of cardiomyocytes that overexpression of the titin N-terminal resulted in severe myofibril disruption. This observation as well as others suggests that telethonin plays a key role in positioning and anchoring the N-terminal of titin to the Z-disk (Gregorio et al., 1998; Zou et al., 2003). Telethonin is phosphorylated by titin kinase, located in the C-terminal of titin and activated by calcium/calmodulin binding during myocyte differentiation. Since the titin kinase domain is situated in the M-line, whereas telethonin is in the Z-disk, it has been proposed that during myofibrillogenesis the cytoskeleton undergoes reorganization and the titin C-terminal becomes transiently located in close proximity to telethonin, thus allowing its phosphorylation (Mayans et al., 1998).

Crystal structure studies have shown that telethonin and titin form a sandwich complex through the interaction of both N-terminals, forming a dimeric assembly between titin and telethonin however the C-terminus of telethonin would also appear to be involved in the assembly of the titin/telethonin complexes (Pinotsis et al., 2006). Studies on the mechanical strength of the titin Z1Z2-telethonin complex have shown that it is able to withstand the force generated passive muscle stretch due to beta strand crosslinking as titin Z1Z2 in the absence of telethonin had reduced resistance to mechanical stress (Lee

et al., 2006). This data strengthens the hypothesis that telethonin is a key component of the N-terminal titin anchor.

Telethonin was the first sarcomeric protein found to cause an autosomal recessive Limb-Girdle Muscular Dystrophy (AR LGMD). Two different mutations in the telethonin gene were identified in patients with LGMD 2G, both mutations giving rise to premature stop codons; the first mutation was a C157T transition in exon 2 and the second mutation was a deletion of two guanine nucleotides within four guanines at the junction of exon 1 and intron 1 (Moreira et al., 2000). The resulting truncated telethonin protein was not detected suggesting that it was rapidly degraded which may cause instability in the sarcomere structure (Moreira et al., 2000). Interestingly, the C-terminal truncation eliminates the domain of telethonin that is phosphorylated by titin kinase. Mutations in telethonin have been found in other muscle disorders for instance in patients suffering from hypertrophic cardiomyopathy (HCM) (two mutations T137I and R153H) and in a patient suffering from dilated cardiomyopathy (E132Q) (Hayashi et al., 2004). In one case, an individual suffering from severe HCM with a heart septal wall thickness of 46mm had a mutation in telethonin (R70W). This individual had no other known mutations in genes associated with HCM, this mutation was in the binding site of telethonin with MLP (Bos et al., 2006). It has been suggested that the titin/MLP/telethonin complex together with α-actinin may play an important role as a stretch sensors controlling cardiac hypertrophy (Hayashi et al., 2004). It is worth noting that telethonin also binds to Ankrd2 (Kojic et al., 2004) that has been suggested as a stretch sensor in skeletal muscle and that the MARP family, of which Ankrd2 is a member, binds to the N2A region of titin and may form a complex with titin, calpain3 and myopalladin (Miller et al., 2003). In cardiomyocytes telethonin binds the potassium

channel (I_{KS}) β-subunit minK suggesting that a T-tubule-myofibril linking system may contribute to a stretch-dependent regulation of K^+ flux (Furukawa et al., 2001). Telethonin can also bind protein kinase D (Haworth et al., 2004), MURF-1, a RING finger protein found in striated muscle (Witt et al., 2005) and the growth factor myostatin. It has been reported that over expression of telethonin inhibits the secretion of myostatin which would indirectly lead to an increase in the number of myoblasts since myostatin is a negative regulator of myoblast proliferation (Nicholas et al., 2002). Recently it was reported that MDM2 binds telethonin and that high levels of MDM2 can change the sub-cellular localization of telethonin, both proteins co-localised in the nucleus. It would appear that MDM2 can down regulate the protein level of telethonin through a ubiquitin-independent proteasomal pathway (Tian et al., 2006). Pertinent to this thesis telethonin is also able to bind members of the FATZ family of proteins (Faulkner et al., 2000; Kojic et al., 2004).

1.8 The MARP family

Since Ankrd1 (C-193/CARP/MARP) and Ankrd2 are similar both in sequence and in behaviour, it is possible that they play similar roles in heart and in skeletal muscle, respectively. Ankrd1 (CARP), Ankrd2 (ARPP) and DARP (Diabetes-related Ankyrin Repeat Protein, have been grouped together into the MARP family of **Mu**scle **A**nkyrin **R**epeat **P**roteins (Miller et al., 2003). The up-regulation in expression of each MARP is induced by different stress stimuli: injury and hypertrophy in heart for Ankrd1 (Kuo et al., 1999); stretch and denervation in skeletal muscle for Ankrd2 (Kemp et al., 2000) and recovery following starvation for DARP (REF) indicating that these proteins could

be involved in muscle stress response pathways. The MARPs bind to the N2A region of titin and they are part of a Titin-N2A based complex together with Calpain3 and Myopalladin. This complex could be a stress sensor sending signals to the nucleus thereby regulating gene expression (Miller et al., 2003).

1.8.1 Ankrd1 (also known as CARP)

The Ankrd1 protein can shuttle between the sarcomere (I-band) and the nucleus. It is a nuclear co-factor downstream of the homeobox gene Nkx2.5 pathway and forms a physical complex with the ubiquitous transcription factor YB-1, thus acting as a negative regulator of HF-1 dependent pathways for ventricular muscle gene expression (Jeyaseelan et al., 1997; Zou et al., 1997) Ankrd1 expression is predominantly in cardiac muscle, with low levels in skeletal muscle. Its expression can be strongly induced in the regenerating myofibres of Congenital and Duchenne Muscular Dystrophy patients (Nakada et al., 2003). It can also be detected in the sarcomeric I-Z-I areas of regenerating skeletal muscle (Nakada et al., 2003) where it interacts with the I-band protein Myopalladin suggesting it may have a role in the maintenance of sarcomeric integrity (Bang et al., 2001b).

1.8.2 Ankrd2 (ANKyrin Repeat Domain 2, also known as ARPP)

Ankrd2 was first discovered as a protein that was up regulated during muscle stretch (Kemp et al., 2000). It is localized in the I-band and near the Z-line (Tsukamoto et al., 2002). The Ankrd2 gene is located in the same region of human chromosome 10 as that of Ankrd1 (position 10q23.1) and its 9 exons encode a protein with a predicted molecular weight of 37 kD; exons 5, 6, 7, and 8 encoding the ankyrin repeats

(Moriyama et al., 2001; Pallavicini et al., 2001). There is a 43 % homology between Ankrd1 and Ankrd2 (Pallavicini et al., 2001). The human Ankrd2 protein shares a 89% similarity at the amino acid level with the mouse Ankrd2 and it is expressed in skeletal muscle and at a lower level in heart, kidney and prostate (Moriyama et al., 2001; Pallavicini et al., 2001). Ankrd2 expression in foetal heart is lower than that in adult heart and it has been suggested by Moriyama and colleagues (Moriyama et al., 2001) that Ankrd2 could be involved regulation of development in heart. In addition to ankyrin repeats domains, Ankrd2 has a nuclear localization signal (KKKRK) and a PEST-like sequence (Kemp et al., 2000; Moriyama et al., 2001; Pallavicini et al., 2001). It also contains several predicted phosphorylation sites for the following kinases: casein kinase I (CKI), casein kinase II (CKII), protein kinase C (PKC), extra-cellular signal regulated kinase (ERK), cAMP-dependent protein kinase, calmodulin-dependent protein kinase II and cGMP-dependent protein kinase (Moriyama et al., 2001; Pallavicini et al., 2001). In myotubes Ankrd2 is localized both in the nuclei in PML nuclear bodies and diffusely in the cytoplasm (Pallavicini et al., 2001). Ankrd2 has been shown to interact with other Z-disk proteins such as telethonin and non-muscle proteins such as p53 and transcription factors such as PML, and YB-1 (Kojic et al., 2004). These interactions support the idea that Ankrd2 could act a transcription co-factor and it has also been hypothesized that Ankrd2 could be a stretch sensor in skeletal muscle shuttling between the nucleus and the cytoplasm (Kojic et al., 2004).

1.9 Myotilin, Palladin and myopalladin family

1.9.1 Myotilin

The myotilin gene maps at the chromosome locus 5q31 and mutations in this gene are responsible for a dominantly inherited limb-girdle muscular dystrophy (LGMD1A). Myotilin is a 57kD myofibrillar protein that is highly expressed in skeletal muscle and only weakly in heart. It has a unique N-terminal rich in serine residues, a 23 amino acid hydrophobic region (57-79 aa), two Ig-like domains (252-341 aa ; 351-441 aa) that share a high sequence homology with the Ig domains 7 and 8 of human titin and a short C-terminal tail (Salmikangas et al., 1999). Myotilin binds F-actin and efficiently cross-links actin filaments into bundles as well as being able to decrease the rate of F-actin depolymerization which suggests that it could be involved in thin filament stabilization. It is able to crosslink actin since it can dimerize via Ig-like domains. Myotilin is localized in the Z-disk where it binds directly to α-actinin-2 and filamin C, the first 214 residues of myotilin bind to the spectrin-like repeats 3 and 4 of α-actinin-2 and the myotilin C-terminal region containing the Ig-like domains binds to the Ig-like domains 19-21 of filamin C. (van der Ven et al., 2000). Over expression of the C-terminal myotilin had an effect on the assembly of myofibrils in differentiating C2C12 myotubes whereas over expression of full-length myotilin induced formation of thick actin cables in non-muscle cells devoid of endogenous myotilin suggesting that myotilin may have a role in stabilizing the assembled actin bundles (Salmikangas et al., 2003). Not only filamin C but also filamin-A, filamin-B and filamin-B_{var-1} variant bind to myotilin (Gontier et al., 2005). Myotilin has also been shown to bind to FATZ-2 (calsarcin-1 /myozenin-2) and to the C-terminal region of FATZ-1 (calsarcin-2/myozenin-1) (Gontier et al., 2005).

Patients suffering from Limb girdle muscular dystrophy type 1 A (LGMD1A) have mutations in myotilin. These mutations were a C450T missense mutation which converted residue 57 from threonine to isoleucine but did not disrupt the binding with α-actinin (Hauser et al., 2000). The other two mutations were S55F and T57I, both located in the N-terminal of myotilin but outside the filamin C binding site (Hauser et al., 2002). Mutations in myotilin as well as ZASP, filamin C, desmin and αβ-crystallin can cause myofibrillar myopathy (Griggs et al., 2007; Selcen and Engel, 2004).

1.9.2 Palladin

Palladin was simultaneously discovered by two different laboratories, the mouse palladin was discovered by (Parast and Otey, 2000), while the human palladin was discovered by (Mykkanen et al., 2001). The human palladin shares a 91% homology with the mouse palladin. Palladin is expressed in muscle and non-muscle fibres. In muscles palladin is highly expressed in smooth and poorly expressed in skeletal, while in non-muscle fibres it is highly expressed in prostate, testis, ovary, small intestine, and colon (Mykkanen et al., 2001). There are three isoforms of palladin and their expression depends on cell type; the first isoform is a 90-92 kD protein which is the most abundant isoform of palladin and widely expressed in many cells and tissues, another isoform is around 140 kD which is less abundant than the previous isoform and is mostly expressed in embryonic mice while in adult mice it is mostly detected in smooth muscles (Mykkanen et al., 2001; Parast and Otey, 2000), the third isoform is a 200 kD isoform first found in developing heart and then in embryonic and neonatal bone (Otey et al., 2005). Palladin contains three IgC2 domains, the first IgC2 domain towards the N-terminal shares high homology with the first IgC2 domain, Z-disk-associated IgC2

domains of titin, and with the C-terminal IgC2 domains of myosin light chain kinase, while the middle and the C-terminal IgC2 domains of palladin share high homology with the myotilin N-terminal IgC2 domain; palladin and myotilin share a high homology at their N-terminal and C-terminal. Alpha-actinin colocalizes with palladin in stress fibres, focal adhesions, cell-cell junctions and the embryonic Z-disk. Palladin plays an important role in the organization of actin cytoskeleton and focal adhesions in cultured trophoblasts and fibroblast cells (Parast and Otey, 2000). The expression level of palladin is highly reduced in a number of tissues including heart, skeletal muscle, liver, and kidney, which indicates that palladin could be involved in establishing the cytoskeletal organization of cells during differentiation being replaced by other proteins when the cells are fully differentiated (Parast and Otey, 2000). Recently palladin has been found mutated members of a family suffering from pancreatic cancer, the mutation caused a change of an amino acid proline (hydrophobic) to serine (hydrophilic) (P239S) in a highly conserved region of palladin, the mutation was not found in healthy members of the family. It has been suggested that this mutated palladin in pancreatic cancer may cause cytoskeletal changes in the pancreatic cancer cells and may be responsible for strong invasive and migratory abilities of these tumours (Ronty et al., 2007).

1.9.3 Myopalladin

Myopalladin is a 145 kD protein that interacts with nebulin, nebulette and α-actinin in the Z-disk and with CARP in the I-band. These interactions are important for the integrity of the sarcomere since over expression of myopalladin leads to the disruption of the sarcomeric structure suggesting that it could link the regulatory mechanisms of

the Z-disk to muscle gene expression through its interaction with Ankrd1 (Bang et al., 2001b). Myopalladin is expressed in skeletal and cardiac muscle and it is localized predominantly in the Z-disk and to narrow segments of the I-band on either side of the Z-disk. Myopalladin contains five Ig domains, the last three Ig domains towards the C-terminal are most related to the Ig domains of palladin, whereas the last two Ig domains towards the C-terminal of myopalladin shares high homology with the Ig domains of myotilin. Apart from the homology at the Ig domain level that myopalladin shares with palladin and myotilin, myopalladin shares 63% homology through its C-terminal with the C-terminal of palladin which includes the last three Ig domains (Bang et al., 2001b). Myotilin, myopalladin and palladin form a family which shares high amino acid homology and also high homology at the level of the Ig domains. All three proteins function as scaffolds that regulate actin organization (Otey et al., 2005).

1.10 The FATZ family

The FATZ (also known as calsarcin and myozenin) family was independently discovered by three different groups (Faulkner et al., 2000; Frey et al., 2000; Takada et al., 2001). The family consists of three proteins FATZ-1 (myozenin-1 or calsarcin-2), FATZ-2 (myozenin-2 or calsarcin-1) and FATZ-3 (myozenin-3 or calsarcin-3) (Frey and Olson, 2002) that are localised in the Z-disk (Faulkner et al., 2000; Takada et al., 2001). Then name FATZ denotes filamin C, alpha-actinin and telethonin binding protein of the Z-disk (Faulkner et al., 2000), while the name calsarcin denotes calcineurin associated sarcomeric protein (Frey et al., 2000). The FATZ family are

sarcomeric proteins localized in the Z-disk of striated muscle (Faulkner et al., 2000; Frey et al., 2000).

FATZ-1 (myozenin-1 or calsarcin-2) and FATZ-3 (myozenin-3 or calsarcin-3) are highly expressed in differentiated skeletal muscle in fast-twitch fibres, whereas FATZ-2 (myozenin-2 or calsarcin-1) is expressed in adult cardiac muscle in slow-twitch fibres (Frey and Olson, 2002; Frey et al., 2000). The three proteins share a high homology at the N- and C-termini and less homology in the intervening region, which may indicate that these conserved regions have functional properties and could be protein binding domains (Frey and Olson, 2002; Frey et al., 2000). The family members tend to interact with the same proteins, for example filamin A, B and C, α-actinin-2 and -3, telethonin (Faulkner et al., 2000; Takada et al., 2001) as well as calcineurin (Frey et al., 2000), myotilin (Gontier et al., 2005) and ZASP. FATZ-1, FATZ-2 and FATZ-3 bind strongly to nine different splice variants of ZASP, some of these splice variants had only the N-terminal PDZ domain and lacked the three C-terminal LIM domains, suggesting that the LIM domains were not involved in the interaction between ZASP and FATZ (Frey and Olson, 2002; Zhou et al., 2001).

The FATZ family members also interact with calcineurin (calcium/ calmodulin-dependent serine, threonine phosphatase). The catalytic activity of calcineurin is not crucial for the interaction with all three FATZ proteins, since it has been shown that these proteins bind to a mutated subunit of CnA lacking enzymatic activity (Frey and Olson, 2002; Frey et al., 2000). Immunostaining experiments showed that the interaction between calcineurin and FATZ occurs in the Z-disk (Frey et al., 2000). Calcineurin can be detected in the nucleus as well as the cytoplasm suggesting that FATZ may have a role in interacting with and localizing calcineurin to the Z-disk (Frey

et al., 2000). There are other examples of intracellular proteins that bind and localize signalling proteins to specific sites, for example; a family of anchoring proteins called AKAPs (A-kinase anchoring proteins) has been shown to tether protein kinase A (PKA) to centrosomes (Edwards and Scott, 2000). There is evidence that over expression of the FATZ proteins can inhibit calcineurin *in vitro*, which allows speculation that the FATZ family can serve as inhibitors or activators of calcineurin (Frey et al., 2000).

1.10.1 FATZ-1 (calsarcin-2, myozenin-1)

Human FATZ-1 was mapped to chromosome 10q22.1 (Faulkner et al., 2000). The FATZ-1 gene has six exons that encode for a 32 kD sarcomeric protein that is localized in the Z-disk. (Faulkner et al., 2000; Takada et al., 2001). This protein is expressed in skeletal muscle and to a lesser extent in heart; its expression is upregulated during differentiation (Frey et al., 2000). The human and mouse FATZ-1 proteins share a 90% identity (Faulkner et al., 2000).

Secondary structure predictions show that FATZ-1 has two alpha helical domains at the N-terminal (A1; 1-72 aa) and at the C-terminal (A2; 87-244 aa) regions, with a glycine rich region (in the middle between residues 95-175) and a short C-terminal tail of approximately 55 amino acids (Takada et al., 2001). These three regions, the two alpha helical and the glycine-rich, have also been named as CD1 (1-71 aa), CD2 (171-299 aa) and GRD (75-171 aa) respectively (Faulkner et al., 2000). As mentioned previously, FATZ-1 binds to several muscle proteins and some of these binding sites have been mapped; both α-actinin and filamin C bind to the full length FATZ-1 protein more particularly its to its C-terminal region (Faulkner et al., 2000). The FATZ-1 binding site on α-actinin-2 was mapped to the region that spans the SR3 and SR4 spectrin-like

repeats (431–719 aa) whereas FATZ-1 binds to filamin C at repeat 23.close to the C-terminal. (Faulkner et al., 2000; Takada et al., 2001). FATZ-1 also binds to telethonin (Faulkner et al., 2000), calcineurin and ZASP (Frey and Olson, 2002; Frey et al., 2000). Recently it was found that the C-terminal of FATZ-1 binds to myotilin. It was also shown that FATZ-1 was able to bind not only the C-terminal of filamin-C, but also to filamin-A, filamin-B and the newly discovered filamin-$_{Bvar-1}$ (van der Flier et al., 2002). From immunofluorescence experiments in CHO cells transfected with both FATZ-1 and myotilin it was noted that the punctuated distribution pattern of FATZ-1 was lost and that the double transfection pattern resembled that of myotilin. This indicates that myotilin might have a direct or an indirect effect in reorganizing the subcellular distribution of FATZ-1, it has also been shown that FATZ-1 and myotilin are localized in the Z-disk (Gontier et al., 2005).

Very recently two synonymous single nucleotide substitutions in FATZ-1 (Ser 50 and Leu 255) were found in the DNA of DCM patients. The DNA of these 185 unrelated DCM patients was amplified by PCR, analyzed by high performance liquid chromatography (DHPLC) and then the abnormal peaks were sequenced to detect any mutations. In the same study in one patient a 2-bp insertion (178insCA) in exon 2 of PDLIM3 was found that resulted in a stop codon (M60Tfs1X). The potential role of these mutations in the pathogenesis of DCM is still unknown however it was concluded that they do not play a significant role in the genetic etiology of the idiopathic DCM (Arola et al., 2007). However considering to the recent report of cardiac hypertrophy in patients as a result of mutations FATZ-2 (Osio et al., 2007) and given that the FATZ family members are part of an intricate network of interactions of Z-disk proteins mutations in FATZ-1 could play a secondary role in DCM.

1.10.2 FATZ-2 (calsarcin-1, myozenin-2)

FATZ-2 (calsarcin-1/myozenin-2) has been mapped on chromosome 4q26-q27. The FATZ-2 gene encodes a 264 amino acid protein, with a predicted molecular weight of 30 kDa (Frey et al., 2000). Human and mouse FATZ-2 have an 88% identity at the amino acid level. FATZ-2 is localised at the Z-disk and was shown to be expressed in skeletal and cardiac muscles during embryogenesis and development, and then expressed exclusively in adult cardiac muscles (Frey et al., 2000) . *In situ* hybridizations using FATZ-2 as a probe showed that it is predominantly expressed in heart muscles (Frey et al., 2000) however FATZ-2 is also expressed in skeletal muscle in slow-twitch fibres whereas FATZ-1 is present in fast-twitch muscle fibres (Frey et al., 2000). FATZ-2 is abundantly expressed in porcine heart with a pattern similar to that of the human FATZ-2, which suggests that pigs could be suitable models for studying the function of FATZ-2 in heart disease (Wang et al., 2006).

FATZ-2 binds to α-actinin-2, α-actinin-3, filamin C and the catalytic subunit of calcineurin (CnA). In Co-IP experiments CnA could only be immunoprecipitated with α-actinin in the presence of FATZ-2 which would suggest that these proteins form a trimeric complex (Frey et al., 2000). The C-terminal region (217-240) of FATZ-2 is important for the calcineurin binding. FATZ-2 and α-actinin-2 co-localise in the Z-disk and calcineurin is also localized in the Z-disk (Frey et al., 2000). Both FATZ-2 and FATZ-1 bind to ZASP, telethonin (Frey et al., 2004) and myotilin, (Gontier et al., 2005).

FATZ-2 is not required during embryogenesis and development since mice lacking FATZ-2 were normal and did not show any abnormalities. However in these mice the expression of calcineurin was increased supporting the idea that FATZ-2 negatively

modulates the activity of calcineurin. The up-regulation of calcineurin activated a foetal gene program associated with cardiac hypertrophy and although the hearts of FATZ-2 null mice showed no hypertrophy there was a marked induction of the foetal gene program genes, ANF and BNP, suggesting that they are regulated by calcineurin (Frey et al., 2004). In FATZ-2 deficient mice the Z-disks of the heart appeared fuzzy and wider than normal with a significant increase (36%) in diameter. FATZ-1 and FATZ-3 expression was not upregulated in the heart FATZ-2 null mice therefore they do not appear to compensate for the lack of FATZ-2 (Frey et al., 2004). To better understand the consequences due to the absence FATZ-2, transgenic mice expressing a constitutively active form of calcineurin in heart were bred with FATZ-2 null mice. Analyses of progeny hearts showed a high level of cardiac hypertrophy with an almost a fourfold increase in heart mass compared with normal mice. In addition calcineurin transgenic mice lacking FATZ-2 had a short lifespan and died by the age of 20-28 days (Frey et al., 2004).

Recently mutations in FATZ-2 gene were found to co-segregate with hypertrophic cardiomyopathy (HCM). These mutations were a T to C missense which gave rise to a S48P substitution in 6 family members affected with HCM and another missense mutation A to G giving rise to an I246M substitution. The mutations were only detected in individuals with HCM and not in controls and unaffected family members (Osio et al., 2007). This linking of FATZ-2 to a genetic cardiomyopathy is very interesting and the authors suggest that these FATZ-2 mutations cause HCM by up-regulating calcineurin and activating pathways controlled by calcineurin. However these mutations are not in the region of FATZ-2 known to bind calcineurin or α-actinin therefore they speculate structural changes may occur that affect the interactions. However they also

admit that there may be completely different reasons, such as FATZ-2 interacting with proteins other than calcineurin to cause this disease. Very recently it has been shown that the FATZ-2 transcription is mediated by the transcription factors NF-kB, NFAT and MEF2 (Wang et al., 2007).

1.10.3 FATZ-3 (myozenin-3/calsarcin-3)

Human FATZ-3 is located on chromosome 5 locus 5q31 and contains 7 exons spanning 19 kb (Frey and Olson, 2002). Two transcripts, one major (~ 3.5 Kb) and one minor (~ 4k b), were detected by Northern blot analysis in mouse whereas in human there appeared to be several transcripts (Frey and Olson, 2002). The gene encodes a protein of 251 amino acids with a predicted molecular weight of 27.6 kD. In the NCBI database there are two other isoforms of FATZ-3 noted; isoforms A and B, respectively 87 and 205 amino acids. Human and mouse FATZ-3 share a 75% identity at the amino acid level. Both in human and the mouse FATZ-3 is specifically expressed in skeletal muscle and there is no detectable expression in cardiac muscle. FATZ-3 is expressed in mainly in fast-twitch fibres and co-localizes with α-actinin in the Z-disk (Frey and Olson, 2002).

FATZ-3 binds to several proteins including calcineurin, α-actinin-2, filamin C, ZASP and telethonin. The binding sites of calcineurin, α-actinin-2, ZASP and telethonin map to the same region of FATZ-3, an N-terminal region, between amino acids 50 and 67. However α-actinin-2 has another binding region between amino acids 186 and 207 and filamin C binds to the region between amino acids 67 and 110 (Frey and Olson, 2002). FATZ-3 as well as FATZ-1 and FATZ-2 binds both the short (without the LIM domains) and the long isoforms (with LIM domains) of ZASP/Cypher (Frey and Olson,

2002). It is notable that the FATZ family including FATZ-3 lack known interaction domains yet are able to bind so many different proteins. Since the N and C- terminal regions of all the FATZ proteins are the most highly conserved regions between the family members it is probable that these regions are the main sites of protein-protein interaction.

1.11 The Enigma family

The Enigma family of proteins is comprised of proteins that possess a PDZ domain at the N-terminal and one to three LIM domains at the C-terminal and are associated with the cytoskeleton and involved in signal transduction pathways. There are two subclasses of the Enigma family defined by the number of LIM domains; the Enigma subfamily: Enigma, Enigma homology protein (ENH) (Kuroda et al., 1996) and ZASP/Cypher (long isoforms have three LIM domains; short isoforms have no LIM domains); the ALP subfamily: comprising of RIL (Kiess et al., 1995), CLP36 (Wang et al., 1995), and actin-associated LIM protein (ALP) (Xia et al., 1997) have one LIM domain. All members have one N-terminal PDZ domain with a high degree of sequence identity, the PDZ domains of Enigma and RIL, CLP36, and ALP are 42, 47, and 44% identical (fig 4). The PDZ domains of the Enigma Family members are distinguished by the amino acids P/S and W in place of G and L in the "GLGF" signature sequence of PDZ domains, that is PWGF whereas ALP has SWGF sequence instead of PWGF (Guy et al., 1999).

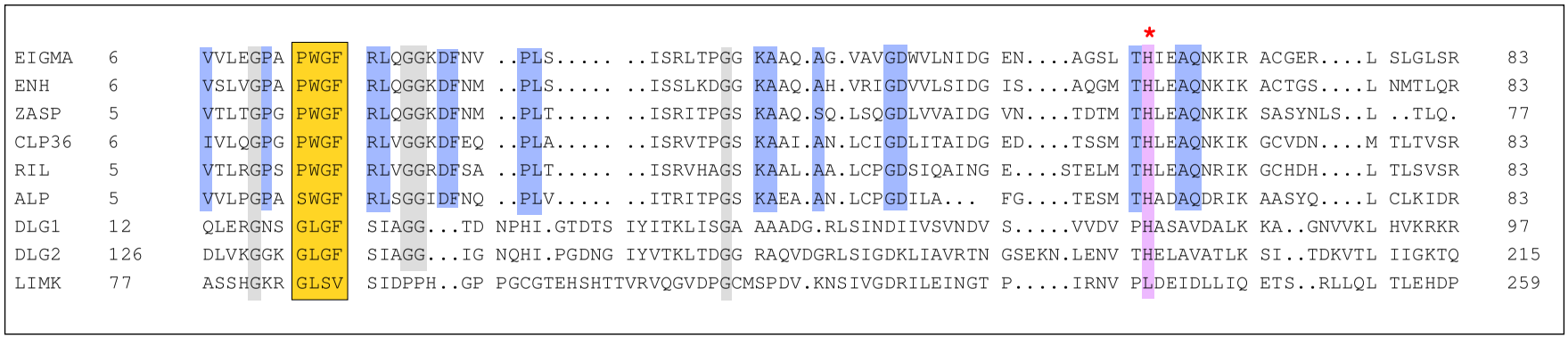

Figure 4. A diagram representing the sequence alignment of the amino acids of the PDZ domains of the ENIGMA family of proteins as well as the DLG and LIMK proteins. The yellow colour highlights the four amino acids that form the carboxylate binding loop GLGF; these are present in the ENIGMA family as PWGF except for ALP which is SWGF. The purple color highlights the histidine which is a conserved amino acid in most of the PDZ domains and is located at position 63 in the ENIGMA family of proteins; the gray color highlights the similarity between the PDZ domains of the ENIGMA family and those of DLG1, DLG2 and the LIMK. The blue colour highlights the sequence similarity between the PDZ domains of the ENIGMA family. (figure modified from Guy et al., 1999).

1.11.1 Enigma

ENIGMA is also known as LIM mineralization protein (LMP), PDZ and LIM domain protein 7 (PDLIM7). Enigma is expressed in brain and skeletal muscle, where it localizes in the Z-disk (Guy et al., 1999). In cultured cells it is detected in the cytoplasm and membrane ruffles rich in actin filaments (Barres et al., 2005; Borrello et al., 2002). The Enigma protein is known to interact and co-localize with the short isoform of RET/PTC2, a chimeric oncoprotein isolated from papillary thyroid carcinoma and also with the short isoform of RET-wt and of its mutants (RET-C634R and RET-M918T) that are linked with multiple endocrine neoplasia (MEN2) syndrome. However Enigma binds very poorly and does not co-localize with the long isoforms of RET (Borrello et al., 2002)

1.11.2 Enigma homologue protein (ENH)

The name ENH comes from the high level of homology that is shared between the ENH and enigma protein, there is a 37% identity between the two proteins (Kuroda et al., 1996). ENH is expressed in heart and skeletal muscle (Kuroda et al., 1996). It interacts with α-actinin through its PDZ domain and colocalizes with it at the Z-disk (Nakagawa et al., 2000; Niederlander et al., 2004). The LIM domains of EN bind to protein kinase C ß (PKCß) (Nakagawa et al., 2000). ENH is expressed also in various cancer cell lines (Nakagawa et al., 2000).

There are four isoforms of ENH: ENH1, ENH2, ENH3 (Kuroda et al., 1996) and ENH4 that was discovered later (Niederlander et al., 2004). All four isoforms have an N-terminal PDZ domain however only ENH1 has three LIM domains at the C-terminal, while the other isoforms lack the LIM domains. This is similar to ZASP/Cypher that has

isoforms with and without LIM domains. The distribution pattern of different isoforms is specific, the short ENH4 isoform is expressed only in skeletal muscle, the ENH3 isoform both in skeletal and cardiac muscle, the ENH2 isoform in skeletal and ENH1 isoform in cardiac muscle (Kotaka et al., 1999; Niederlander et al., 2004).

1.11.3 ALP (Actinin associated LIM protein)

ALP is a 39kDa muscle protein containing an N-terminal PDZ domain and a C-terminal LIM domain. Genetic mapping studies showed that ALP is located at the 4q35 locus on chromosome 4. It is found to be highly expressed in differentiated skeletal muscles, enriched in smooth muscle tissues such as arteries and a splice isoform is expressed at a low level in heart. (Xia et al., 1997). The ALP isoform in skeletal muscle (ALP_{SK}) contains a central exon encoding 112 amino acids, which in the heart isoform (ALP_H) is replaced by an exon encoding only 64 amino acids.The ALP-PDZ domain is 75 amino acids and shares a 55 %, 48 % and 45 % amino acid identity with the PDZ domains of CLP-36, RIL, and enigma respectively whereas the LIM domain of ALP shares a higher homology with the LIM domains of CLP36 and RIL about 67% (Xia et al., 1997). ALP also has a third domain which is the ZM motif that is also present in CLP-36 and ZASP (Klaavuniemi et al., 2004). Recently a third isoform of ALP has been found in zebrafish but this lacks the ZM motif (Te Velthuis et al., 2007).

Studies using cultured myoblasts showed that the PDZ domain of ALP binds to the spectrin-like motifs of α-actinin-2, whereas the ZM motif of ALP was responsible for the interaction of ALP with the rod domain of alpha-actinin-2 and its localization at the Z-disk (Klaavuniemi et al., 2004). A mutation in the PDZ domain (L78K) abolished the binding of the PDZ domain to alpha-actinin (Xia et al., 1997) when the PDZ domain

was used alone whereas when the full length ALP protein was used in binding experiments this mutation (L78K) only reduced the binding with alpha-actinin-2 to 87% (Henderson et al., 2003). Immunostaining of intact myocardium showed that ALP is present in the intercalated discs, where it binds to α-actinin and γ-catenin. Disruption of the ALP gene causes right ventricular (RV) chamber dilation and dysfunction (Pashmforoush et al., 2001).

1.11.4 RIL (Reversion induced protein)

The reversion induced protein (RIL) was first discovered in mice by (Kiess et al., 1995) It is located on human chromosome locus 5q31.1 and has seven exons that code for 330 amino acid protein. It is expressed in brain and lung and in a variety of cultured cells lines but not in muscle (Bashirova et al., 1998; Kiess et al., 1995; Schulz et al., 2004; Vallenius et al., 2004). RIL localizes in dendritic spines in cultured neurons (Schulz et al., 2004) and along stress fibres (Vallenius et al., 2004). It has an N-terminal PDZ domain (4-84 aa) and a C-terminal LIM domain (253-303 aa) (Bashirova et al., 1998; Cuppen et al., 1998; Kiess et al., 1995). A remarkable point about RIL is that its PDZ can bind to its LIM domain. RIL contains a tyrosine phosphorylation site ([RK]-(2,3)-[DE]-x(2,3)-Y) within the LIM domain (Y-274), and it has been shown that the LIM domain of RIL can be phosphorylated by tyrosine *in vitro* and *in vivo,* and can be dephosphorylated *in vitro* by the PTPase domain of protein tyrosine phosphatase (PTP-BL) (Cuppen et al., 1998). It is expressed in brain and heart of adult mice. In brain there is another isoform of RIL encoded by a transcript lacking exon six, the exon that codes for the LIM domain (Bashirova et al., 1998; Kiess et al., 1995). There is a high (96%) identity between mouse and human RIL.

The C-terminal of RIL can bind to the second and the fourth PDZ domains of PRP-BL (which contains five PDZ domains). Surprisingly deleting the last four amino acids of RIL did not affect its binding to the PDZ II and PDZ IV domains of PRP-BL. This is an unusual characteristic as PDZ domains usually bind the last four amino acids of the C-terminal their binding proteins (Cuppen et al., 1998). RIL binds to α-actinin and localizes to actin stress fibres as does CLP-36 and also enhances the binding of α-actinin to actin filaments suggesting that RIL has a role in modulating actin stress fibre dynamics through its binding to α-actinin (Vallenius et al., 2004).

RIL has been found to be deleted in patients with myelodysplasia and myeloid leukemia (Bashirova et al., 1998). Recently, it was found that RIL was highly methylated in 60% of patients (55 out of 92) with acute myeloid leukemia (AML) and colon cancer, whereas in normal tissues RIL was not or only poorly methylated. These data lead to the speculation that RIL could be a good candidate for a tumour suppressor gene (TSG) silenced by hypermethylation (Boumber et al., 2007).

1.11.5 CLP-36 (hCLIM1, Elfin)

C-terminal LIM domain protein (CLP) (Wang et al., 1995) also known as, human 36-kDa carboxyl terminal LIM domain protein (hCLIM1) (Kotaka et al., 1999) and Elfin (Kotaka et al., 2001), is a 36kD protein first discovered in rat. CLP-36 is highly expressed in heart, lung and liver, moderately in spleen and skeletal muscle and at low levels in testis and brain tissue (Wang et al., 1995). CLP-36 belongs to the Enigma family of proteins, it has an N-terminal PDZ domain (1-89 amino acids) as well a LIM domain at the C-terminal region (258-310 amino acids). It also shares an overall identity of 41.1% with the rat RIL protein (Kiess et al., 1995; Wang et al., 1995).

The rat CLP-36 shares an 87.8% homology at the amino acid level with the human CLP-36 (hCLlM1). FISH and radiation hybrid experiments showed that the human HCLIM1 gene maps on chromosome 10, position 10q36 (Kotaka et al., 1999). The CLP-36 protein belongs to the ZM motif family, as it contains a central ZM motif between the PDZ and the LIM domains (Klaavuniemi et al., 2004).

In the epithelial cells the LIM domain of CLP-36 binds to C-terminal EF hand region of α-actinin-1 and -4. Analyses such as immunoprecipitation and matrix-assisted laser desorption/ionization time-of-flight mass spectrometry indicate that both α-actinin-1 and α-actinin-4 form complexes with CLP-36. The CLP36-LIM domain also binds to the C-terminal EH-hand region of α -actinin-2; this interaction is localized at the Z-disk and is abrogated when the LIM domain is truncated. On the other hand the PDZ domain of CLP-36 binds to the spectrin-like repeats of all the α-actinin isoforms (Bauer et al., 2000; Kotaka et al., 2000; Vallenius et al., 2000). Vallenius and colleagues have shown that by deleting the first 24 amino acids of the CLP-36 PDZ domain they can eliminate the binding of CLP-36 to α-actinin and consequently its localization to stress fibres (Vallenius et al., 2000). Another binding protein of CLP-36 is vinculin; a protein that serves as an anchor for actin and actin-binding proteins in the cell membrane. Vinculin and CLP-36 colocalize at the intercalated disks that are the specialized regions of the plasma membrane that connect the cardiac muscle cells. The interaction and localization of CLP-36 and vinculin is thought to be mediated via the interactions of the two proteins to α-actinin (Kotaka et al., 2000).

1.11.6 ZASP/Cypher/Oracle

Z-disk alternatively spliced PDZ motif protein (ZASP) (Faulkner et al., 1999) is also known as Cypher (Zhou et al., 1999) or Oracle (Passier et al., 2000) in mice. ZASP is a 32 kD protein that maps on chromosome 10q22.3-10q23.2. The protein is highly expressed in skeletal and to a lesser extent in heart muscles in embryonic and adult tissue. Immunostaining experiments showed that ZASP is localized in the Z-disk (Faulkner et al., 1999). ZASP belongs to the Enigma family of proteins, the members of which all have a N-terminal PDZ domain and one or more LIM domains at the C-terminal (Te Velthuis et al., 2007). The human ZASP gene consists of 16 exons and has several isoforms; to date six isoforms have been found C1/Z1, C/Z2, C/Z3, C/Z4, C/Z5 and C/Z6. The human isoforms 2 to 5 contain both an N-terminal PDZ and three C-terminal LIM domains whereas isoforms 1 and 6 contain only the PDZ domain. The PDZ domain of ZASP is encoded by exons 1, 2 and 3, while the LIM domains are encoded by exons 12-16 (Vatta et al., 2003). The ZASP isoforms containing exon 4 are expressed in cardiac muscle, whereas the isoforms containing exon 6 are expressed in skeletal muscle (Huang et al., 2003). ZASP also contains a third domain known as the ZM motif which is encoded by exons 4 and 6 (Klaavuniemi et al., 2004).

ZASP interacts with α-actinin in two different regions, the PDZ of ZASP binds to the EH-hand region of the C-terminal of α-actinin whereas the ZM motif that binds to the rod region of α-actinin. ZASP co-localizes with α-actinin in the Z-disk whereas the LIM domains interact with and are phosphorylated by all 6 isoforms of protein kinase C (PKC α, ß1, γ, ζ, δ, and ε), and ZASP is by PKC (Klaavuniemi and Ylanne, 2006; Zhou et al., 1999).

ZASP is important for the stability of the Z-disk. In fact, ZASP knockout mice die in the first 24 hour after birth from a severe form of congenital myopathy as a result of functional failure of striated muscles, these mice also showed symptoms of heart failure. The structure of the Z-disk was analyzed in ZASP null mice; contracting skeletal and cardiac muscle tissue showed abnormality in the Z-disk, while a normal structure was found in the non-contracting embryonic diaphragm muscles. These observations suggested that although ZASP may not be required for the formation of protein complexes during sarcomerogenesis, it is however essential in maintaining Z-disk stability during muscle contraction (Zhou et al., 2001). Mutations in exon 4 of ZASP gave rise to mutations in the ZASP protein (T213I and S196L) found in patients with isolated non-compaction of the left ventricular myocardium (INLVM) whereas mutations in exon 6 resulted in mutations (D117N and K136M) in the ZASP protein found in patients with INLVM and DCM. Both sets of mutations were located in the region coding for the ZM motif (Klaavuniemi et al., 2004; Vatta et al., 2003).

The PDZ of ZASP is a classical class I PDZ domain which binds to the C-terminal of aα-actinin-2 (calmodulin-like domain/ EF-hand region). The ZASP-PDZ domain consists of 85 amino acids and the crystal structure shows a high similarity with the third PDZ domain of the human disk large protein (DlgA). The structure of the ZASP PDZ domain is similar to other PDZ domains in that it consists of 6 beta sheets and 2 alpha helices organized as follow (ß1, ß2, ß3, α1, ß4, ß5, α2 and last ß6). ß2 and α2 form the groove that starts from the conserved 'PWGF' loop (residues P9, W10, G11 and F12) in the PDZ domain of human ZASP and (residues P11, W12, G13 and F14) in the PDZ domain of Cypher, the mouse form of ZASP. The ZASP PDZ domain contains a unique tryptophan at the N-terminal portion of ß2. This groove is the active site for

interaction in PDZ class I and it is the site of the interaction between the α-actinin C-terminal region and the ZASP-PDZ domain (Au et al., 2004). It has also been shown that a mutation in the PDZ of ALP (L78 to K78) abolished its binding with α-actinin (Xia et al., 1997). Therefore mutations were made in the PDZ region of Cypher in order to study in more detail its interaction with α-actinin; these mutations were G14 to A14, F15 to A15 and L76, L77 and L78 to K (Au et al., 2004; Zhou et al., 2001). These mutations managed to disrupt the binding of Cypher with α-actinin and hence its localization in the Z-disk (Zhou et al., 2001) indicating that the mutations may disrupt the folding of the Cypher PDZ domain .

1.12 PDZ domains

PDZ proteins were first recognized as a group of proteins found at cell-cell junctions that had a common structural domain of 80-90 amino acid residues named PDZ for the first identified three proteins **P**SD-95 (a 95 kDa neuronal PDZ protein that associates with receptors and cytoskeletal elements at synapses), **D**lg (the *Drosophila melanogaster* Discs large protein), and **Z**O-1 (the zonula occludens 1 protein that is involved in maintenance of epithelial polarity) (Cho et al., 1992; Kim et al., 1995; Woods and Bryant, 1993) Originally the domain was known as Discs-large homology regions (DHRs) or GLGF repeats since there are four highly conserved residues within the domain (Gly-Leu-Gly-Phe) (Hung and Sheng, 2002). The PDZ domains have been found in a wide variety of proteins from bacteria to mammals, they are usually around 90 kDa and are involved in protein-protein interactions normally binding proteins through their C-terminals (last 4 to 6 amino acids) but in some cases they can also bind internal regions of proteins (Bezprozvanny and Maximov, 2001).

SMART (a simple modular architecture research tool) database lists about 1,163 PDZ domains in 484 human proteins, 259 PDZ domains in 153 *Drosophila melanogaster* proteins, 130 PDZ domains in 95 *Caenorhabditis elegans* proteins and 26 PDZ domains in 23 *Arabidopsis thaliana* proteins while there are only 3 PDZ-like domains in *Saccharomyces cerevisiae* and 5 in *Escherichia coli* (Schultz et al., 2000). PDZ domains also exists in plants but they are quite rare (Venter et al., 2001) and it has been suggested that PDZ-like domains may have entered the plant and bacterial genomes by horizontal genetic transfer (Pallen and Ponting, 1997). It is interesting that the PDZ-like domains in plants and bacteria share a similar secondary and tertiary structure but have different topology (Hung and Sheng, 2002).

PDZ domains can occur as a single copy within the protein such as (Veli1 and ZASP) or as multiple copies, which is the most common form of PDZ containing proteins. The number of PDZ copies can reach up to 13 as for example in MUPP1 (multi-PDZ domain protein1) (Harris and Lim, 2001). One of the speculations regarding the existence of multiple PDZ domains in a single protein, is that this multiplicity can serve as a (glue) binding different proteins simultaneously to form supramolecular complexes that can serve in cell signalling and protein targeting (Schultz et al., 1998).

1.12.1 Structure and binding characteristics of PDZ domains

In a review Huang and Sheng, give an overview of X-ray crystallographic studies of PDZ domains in complex with their cognate peptide ligands a method that enabled the identification of the structural basis for the binding specificity of PDZ domains (Hung and Sheng, 2002). The first solved PDZ domain crystal structure was that of the PDZ3 domain of PSD-95 (Doyle et al., 1996) followed by other PDZ structures, such as PDZ2

of PSD-95, the PDZ of CASK, syntrophin, Neuronal nitric oxide synthase. These structures of these proteins were solved by x-ray crystallography and/or NMR (Hung and Sheng, 2002). The general structure of the PDZ domain consists of six beta sheets (ßA- ßB- ßC- ßD- ßE and ßF) and two alpha helices (αA and αB). The six beta sheets fold as a beta sandwich domain. The N- and C-terminals of the PDZ domain are close to each other in the folded structure, which makes these domains highly modular and raises the speculation that these domains could have entered existing proteins without any significant structural change during evolution (Harris and Lim, 2001). Both the ßB and the αB of the PDZ domain form a groove in which the end of the peptide or the C-terminal of the protein bind as an anti parallel beta sheet (Fig 5). This mechanism is known as beta strand addition (Harrison, 1996). Structural analyses of both the free and complexed peptide of the PDZIII of PS D-95 show that both forms are almost identical therefore the binding of the peptide does not change the structure of PDZ domains (Doyle et al., 1996). Between the ßA and the ßB sheets there is a conserved loop (R/K-XXX-G-ΦGΦ or GLGF motif) which creates a hydrophobic cavity that surrounds the C-terminal of the binding protein. Studies have shown that in some PDZ domains the first glycine of the GLGF motif can be substituted by a threonine or a serine but the second glycine is highly conserved (Jelen et al., 2003).

1.12.2 Why do PDZ domains bind specifically to the C-terminal of proteins?

The PDZ domain structure is folded in a way that is suitable for binding to a free carboxylate group at the end of the binding protein or peptide. The ßA and ßB are connected to each other through a loop which contains a highly conserved arginine or lysine residue (at position 318 in PDZ3 of PSD-95) of the Gly-Leu-Gly-Phe (GLGF)

sequence motif, this loop is also known as "carboxylate-binding loop". Through this loop both ßA and ßB form a pocket which has hydrophobic characteristics that surrounds the C-terminal of the peptide. The GLGF motif contains three main-chain amide protons that form hydrogen bounds with the C-terminal of the binding protein or ligand plus the guanidinium group of arginine at position 318 interacts with the carboxylate anion via a water molecule (Doyle et al., 1996). "*Since a free carboxylate binding group only exists at the very end of the polypeptide chain, the interactions between the carboxylate-binding loop and the carboxylate oxygens form the structural basis for the PDZ recognition of C-terminal peptides*" (Sheng and Sala, 2001). The pocket that is formed by the ßA and the ßB sheets with the carboxylate binding loop in the middle is generally hydrophobic in many PDZ domains, which makes it common that most if not all PDZ domains select a peptide with a hydrophobic C-terminal. In the case of the PDZ 3 domain of PSD-95, valine is the preferred amino acid at position 0 the last reside of the peptide (Niethammer et al., 1998). The amino acid at position 0 varies between different PDZ domains; this is due the differences in the size and geometry of the hydrophobic pocket in these domains. Normally valine, leucine, isoleucine, phenylalanine or alanine are found at position 0 of the PDZ binding peptide (Songyang et al., 1997). However the hydrophobic amino acid at the end of the peptide is not always selective as is the case of the PDZ domain of PSD-95, it can bind as well to a peptide that ends with an isoleucine or leucine even if the preferred amino acid is valine (Cohen et al., 1996; Songyang et al., 1997).

Not only is position 0 important or crucial for the interaction with PDZ domains, position 2 is also very important and plays a big role in the classification of PDZ domains. For example the PDZ domains of PSD-95 and some other PDZ proteins select

a threonine or serine at position 2. The crystal structure of this domain shows that the threonine at position 2 forms strong hydrogen bound with the N-3 nitrogen of histidine-372, which is in the first position of the αB1. This bond can also occur with the serine at position 2 of the peptide. These type of PDZ domains are classified as PDZ class I. Proteins containing class II PDZ domains such as LIN-2/CASK and p55 have valine instead of histidine at position αB1 which preferentially binds to a phenylalanine or tyrosine at position 2 of the peptide (Songyang et al., 1997). For class III PDZ domains such as nNOS, the domain contains a tyrosine at the αB1 position that selects for negatively charged amino acids at position 2 of the C-terminal of the ligand such as aspartate (Stricker et al., 1997; Tochio et al., 1999). Positions 1 and 3 of the PDZ binding peptide are predicted to have an influence on the specificity of the PDZ domain binding but not as strong as that of positions 0 and 2 (Sheng and Sala, 2001). For example; substitution of D for S (–QT**S**V to –QT**D**V) at position 1 of the CRIPT C-terminal protein changed the binding of the peptide from a PDZ III to a PDZ II (Niethammer et al., 1998). Position 3 of the CRIPT protein which contains glutamine (**Q**TSV) forms hydrogen bounds via its oxygen with the residues Asn-326 ßB2 and Ser-339 ßC4 in the PDZ domain of PSD-95 (Doyle et al., 1996). Even though the glutamine at position 3 interacts with two amino acids on the PDZ domain (Asn-326 ßB2 and Ser-339 ßC4), position 3 is not as critical as position 2 for binding to PDZ domains (Songyang et al., 1997). Not only positions 0, 1, 2 and 3 influence the binding, it has also been demonstrated that positions up to 8 can influence the binding of the C-terminal to PDZ domains (Kozlov et al., 2000; Niethammer et al., 1998; Songyang et al., 1997).

PDZ domains in some rare cases can bind to internal sequences however this can occur only if these sequences form a specific tertiary structure that mimics a chain terminus. The best studied example of this is the interaction between the PDZ domain of nNOS and the PDZ domain of either syntrophin or PSD-95. The internal sequence of the nNOS PDZ domain forms a heterodimer with either the PSD-95 or the syntrophin PDZ domain. This occurs because the nNOS PDZ domain contains a 30 residue extension, which forms a ß-hairpin structure that can dock inside the peptide binding pocket of the syntrophin or the PSD-95 PDZ domain, forming an unusual head-to-tail interaction (Christopherson et al., 1999).

1.12.3 Classification of PDZ domains

PDZ domains can be classified using two different approaches. The first type of classification is based on the sequence of the ligand or the C-terminal of the binding protein. Through that approach PDZ domains were classified into three different classes; PDZ I, II, and III and as mentioned above, position 2 is very important for this type of classification. In class I PDZ domain proteins, for example PSD-95, Dlg and ZO1, the amino acids serine or threonine are usually found at position 2 and the binding peptide sequence is **X-[S/T]-X-Φ** (where Φ is any hydrophobic amino acid and X is any amino acid). Class II PDZ domain proteins, for example PICK2 and CASK (calcium/calmodulin-dependent serine protein kinase), usually have a hydrophobic residue at position 2 and a common binding peptide sequence of **X-Φ-X-Φ** (Songyang et al., 1997). PDZ class III proteins which include nNOS (neuronal nitric oxide synthase) have a preference for a negatively charged residue on the position 2 of the binding peptide, the common motif being**-X-[D/E/K/R]- Φ** (Stricker et al., 1997). In

some cases PDZ domains are able to bind to peptides from two different classes indicating that these classifications are still far from being perfect. For example syntenin, a 32kDa protein that interacts with many cell membrane receptors, contains two PDZ domains, the PDZI domain is able to bind peptides from class I and III, while the PDZ2 domain is able to bind peptides from classes I and II (Kang et al., 2003).

The classification used by the Eukaryotic Linear Motif (ELM) resource for predicting functional sites in eukaryotic proteins also depends on the last four amino acids of the PDZ binding peptide and is quite similar to that outlined above only more precise in choosing the sequence of the four amino acids (www.elm.eu.org). This program uses the **-X-[S/T]-X-[VIL]** motif for ligands binding to class I PDZ domains, the **-X-[VYF]-X-[VIL]** motif for ligands binding class II PDZ domains and the **-X-[DE]-X-[VIL]** motif for ligands biding to class III PDZ.

The second approach of classification is based on the two critical positions of the PDZ domain; the first position is that of the amino acid immediately following the second ßB strand referred to as Pos1 and this is usually a glycine (G). The second critical amino acid position is the first position in the second αB helix designated as Pos2; this is usually a histidine (H). Based on this approach and by analyzing the PDZ domain protein listed in the SMART database (http://smart.embl-heidelberg.de) Bezprozvanny and Maximov, classified the PDZ domains into 25 different groups based on the polarity and/or bulkiness of these two amino acids (Bezprozvanny and Maximov, 2001). However Vacarro and Dente (Vaccaro and Dente, 2002) have shown that this type of PDZ domain classification based on only the two conserved amino acids in the hydrophobic pocket is difficult, especially since there are other positions involved in the

recognition of the binding peptide. Two of the 25 groups did not correspond to any known PDZ domains, (G, n) and (a, p) that should have Glycine (Pos1) and a negative amino acid (Pos2) and an aromatic amino acid (Pos1) and a polar amino acid (Pos2), respectively. Another problem is that of the remaining 23 groups only 9 had known ligand sequences. Of these one corresponded to PDZ domain proteins classified as binding to class I motifs, this group had G at Pos1 and H at Pos2. Four groups can be unified as PDZ class II and one group includes PDZ domains that are known to have dual specificity (Vaccaro and Dente, 2002). Vacarro and colleagues have shown experimentally that the substitution of the histidine in the crucial position αB (Pos 1) of hINADL-7 (class I binding PDZ domain) is not sufficient to change its binding specificity and ligand preference (Vaccaro and Dente, 2002). In order to classify PDZ domains on the basis of their hydrophobic pocket it is important to consider all the positions that are responsible and can influence the binding plus the corresponding sequence of the ligands. In conclusion, it would appear that the classification of PDZ domains and the specificity of their ligands are still not very clear and it will require further experimental and bioinformatics studies to be done.

1.12.4 The effect of phosphorylation on C-terminus binding

Most ligands that bind PDZ domains have a serine, threonine or tyrosine reside at the position 2 or 3 of the peptide. I have mentioned before that these positions are important for the interaction between the ligand and the PDZ domain, especially position 2. The phosphorylation of the amino acids in these positions can affect the binding positively or negatively. For example: PKA kinase phosphorylation of the amino acid at position 2 of the C-terminus of the inward rectifier K channel (Kir 2.3) protein resulted in

disruption of the binding of this protein with the PDZ domain of PSD95 (Cohen et al., 1996). On the other hand, recent studies demonstrated that phosphorylation can also increase the strength of the interaction. Phosphorylation of the C-terminal peptide of the mitochondrial ribosomal protein MRP2 increased its binding to the three different PDZ-containing proteins PDZK1 (PDZ domain containing-protein), IKEPP (intestinal and kidney enriched PDZ protein) and EBP50 (ezrin-radixin-moesin binding phosphoprotein-50) (Hegedus et al., 2003). Normally in proteins with internal PDZ domains either hetero or homo interactions occur usually between PDZ domains of the same protein, for example, the PDZ 3 and 4 of INAD can bind to each other and form homo-dimers (Xu et al., 1998).

1.12.5 The multiplicity and function of PDZ domains

As mentioned above, PDZ domains can occur as a single copy as in ZASP, RIL and Veli1 or as multiple copies in the same protein normally as tandem repeats one after the other. It has been shown that 18% of the human PDZ-domain containing proteins have three or more PDZ domains in the same protein, the highest number being in the MUPP1 protein that contains 13 PDZ domains. PDZ containing proteins can also contain other domains in the same protein such as LIM domains as in the Enigma family of proteins (Harris and Lim, 2001) (Fig 6).

Based on experimental data several hypotheses have been made regarding the frequency of PDZ domains. For example, syntenin that has two PDZ domains in tandem needs both for binding other proteins. The PDZ2 domain of syntenin can bind the C-terminal of syndecan, neurexin, and ephrin-B1 but only with the help of PDZ1 or another copy of PDZ2 but not alone (Grootjans et al., 2000). In this case it appears that multiplicity is

crucial for binding. Another study showed that some PDZ domains can play a role in influencing the folding of an adjacent PDZ domain. For example, nuclear magnetic resonance (NMR) and circular dichroism spectroscopy (CD) experiments showed that when alone the PDZ5 domain of GRIP was unstructured and lost its binding with GluR2. However when PDZ5 was connected with the PDZ4 domain of GRIP it became highly structured and the binding with GluR2 was restored (Zhang et al., 2001). It has been suggested that multiple PDZ domains can allow a protein to bind several other proteins simultaneously, thereby assembling large proteins complexes (Harris and Lim, 2001; Sheng and Sala, 2001). PDZ-based complexes are often localized to specific subcellular compartments where PDZ-based scaffolds have been shown to organize signal transduction pathways. For example, the photo-transduction pathway in *Drosophila*, where ion channels and signalling molecules are co-assembled by the multi-PDZ protein InaD (Montell, 1998; Tsunoda and Zuker, 1999). The first human disease related to a mutation in a PDZ domain was the Usher syndrome type 1C, an autosomal recessive disorder characterized by congenital sensorineural deafness, vestibular dysfunction, and blindness (Montell, 2000; Verpy et al., 2000). In a very recent study it was found that the over expression of the PDZ domains of syntenin (2 PDZ domains) increased cancer cell invasion *in vitro*. Therefore syntenin could be a potential biomarker and drug target for breast, gastric and melanoma cancer (Meerschaert et al., 2007). An *in vitro* study on the ZASP/Cypher protein showed that mutations (G14A, F15A and L78K) in its PDZ domain blocked its binding with α-actinin 2 therefore it was no longer able to co-localize in the Z-disk with α actinin 2 but rather showed a diffused pattern inside the cell. This demonstrates the role of PDZ

domains in binding and localizing proteins to different subcellular regions (Zhou et al., 2001).

PDZ domain proteins can also contain other domains such as LIM, SAM, SH3, CaM, GUK and ankyrin repeats (Jelen et al., 2003). A recent study on PDZ/LIM family proteins noted that there are ten mammalian PDZ proteins that contain both PDZ and several LIM-domains. These proteins are members of the Enigma family proteins [ALP, RIL, Elfin (CLP36), Mystique, Enigma (LMP-1), enigma homologue (ENH), ZASP (Cypher/ Oracle)], LMO7 and the two LIM domain kinases (LIMK1 and LIMK2) (Te Velthuis et al., 2007). It has been suggested that cytoskeletal proteins belonging to the PDZ-LIM family serve as adapters for direct binding of LIM- proteins to the cytoskeleton (Vallenius et al., 2000). The precise function of PDZ domains is still not clear and also their classification needs to be better defined. Studies to-date on PDZ proteins definitely show that they have an important role in multiple protein-protein and in creating supramolecular complexes which are involved in cell signalling and subcellular localization.

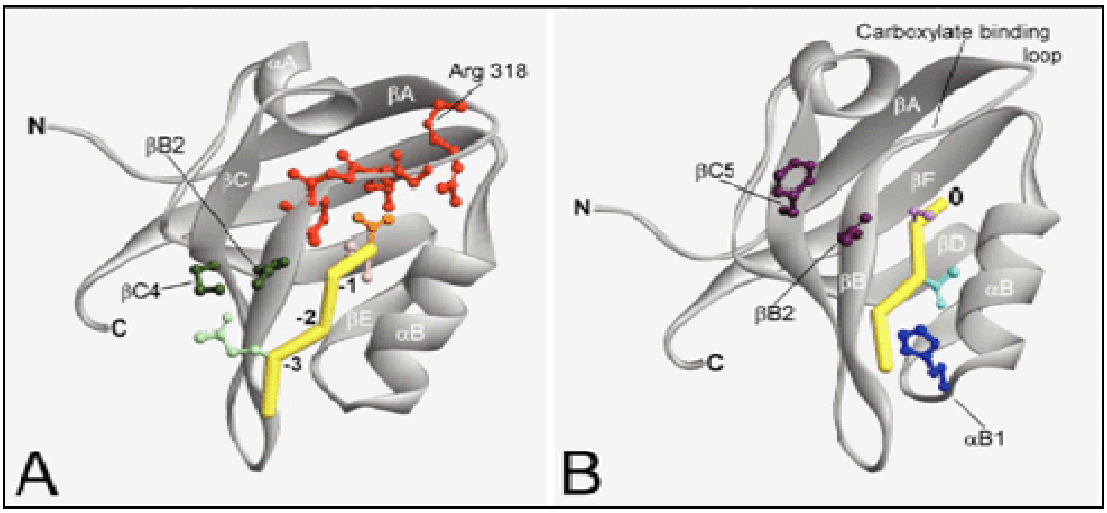

Figure 5. The structure of a PDZ domain complexed with a C-terminal peptide ligand, based on PDZ3 of PSD-95 complexed with CRIPT (Doyle1996; Niethammer 1998). The ribbon diagram of the PDZ domain (gray) is shown bound to the peptide ligand (yellow). The structures in A and B are slightly rotated relative to each other to show particular sets of interactions. A. The free carboxylate group (orange) of the C-terminal residue (0 position) of the peptide interacts with the conserved amino acids (Arg-318 and G-L-G-F) of the carboxylate binding loop (red). The side chain of the -3 residue (glutamine; light green) interacts with βB2 (asparagines, red) and βC4 (serine; dark green). B. The hydroxyl group of the -2 residue (threonine; light blue) interacts with the side chain of αB1 (histidine; dark blue). The side chain of the -1 residue (serine; light purple) of the CRIPT peptide shows no interactions with the PDZ domain. However, ¯B2 and ¯C5 residues (dark purple) are likely to influence selectivity at the -1 position of the peptide ligand (Sheng and Sala, 2001).

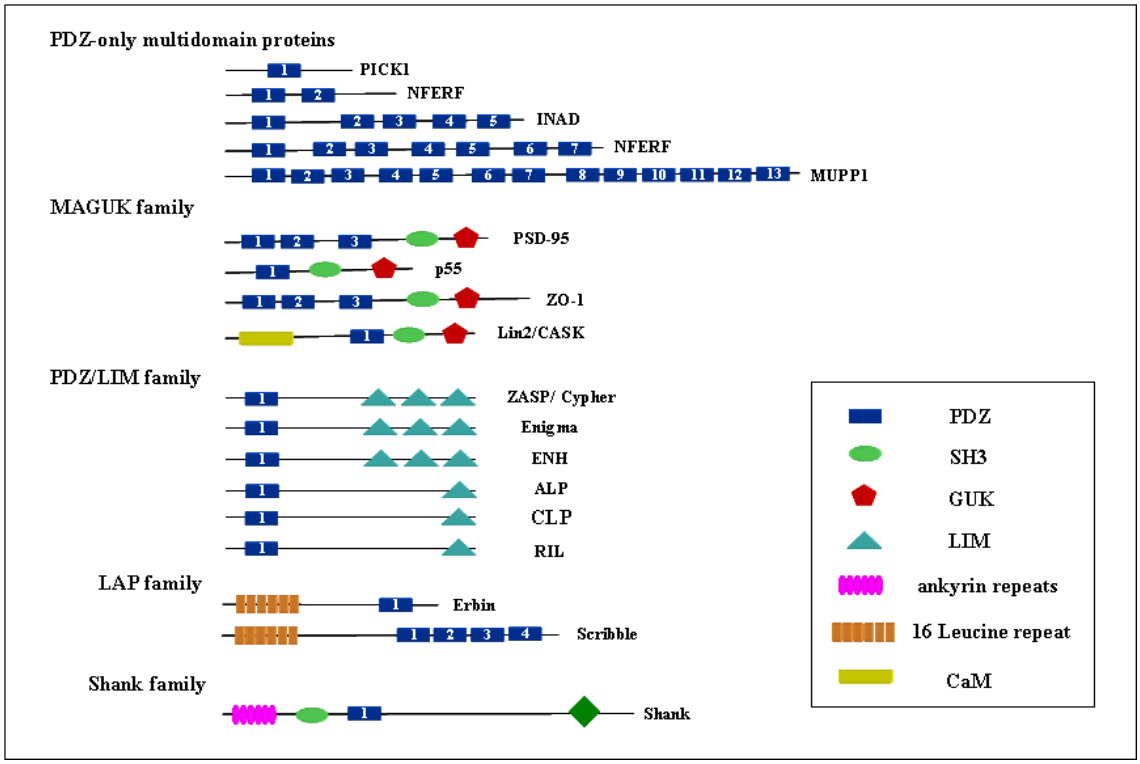

Figure 6. Modified figure showing the modular organization of PDZ-containing proteins. Representative members of the PDZ families are represented schematically (Jelen et al., 2003).

Chaper 2 MATERIALS and METHODS

2.1 AlphaScreen

AlphaScreen is an **A**mplified **L**uminescent **P**roximity **H**omogeneous **A**ssay that is non-radioactive, homogeneous proximity assay that relies on hydrogel coated Donor and Acceptor beads providing functional groups for conjugation to biomolecules. In the AlphaScreen assays, a signal is generated when a donor and an acceptor bead are brought into proximity by an interaction between the two conjugated biomolecules. The laser excitation at 680 nm of a photosensitiser (phthalocyanine) present on the Donor bead results in the production of singlet oxygen. The short lifetime of singlet oxygen in aqueous solution (~4 μsec) allows diffusion over a distance up to ~200 nm. The singlet oxygen migrates to react with a thioxene derivative in the Acceptor bead generating chemiluminescence at 370 nm that further activates fluorophores contained on the same bead emitting light at 520– 620 nm. This reaction cascade results in amplification of the signal that can be detected at the attomolar level. In the absence of a specific biological interaction, the singlet state oxygen molecules gave a very low background signal. The half-life of the decay reaction is 0.3 sec, which allows the technology to operate in a time-resolved mode ensuring a reduced background by minimizing the effect of auto-fluorescence. Also a long excitation wavelength of 680 nm combined with a shorter emission wavelength of 520–620 nm reduces interference from biological or assay components.

The AlphaScreen method was used to evaluate the strength of protein-protein bindings, to study the interactions occurring when more than one binding partner of a protein is present and also to eliminate the suspicion that there is an intermediary protein present as can be the case in experiments using cell lysates and *in vitro* transcripted translated protein. The AlphaScreen was done in collaboration with the Genome Research Group, CRIBI, University of Padua. This group has a Fusion-alpha microplate analyzer (Packard Bioscience) which is a universal multiplate analyzer designed to measure top and bottom fluorescence intensity, time-resolved, fluorescence, absorbance and luminescence. At present the protocol used is to biotinylate the protein to be used as Donor (usually a His tagged protein) and bind it to Streptavidin-Donor beads. The proteins used as Acceptors (Glutathione S-transferase [GST]-tagged proteins) are bound to the Glutathione-Acceptor beads, the opposite combination is also possible as both GST and His detection kits are available.

2.1.1 AlphaScreen Experiments

Alphascreen experiments were performed using His tagged proteins, GST fusion proteins or peptides. Experiments were done using 384-well plates (OptiPlate-384 white opaque, Packard BioScience*)* in a final volume of 25 µl per well. Both the GST detection and the His detection Kits for AlphaScreen were used according to the manufacturer's specifications (Perkin Elmer). The acceptor and donor beads were used at a concentration of 0.02 µg/µl (6.5 pM). First the protein to be tested was added to the wells and the acceptor beads were immediately added. The following steps were done in the dark. The plate was incubated for 30 minutes at RT before adding the donor beads and incubated for 3 hours, then kept for 15 minutes at 28 ˚C to equilibrate the temperature before reading. The signal was read at 28°C using a Fusion

Alpha™Multilabel Reader (PerkinElmer™) at 300 ms excitation, 700 ms emission.3. When testing a protein for binding it was titrated against the partner protein in order to establish the concentration of both proteins that resulted in a significant value for the ratio of the signal(S) to noise (N), normally in the range of S/N 8-50. In every experiment negative controls without one or both proteins were used to measure the background (noise) level. The experiments were repeated at least 3 times, to reduce the possibility of false results. Also biotinylated GST (0.5nM) or biotinylated His (1nM) were used as internal controls to normalize the signal readings. In competition experiments the binding proteins were first added to the wells at a fixed concentration that would result in binding in the absence of a competitor. Then the protein used as competitor was added at decreasing concentrations.

The Ratio is calculated as the mean of the normalized Signal divided by the mean of the normalised Noise ie $R = \frac{Sm}{Nm}$

The confidence of the ratio is calculated from the standard deviation of the Signal and the Noise.

$$\Delta R = R\sqrt{\left(\frac{\delta Sm}{Sm}\right)^2 + \left(\frac{\delta Nm}{Nm}\right)^2}$$

Sm = normalized signal mean; dSm= mean standard deviation of normalized signal

Nm = normalized noise mean; dNm= mean standard deviation of normalized noise

For competition experiments using AlphaScreen the concentration at which both proteins gave good binding was kept fixed and the possible competitor protein was added at variable concentrations. The result was plotted as the ratio obtained by dividing the signal in the presence of the competitor by that of the signal in the absence of the

competitor. The experiments were repeated at least three times and the values for the mean as well as the standard deviation from the mean of the samples were plotted.

2.2 Antibodies

2.2.1 Primary Antibodies

The following antibodies were obtained commercially.

Anti-c-myc mouse monoclonal clone 9E10, ascites fluid (M5546, SIGMA)

Anti-FLAG M2 mouse monoclonal antibody (F 2426, SIGMA)

Anti-HA (F-7) mouse monoclonal antibody (sc-7392, Santa Cruz Biotechnology)

Anti-GFP polyclonal antibody (46-0092, Invitrogen)

Anti-GST polyclonal antibody made in goat (27457701, GE Healthcare):

Anti-6xHis monoclonal antibody albumin free (631212, BD Biosciences)

Anti-GFP HRP conjugated polyclonal antibody made in goat (66633-100, Abcam), allows the detection of the GFP fusion protein without the detection of the heavy and light chain of the IgG.

The following antibodies were produced in house by Dr. G Faulkner, MMB, ICGEB. The antibodies were made in mouse to the respective human muscle proteins.

Anti-FATZ-1 polyclonal antibody made in mouse: this antibody was raised against a recombinant His tagged human full length FATZ-1 (1-299 aa) protein.

Anti-FATZ-2 polyclonal antibody made in mouse: this antibody was raised against the human recombinant His tagged human full length FATZ-1 (1-264 aa).

Anti-ZASP polyclonal antibody made in mouse: this antibody was raised against the human recombinant His tagged human full length ZASP-1 (1-283 aa).

Anti-Ankrd2 polyclonal antibody made in mouse: this antibody was raised against the human recombinant His tagged human partial full length Ankrd2 (5-333 aa).

Anti-Ankrd2 monoclonal antibody clone 2F10 (ascites fluid): the monoclonal antibody was produced using the Ankrd2 C-terminal (297-333 aa) protein. The position of the epitope was pin-pointed to the last 20 amino acids of the C-terminal of Ankrd2 using GST fusion proteins for different regions of the Ankrd2 protein.

2.2.2 Secondary antibodies

These antibodies were obtained commercially.

Anti-mouse IgG AP-conjugated antibody (Sigma, A3562)

Anti-rabbit IgG AP-conjugated antibody (Sigma, A3687)

Anti-goat IgG AP-conjugated antibody (Sigma, A4187)

Anti-mouse conjugated to fluorescein isothiocyanate (FITC) antibody (Sigma, F4018)

Anti-goat Alexa 546 antibody (Molecular Probes, A21085): anti-goat IgG conjugated to the fluorescent dye Alexa 546 that absorbs light at 556 nm and emits light at 573 nm.

Anti-mouse HRP conjugated antibody: anti mouse immunoglobulins conjugated with horseradish peroxidase was used for chemiluminescence detection (A-9044, GE Healthcare Biosciences).

2.3 Bacterial strains and growth media

The following *E.Coli* strains were used for this work:

DH5α recA1$^-$ strain (F$^-$, recA1$^-$, endA1, gyrA96, thi-1, hsdR17 (rk$^-$, mk+), supE44, elA1) for the propagation of eukaryotic expression vectors; the K-12 derived *E.Coli* strain

M15[pREP4] (Nal^S, Str^S, rif^S, lac^-, ara^-, gal^-, mtl^-, F^-, $recA^+$, uvr^+) for the expression and purification of His tag recombinant proteins.

BL21 (DE3) pLys S strain (F^-, ompT, $hsdS_B$ (r_B^- m_B^-), dcm, gal, (DE3), pLysS, Cm^r) (Promega) for the expression and purification of Glutathione-S-transferase (GST) recombinant proteins. Both the M15 and the BL21 strains allow high levels of expression of recombinant proteins after Isopropyl-β-D-thiogalactoside (IPTG) induction.

BL21-CodonPlus-RIL strain[a]: *E. coli* B F– *ompT hsdS*(r_B– m_B–) *dcm*+ Tet^r *gal endA* Hte *[argU ileY leuW* Cam^r], this strain is mainly used if the protein sequence contains a high percentage of arginine, isoleucine and leucine.

BL21-CodonPlus-RP strain[a]: *E. coli* B F– *ompT hsdS* (r_B– m_B–) *dcm*+ Tet^r *gal endA* Hte [*argU proL* Cam^r], this strain is normally used when the protein sequence is rich in proline and arginine.

The bacterial cultures were grown in one of the following media:

Luria Broth (LB): 10 g bactotryptone, 5 g yeast extract, 5 g NaCl (for 1 L).

Terrific Broth (TB): 12 g bactotryptone, 24 g yeast extract, 4 ml glycerol (for 1 L). Before use KH_2PO_4 at 17mM final concentration and K_2HPO_4 at 72 mM final concentration should be added.

2.4 Baculovirus expression system

Baculovirus expressing the human muscle protein FATZ-3 was made using the Bac-to-Bac baculovirus expression system (Invitrogen). The *Spodoptera frugiperda* (Sf9) insect cell line was used for baculovirus transfection and infection.

Steps of baculovirus preparation: Human FATZ-3 cDNA was inserted into the pFastBacHT vector at the *BamHI-HindIII* restriction site. The pFastBacHT vector contains Tn7R and Tn7L which are two sequences homologous with the mini-attTn7 sequence that is present in the baculovirus shuttle vector (bacmid 136 kb), and allow homologous recombination transposition of the gene of interest and into the bacmid. In order to allow the homologous transposition of FATZ-3 into the bacmid genome FATZ-3 pFastBacHT was transformed into the *E. coli* strain DH10Bac that contains the bacmid genome. Transformed DH10Bac cells were incubated for 48 hr at 37 °C. After 48 hr white and blue colonies were grown, selection was for the white colonies (positive colonies). White colonies were analysed further by PCR in order to confirm the presence of FATZ-3 in the bacmid genome. This bacmid DNA was then purified using a high purity plasmid miniprep kit (Marligen Biosciences). The bacmid containing FATZ-3 (1 ug of DNA) was transfected into Sf9 cells on 35 mm dishes ($9x10^5$ cells). Cells were then incubated at 27°C for 72 hr or until signs of viral infection started to appear. Then the virus (P1) was harvested from the cell culture medium. The virus from the P1 stock was amplified by infecting Sf9 cells with a multiplicity of infection (MOI) ranging from 0.05 to 0.1 pfu per cell; the amount of the P1 virus required for this amplification was calculated according to the formula:

$$\text{Inoculum required (ml)} = \left(\frac{\text{MOI (pfu / cell)} \times \text{number of cells}}{\text{titer of viral stock (pfu / ml)}} \right)$$

The amplified virus (P2) was harvested from the media after 48 hr. and the efficiency of the P2 stock virus was tested by infecting a constant number of Sf9 cells ($2x10^6$ in a 35mm dish) with different amounts of the virus (5, 50, 150 and 500ul). The amount of

virus giving the optimum protein expression was noted and a time course experiment made using this fixed amount of the P2 virus to infect same number of Sf9 cells in 4 different 60mm plates to determine when the virus starts to express the recombinant protein. One plate was harvested every 24 hours until 96 hr (24, 48, 72, 96hr). The results of these experiments are detailed in chapter 3 (Results).

2.5 Cell culture

2.5.1 C2C12 cells

C2C12 are mouse myoblasts that on the addition of differentiating medium or at confluency differentiate rapidly, forming contractile myotubes. Growth conditions: DMEM supplemented with 10 % v/v Foetal Calf Serum and 50 µg/ml gentamycin. Differentiation conditions: DMEM supplemented with 0.4 % Ultroser G and 50 µg/ml gentamycin.

2.5.2 COS-7 cell line

The COS-7 cell line is derived from CV-1, a simian cell line (cercopithecus aethiops), by transformation with an origin-defective mutant of SV-40. Growth conditions: DMEM supplemented with 10 % Foetal Calf Serum and 50 µg/ml gentamycin.

2.5.3 Sf9 cell line

The Sf9 cell line was derived from pupal ovarian tissue of the *Spodoptera frugiperda*. The Sf9 cell line is highly susceptible to infection with *Autographa california* nuclear polyhedrosis virus (AcNPV baculovirus), and can be used with all baculovirus expression vectors. Sf9 cells are commonly used to isolate and propagate recombinant baculoviral stocks and to produce recombinant proteins. Growth conditions: Grace's

insect medium (Invitrogen Corporation) supplemented with 10 % Foetal Calf Serum and 50 μg/ml gentamycin.

2.6 Gene amplification and cloning

2.6.1 Amplification and cloning of full length FATZ-3

Human full length FATZ-3 was amplified from human skeletal muscle mRNA (Invitrogen) using the "OnestepRT-PCR" Kit (QIAGEN). Primers were designed with a *BamHI* restriction site on the forward primer and a *HindIII* restriction site on the reverse primer, to allow cloning in other vectors with the same restriction sites. The concentration of primers and mRNA was optimized and the final amplification conditions were as follows: 50 °C for 30 min, 95 °C for 15 min, followed by 40 cycles of 94 °C for 1 min., 62 °C for 1 min., 72 °C min for 1 min. then 72 °C for 10 min. The PCR product separated on a 1% agarose gel, the band of DNA corresponding to FATZ-3 was cut from the gel and then purified using the QIAEX purification Kit (QIAGEN). This FATZ-3 DNA was digested with enzymes for 3 hr at 37 °C, and then purified again using the QIAEX purification Kit (QIAGEN) ready for cloning into a variety of vectors.

N-terminal eukaryotic expression vectors: The full-length cDNA of human FATZ-3 was cloned into in the *BamHI-HindIII* restriction sites in the following the eukaryotic expression vectors.

pCMV-tag-3B (Stratagene): contains an N-terminal c-myc (EQKLISEEDL) tag

pCMV-tag-2B (Stratagene): contains an N-terminal FLAG (DYKDDDK) tag.

pFastBacHT FATZ-3: contains an N-terminal 6His tag used to express FATZ-3 in Sf9 insect cells.

pcDNA3-HA: FATZ-3 cDNA was cloned into the *BamHI-EcoR1* restriction sites in a modified pcDNA3 vector (Invitrogen) with a N-terminal HA tag (YPYDVPDYA).

pEGFP-C1 FATZ-3: FATZ-3 cDNA was cloned into in the *BglII-HindIII* restriction sites. The FATZ-3 was digested *BamHI-HindIII* and inserted into the *BglII-HindIII* site of the vector.

C-terminal eukaryotic expression vectors: The full-length cDNA of human FATZ-3 was cloned into in the *BamHI-HindIII* restriction sites in the following eukaryotic expression vectors.

pCMV-tag-5A (Stratagene): contains a C-terminal c-myc (EQKLISEEDL) tag

pCMV-tag-4A (Stratagene): contains a C-terminal FLAG (DYKDDDK) tag.

Bacterial expression vectors: The full-length cDNA of human FATZ-3 was cloned into the *BamHI-HindIII* restriction sites in the following bacterial vectors.

pGEX-6PH-3: contains a N-terminalGST tag. The vector is a modified form of the pGEX-6P-3 vector (GE Healthcare) containing *BamHI-HindIII* restriction sites.

pQE30-FATZ-3 (QIAGEN)**:** contains a N-terminal six histidine (6xHis) tag

pPROEXHTa contains a N-terminal six histidine (6xHis) tag with a TEV protease cleave site (leu, tyr, phe, gln) for removing the 6His tag.

2.6.2 Amplification and cloning of regions of FATZ-3

Regions of FATZ-3 cDNA were amplified by PCR using the full length FATZ-3 cDNA as template and with a BamHI restriction site on the forward primer and *HindIII* on the reverse primer. They were then cloned into the various expression vectors noted above using these restriction sites. Three regions were chosen based on a theoretical prediction of the secondary structure of FATZ-3 obtained using the Predictprotein program

(PredictProtein: B Rost, G Yachdav and J Liu (2004) The PredictProtein Server. Nucleic Acids Research 32(Web Server issue):W321-W326).

FATZ-3 (1-240 bp) expressing the protein **F ATZ-3 mutant sN (1-80 aa)**

FATZ-3 (241-540 bp) expressing the protein **FATZ-3 mutant Cen (81-180 aa)**

FATZ-3 (541-753 bp) expressing the protein **FATZ-3 mutant sC (181-250 aa)**

In order to obtain better protein expression FATZ-3 was divided into two main regions.

FATZ-3 (1- 240 bp) expressing the protein **F ATZ-3 mutant LN (1-180 aa)**

FATZ-3 (240-753 bp) expressing the protein **F ATZ-3 C terminal (80-251 aa)**

FATZ-3 (198-753 bp) expressing **protein FATZ-3 P (66-139 aa).** This region of FATZ-3 was cloned and expressed as a His tag recombinant protein to be used for antibody production. It was specifically chosen because it had low homology with other members of the FATZ family.

FATZ-3 (196-251aa): primers where designed to amplify the last 168 bp of FATZ-3 with the addition of the *BamHI-HindIII* restriction sites at the ends. The amplified DNA was cloned into pGEX-6PH vector which was used to express an N-terminal GST FATZ-3 (196-251 aa) fusion protein. This deletion mutant containing the last 56 aa of FATZ-3 was sent to our collaborator Prof. Olli Carpen (Helsinki) for use in *in vitro* phosphorylation studies.

Eight of the **FATZ-3 deletion mutants** published by Frey and Olson (Frey and Olson, 2002) were amplified by PCR with *BamHI-HindIII* restriction sites and then cloned into the various expression vectors noted above. These FATZ-3 deletion mutants encode the following FATZ-3 partial proteins F1 (1-110 aa), F2 (37-110 aa), F3 (109-251 aa), F4 (109-207 aa), F5 (73-251 aa), F6 (50-251 aa), F7 (50-186 aa) and F8 (50-110 aa). Since there were difficulties expressing the smaller deletion mutants *in vivo*, probably due to

their size and susceptibility to degradation it was decided to use a larger tag. The DNA's of the deletion mutants were cloned into the *BiglII-HindIII* site of the eukaryotic expression vector pEGFP-C1. The GFP is 27 kDa alone and these FATZ-3 fusion proteins expressed with the GFP tag ranged from 33.7 to 48.7 kDa.

2.6.3 Myotilin

Myotilin deletion mutants, M1 (1-250 aa) and M2 (185-498 aa) were designed by our collaborator Prof. Olli Carpen, Turku, Finland. The DNA encoding these deletion mutants of myotilin were amplified by PCR in order to insert suitable restriction sites, *BamHI-HindIII* and *BamHI-EcoRI* respectively, for cloning in the pCMV-tag-2B-FLAG vector. These constructs were produced *in vivo* for binding studies.

2.6.4 Amplification and cloning of FATZ-1, -2, -3 and myotilin lacking last 15 bp

Primers were designed to produce FATZ-1, -2, -3 , myotilin and a myotilin deletion mutant (M2) without the last 15 bp corresponding to the last 5 amino acids of the protein. The amplified DNA was cloned into the pGEX-6PH vector for the production of GST protein and also into the eukaryotic expression vector pCMV-tag 3B. These constructs were produced in order to study the binding of the FATZ-1, -2-, -3 and myotilin proteins without the last 5 amino acids to the ZASP, ALP and CLP PDZ. The full length human myotilin cDNA was kindly supplied by our collaborator Prof. Olli Carpen (University of Turku, Finland). Primers were designed in order to amplify the full length myotilin with BamHI-EcoRI restriction sites. The gene was then digested by *BamHI-EcoRI* restriction enzyme and inserted in the eukaryotic vector pCMV-tag-2B-FLAG through its restriction *BamHI-EcoRI*, in order to study protein-protein interaction in vivo.

2.6.6 PDZ-ZASP pPROEXHTa

The PDZ (1-85aa) region of ZASP had been cloned previously into expression vectors in our laboratory. PDZ-ZASP was cut by *BamHI-HindIII* and cloned in the prokaryotic vector pPROEXHTa, that allows the production of the protein with a 6His tag and a TEV protease cleavage site (leu, tyr, phe, gln). This PDZ-ZASP pPROEXHTa vector was sent to our collaborator Prof. Olli Carpen (University of Turku, Finland) for structural studies.

2.6.7 PDZ-ZM-ALP pGEX-6P

Primers were designed with *BamHI-HindIII* restriction sites to amplify the first 501 bp of ALP encoding amino acids 1-167aa that contain both the PDZ domain and the ZM motif. The PDZ-ZM-ALP was amplified, digested and cloned into the pGEX-6PH vector for the expression and purification of an N-terminal GST tag fusion protein for use *in vitro* studies such as AlphaScreen.

2.7 In vitro binding

Equal amounts of GST (GST and GST-PDZ-ZASP) proteins bound to glutathione-Sepharose 4B resin were incubated for three hours at RT with *in vitro* transcribed and translated (IVTT) ^{35}S labelled proteins: FATZ-3, FATZ-3 lacking the last 5 amino acids. The resins were briefly centrifuged and washed several times before being subjected to SDS-PAGE as was the IVTT protein, 30 % of the total amount used in each of the binding reactions. The gels were dried and exposed either to BioMax autoradiography film or to SR Packard phosphor screens; the analysis was done using a Packard Cyclone Phosphor Imager (Packard Instrument Co).

2.8 In vitro transcription and translation

The TNT Coupled Reticulocyte Lysate System (Promega) was used to produce IVTT proteins such as full length human FATZ-1, human FATZ-1 lacking the last 5 amino acids, full length human FATZ-2, human FATZ-2 lacking the last 5 amino acids, full length human FATZ-3, human FATZ-3 lacking the last 5 amino acids, human myotilin full length and the myotilin mutant lacking the last 5 amino acids. This system allows the production of both radioactive and non-radioactive proteins.

Each transcription/translation reaction was performed using 25 µl of TNT Rabbit Reticulocyte Lysate, 2 µl of TNT Reaction buffer, 1 µl of T7 RNA polymerase, 2-5 µl of the appropriate radiolabeled aminoacid was used (Pro-mix [^{35}S] cell labelling mix, GE Healthcare Biosciences), 1 µl of the amino acid mixture minus methionine/cysteine, 1 µl of RNasin ribonuclease inhibitor, DNA template (0.5-1 µg) and nuclease free water to a final volume of 50 µl. The reaction was performed at 30°C for 90 minutes. Samples were tested for the presence of the desired protein by SDS-PAGE and then the gel was dried, exposed either to BioMax autoradiography film or to SR Packard phosphor screens. The analysis was done using a Packard Cyclone Phosphor Imager (Packard Instrument Co).

2.9 PDZ Array

The PDZ array membranes (Panomics) were used according to the protocols in the manufacturer's handbook. The array membranes have a notch at the top right hand corner for orientation purposes. When biotinylated peptides were used as ligands 1.5 µg of the peptide was mixed with 15 µl of Streptavidin-HRP (DAKO) and incubated at 4°C for 30 min before adding to 5 ml of Blocking Buffer (Panomics CS7660) and kept at

4°C until ready to use. When a His –tagged purified protein was used instead of a biotinylated peptide as ligand it was diluted in blocking buffer to obtain a protein concentration of 15 μg/ml. The membranes were incubated for 1 hr at room temperature (RT) in blocking buffer and then rinsed with wash buffer before adding the peptide or the purified protein. They were then incubated with gentle shaking for 1-2 hr at RT and washed three times with wash buffer for 10 min (each wash) at RT. When His –tagged purified protein was used the membrane was incubated with anti-histidine HRP conjugate diluted in wash buffer and incubated for 1-2 hr at RT. After incubation the membranes were washed three times in wash buffer at RT then treated with the provided solutions for chemiluminescence and after incubation for 5 min at RT the membranes were exposed to Hyperfilm for ECL (Amersham).

2.10 Peptides

Peptides were produced in the Protein Structure and Bioinformatics laboratory, ICGEB. The peptides, corresponding to the last 5 residues of the FATZ family of proteins and myopalladin, were synthesized on solid phase (Fmoc/t-Bu chemistry). The synthesis was automatically performed on a 0.05 mmol scale with a Gilson AspecXl Solid Phase Extraction instrument modified in-house. Biotin was manually added at the peptide N-terminus as a Biotin 4-nitrophenyl ester at the end of the synthesis. After cleavage from the resin the peptides were precipitated with diethyl ether, washed and freeze-dried. The peptides were purified by RP-HPLC on a Zorbax 300SB-C18 column (Agilent) using a linear gradient from Eluent A (0.1% trifluoroacetic acid in water) to Eluent B (0.1% trifluoroacetic acid in acetonitrile) using UV monitoring at 214 nm. The collected

fractions were analyzed by ESI-MS on a API150EX single quadrupole mass spectrometer (Applied Biosystems), pooled and freeze-dried.

List of peptides: The following peptides where used for both AlphaScreen studies and the TransSignal PDZ array domains experiments.

Biotin-GABA-GABA-EpSEEE; -ESEEE, -EpSEEL; -ESEEL; -EpTEEL; -ETEEL; -EpSEDL;-ESEDL; -EpSEDL; -ESDEL and –EpSDEL. For competition experiments the same peptides without biotin but with GABA were used.

2.11 Protein Production

2.11.1 Production and purification of native 6His-tagged proteins

The pQE30 (QIAGEN) and the pPROEXHT (Life Technologies) vectors were used for the expression of His-tagged proteins. The difference between these vectors is that the pPROEXHT contains a TEV protease cleavage site, whereas the pQE30 does not. His tagged proteins required for structural studies such as C-terminal FATZ-3 (81-251 aa) and the PDZ-ZASP (1-85 aa) were produced using the pPROEXHT vector that had a cleavable 6His tag. The protocols used for production and purification were the same for both vectors. The *E. coli* strain M15(pREP4) was transformed and after induction colonies were screened for expression of the recombinant His tag protein. A fresh colony expressing FATZ-3 was inoculated into LB (500ml), grown overnight at 37°C with shaking and the next day this culture was used to inoculate LB (500 ml) with ampicillin (100 μg/ml) and kanamycin (30 μg/ml) selection and grown at 37°C with shaking until an OD_{600} of 0.6. At this point the 1-2 mM IPTG was added for induction of the recombinant protein and the culture was grown at 37°C or at room temperature (native protein protocol) for 4-5 hours. Then cells were harvested by centrifugation at

6,000 rpm for 15 minutes, the pellet resuspended in the lysis buffer (Tris 50mM, NaCl 300mM, Imidazole 10mM pH8) and kept on ice for 45 minutes. The suspension was sonicated and then centrifuged 10 minutes at 14000 rpm to remove cellular debris. The supernatant was transferred to a fresh tube, mixed with 1 ml of Ni-NTA (QIAGEN) resin and incubated for 1 hour at 4°C with gentle mixing. The Ni-NTA (nitriltriacetic acid) resin is a metal chelant adsorbent attached to Sepharose CL-6B which binds with high affinity to the 6xHis tag. The resin was washed three times for 10 minutes in wash buffer (Tris 50mM, NaCl 300mM, imidazole 20mM pH8). The recombinant protein was eluted by the addition of 1 ml of the elution buffer (Tris 50mM, NaCl 300mM, imidazole 250mM pH8). Protein levels and purity were checked by SDS-PAGE followed by Coomassie Blue staining. The proteins produced were used for AlphaScreen or structural studies.

List of 6His tagged fusion proteins produced and purified for the project

1) Full length FATZ-3 (1-251 aa)
2) C-terminal FATZ-3 (81-251 aa)
3) C-terminal FATZ-3 (81-251 aa) the His tag of this protein could be cleaved using the TEV protease
4) PDZ-ZASP (1-85 aa) the His tag of this protein could be cleaved using the TEV protease
5) *alpha-actinin-2 (1-894 aa)*

2.11.2 Production and purification of GST recombinant proteins

GST-recombinant proteins were produced and purified using the Glutathione S-transferase Gene Fusion System (GE Healthcare) for the expression, purification and detection of fusion proteins produced in *E.Coli*. The pGEX plasmids are designed for

inducible, high-level intracellular expression of genes or gene fragments as GST fusion proteins. cDNA of different proteins were inserted into pGEX plasmids, these vectors were then transformed in the *E.Coli* strain BL21 (DE3)-pLys S (Promega) that is engineered to contain the pLys plasmid encoding the T7 lysozyme. RIL, RP or RLP variants of BL21 (DE3)-pLys S (Promega) containing extra codons were used when the protein to be expressed was rich in arginine (R), isoleucine (I), leucine (L) or proline (P). Colonies were screened for expression of the recombinant protein. A positive colony was grown in LB in the presence of ampicillin (100 μg/ml) (SIGMA) at 37°C with shaking overnight until the bacterial culture reached the OD_{600} of 0.6. At this point the GST-recombinant protein expression was induced by the addition of 0.5-1 mM IPTG and the bacteria grown for a further 3-4 hours with mixing at room temperature or at 37°C. Then the cells were collected by centrifugation at 6,000 rpm for 15 minutes, resuspended in lysis buffer (Hepes 25mM pH 7.6, NaCl 300mM, EDTA 1mM, DTT 1mM, Lysozyme, protease inhibitor cocktail Roche, Triton 100, 0.5%) and kept on ice for 20 minutes. The composition of the lysis buffer varied depending on the protein to be purified. At this point the suspension was sonicated, and then centrifuged at maximum speed to remove cell debris. The supernatant was recovered and incubated for 1 hour with Glutathione Sepharose-4B beads (GE Healthcare), at 4°C with mixing. During this step the recombinant GST proteins should bind to the glutathione conjugated beads. Then the solution was briefly centrifuged and the recovered resin was washed three times with lysis buffer for five minutes with mixing at 4°C. After a final wash in PBS (Phosphate buffered saline), the GST-recombinant proteins were eluted from the beads by the addition of 200 μl of 20 mM Glutathione (SIGMA) for 10 minutes at room temperature. As an alternative, proteins can be kept bound to the resin

for use in GST pull down experiments. The amount and purity of the proteins was determined by SDS-PAGE and subsequent staining with Coomassie Brilliant Blue R (Coomassie Blue 0.4%, Acetic Acid 10%, and Methanol 40%). Native GST fusion proteins were used for GST pull-down assays and AlphaScreen experiments.

List of GST fusion proteins produced and purified for the project

1) Full length human FATZ-3 (1-251 aa)
2) Human FATZ-3 mutant (81-251 aa)
3) Human mutant FATZ-3 lacking the last 5 amino acids (1-246 aa)
4) Human full length FATZ-1 (1-299 aa)
5) Human FATZ-1 lacking the last 5 amino acids (1-294 aa)
6) Human full length FATZ-2 (1-264 aa)
7) Human FATZ-1 lacking the last 5 amino acids (1-259 aa)
8) Human full length myotilin (1-498 aa)
9) Human myotilin mutant lacking the last 5 amino acids (1-493aa)
10) Human myotilin deletion (1-250 aa)
11) Human myotilin deletion (185-498 aa)
12) Human myotilin mutant lacking the last 5 amino acids (185-493 aa)
13) Human myotilin deletion (441-493 aa),
14) Human palladin (716-772 aa)
14) Human PDZ-ZASP (1-85 aa)
15) Human PDZ-ALP (1-80 aa)
16) Human PDZ-ZM-ALP (1-167 aa).

2.12 Structural Biology Protocols

2.12.1 Production and purification of the C-terminal FATZ-3 (81-251aa) for protein crystallization: Small scale production and purification

The C-terminal region of FATZ-3 in the pPROEXHT vector was used to transform BL21 (DES) RIL bacteria. A fresh colony was picked the next day, inoculated into 50 ml of LB media containing 100ug/ml ampicillin (Sigma) and grown overnight at 37 °C. The 50 ml culture was used to inoculate a 500 ml culture to an optical density of 0.10 at 600 nm, the culture was incubated with shaking at 37 °C until the OD_{600} reached 0.60, and then IPTG was added to a final concentration of 1mM. The culture was incubated at RT for 5 hr and then the cells were collected by centrifugation at 6,000 rpm for 15 min. These cells were resuspended in a $1/10^{th}$ of the culture volume with lysis buffer (20mM Tris pH 8, 50mM NaCl, 10mM imidazole and complete EDTA-free protease inhibitor cocktail, Roche) and left on ice for 1hr. Cells were disrupted by sonication on ice, and the soluble phase was separated from the inclusion bodies and cellular debris by centrifugation at 12,000rpm for 15 min.

The protein purification was made in three steps:

Affinity purification: The supernatant was transferred to a fresh tube, mixed with 1 ml of Ni-NTA resin (QIAGEN) and incubated for 1 hour at 4°C with gentle mixing. Then the resin was centrifuged and washed three times for 10 minutes in wash buffer (Tris 50mM, NaCl 300mM, imidazole 20mM pH8). The concentration of imidazole in the wash buffer varied depending on the stability of the protein binding to the Ni-NTA resin. The recombinant protein was eluted in 5 fractions by adding 1 ml of elution buffer (Tris 50mM, NaCl 300mM, Imidazole 250mM pH8) for each fraction. Protein level and purity were checked by SDS-PAGE followed by Coomassie Blue staining. The

concentration of the protein was measured by UV at wave length 280nm. The protein was dialyzed against (20mM Tris pH8, 75 mM KCl) buffer to remove imidazole. Dialysis was done overnight at 4°C, and then the protein was centrifuged to remove precipitates formed during dialysis. Any precipitated material was checked by SDS-PAGE to control if there was purified protein present. To cleave the 6His tag from the protein the supernatant containing purified protein was treated with Ac-TEV protease (Invitrogen) with an enzyme/substrate ratio of 10U for 100ug of protein, the reaction was made overnight at 4°C, then the protein before and after cleavage was checked by SDS-PAGE to confirm the removal of the His tag.

Ion exchange chromatography: In order to achieve the highest purification level and to remove the protease, anion exchange chromatography was used. The sample was loaded on a MonoQ HR 5/5 column (Amersham Biosciences), containing a matrix (10 µm hydrophilic polymer particles) covalently bound to a quaternary amino group that is a strong anion exchanger. Elution was performed with a 20 CV linear gradient from 0% to 100% of Elution Buffer (20 mM Tris pH 7.5,1 M KCl). Peak fractions obtained from elution were analyzed by SDS-PAGE (12%). Fractions containing pure C-terminal FATZ-3 were pooled, and concentrated using a Vivaspin 5 ml concentrator (VIVA Science).

Gel filtration chromatography: The molecular weight of native proteins and their aggregation state can be determined by size exclusion chromatography. Compounds of similar molecular shape and density like globular proteins are related by a sigmoidal relationship existing between their distribution coefficient (K_d) and the logarithms of their molecular weights.

K_d of each gel filtration column is defined as:

$$K_d = \frac{Ve - V_0}{Vt - V_0}$$

Where V_e, V_t and V_o represent the elution, total and void column volume respectively.

The elution position of the C-terminal FATZ-3 protein relative to proteins of known molecular mass was determined using 10/30 Superdex200 HR gel filtration chromatography (Amersham Biosciences). The column was eluted at a flow rate of 0.5 ml/min with 20 mM Tris pH 7.4 and 500 mM NaCl. The K_d was determined from the chromatogram for pre-mixed standard proteins of known molecular mass (Gel Filtration Calibration Kits HMW and LMW, Amersham Biosciences) and for the samples. It was then plotted against the logarithm of the molecular mass of the standard proteins. The standard curve obtained was used to calculate the apparent molecular mass of the C-terminal FATZ-3 protein and showed that this behaved as a dimer. The purified protein was then concentrated using the Vivaspin concentrator(VIVA Science) and its concentration was measured by UV at 280 nm. The protein (50ul) had a concentration of 0.5 mg/ml.

2.12.2 Large scale production and purification of C-terminal FATZ-3 protein

Several scale-up trials were made to optimize suitable buffer conditions, since the buffers and the purification protocols that worked when using small scale conditions did not work when using large scale conditions. The protocol was similar to that for the small scale except for the volumes and the use of a French Press for disruption of the cells. A 12 L culture of BL21 (DES) RIL bacteria transformed with the pPROEXHT

containing C-terminal FATZ-3 vector was grown to an OD_{600} of 0.1 at 37°C. The 12 L culture was then incubated at 25°C until the OD_{600} was 0 6, then induced by adding IPTG (1mM) and incubating with shaking for a further 5 hours at 25°C. Cells were centrifuged at 6,000 rpm and resuspended in $1/10^{th}$ of the volume with lysis buffer containing 50 mM MES pH6, 300 mM NaCl, 10 mM imidazole and complete EDTA-free protease inhibitor cocktail (Roche). The lysate was left on ice for 1 hour and then disrupted using a French Press, a very efficient method of disruption, and then centrifuged at 12,000 rpm for 20 mins.

Protein purification in three steps:

Affinity purification. Supernatant was mixed with 12 ml of Ni-NTA (QIAGEN) resin and incubated for 1 hour at 4°C with mixing. Then washed three times with 200ml washing buffer MES 50mM pH6, NaCl 300mM, Imidazole 15mM. The recombinant protein was eluted in 50 ml elution buffer (MES 50mM pH6, NaCl 300mM, Imidazole 250mM). Protein levels and purity were checked by SDS-PAGE followed by Coomassie Blue staining. Samples then were dialysed against MES pH 5, KCl 75mM.

Cation exchange chromatography. The C-terminal FATZ-3 protein was stable in the MES buffer at pH6 for this reason we used cation exchange as the second step in the purification since there were problems using ion exchange chromatography with Tris pH6 in the scale-up experiments. The sample was loaded on a Source 15S column (Amersham Biosciences). Elution was performed with a 20 CV linear gradient from 0% to 100% of elution buffer (20 mM Tris pH 7.5, 1 M KCl). Peak fractions from the elution were analyzed using 12% SDS-PAGE. Fractions containing purified C-terminal FATZ-3 protein were pooled, and concentrated using a Vivaspin 5 ml concentrator (VIVA Science).

Size exclusion chromatography. The purified protein from the cation exchange column was further purified by Gel filtration using a Superdex 200HR 16/60 column (Amersham Biosciences) equilibrated with a buffer containing 20 mM MES pH 6 and 75 mM KCl. Peak fractions were collected, concentrated with a Vivaspin 5 ml concentrator, and then analyzed using 12% SDS-PAGE. The purified protein concentration was measured at 280 nm, the final concentration was about 10 mg/ml in a volume of 120 µl.

2.12.3 Dynamic light scattering (DLS)

Dynamic light scattering measurement is a powerful method to analyze the quaternary structure of a protein and to evaluate its aggregation state. In DLS experiments, the radius (R) of a particle is calculated from its diffusion coefficient (D) *via* the Stokes-Einstein equation reported below, where k_B is the Boltzmann constant, T the temperature, η the solvent viscosity, and $f = 6\pi\eta R$ the frictional coefficient for a compact sphere in a viscous medium.

$$D = \frac{k_B T}{f} = \frac{k_B T}{6\pi\eta R}$$

In the above equation, R is the radius of an hypothetical hard sphere that diffuses with the same strength as the particle under examination. Its value is derived from the diffusional properties and it is considered indicative for the apparent size of the dynamic hydrated particle. In a typical DLS experiment, the photons scattered from the randomly oriented molecules in solution are detected with a single photon counting device. The intensity of the scattering signal is dependent on the molecular weight, density, shape,

concentration of the particles, viscosity, and refractive index of the medium, the magnitude of the particle-particle and solvent-particle interactions. The correlation between the scattering intensities measured during small time increments can be described with an intensity correlation curve. The scattering intensity at the detector is dependent upon the position of the particles relative to the detector that, in the absence of any different forces, is driven by the Brownian motion. The measured intensity correlation curve bears an indirect measurement of the particle's diffusion coefficient D. Moreover an appropriate analysis of the autocorrelation function can also provide useful data regarding sample polydispersity, the technique being sensitive to aggregation. DLS measurements were carried out using a DynaPro MS/X instrument (Protein Solutions, Inc.), scanning different temperatures in the range between 4 °C and 22 °C with a protein concentration of 10mg/ml. The use of quartz microcuvettes allowed the use of very small sample volumes (12 µl or 45 µl), which could be almost completely recovered. DLS measurements were preceded by sample centrifugation at 20,000 g for 30 min to reduce the presence of dust or other particulates, which could interfere with the scattering of photons by the protein molecules. The DLS instrument is provided with the DYNAMICS v6 software for controlling parameters such as temperature, acquisition time and photon flux. Moreover the software calculates an autocorrelation function to fit the measurements to either monomodal or bimodal distribution and gives as output the graphical profiles of this fit, the sum of squares differences between the measured correlation curve and the best fit curve using the cumulants method of analysis (B. J. Frisken, 2001). The numerical values obtained from the fitting included the hydrodynamic radius, the percentage of polydispersity, and the molecular weight of the sample, estimated using a calibration curve prepared from globular protein

standards. Furthermore, the degree of polydispersity obtained from DLS measurements of a protein sample was related to the probability to obtain crystals (Ferre-D'Amare and Burley, 1994). There is a higher probability of obtaining a crystal from a protein solution, which shows a low degree of polydispersity (below 20%).

2.12.4 Circular dichroism (CD)

Circular dichroism spectroscopy is a form of light absorption spectroscopy that measures the difference in absorbance of right- and left-circularly polarized light (rather than the commonly used absorbance of isotropic light) by a substance. It has been shown that the CD spectra between 260 and approximately 180 nm can be analyzed for the different secondary structural types: alpha helix, parallel and antiparallel beta sheet, turn, and other secondary structure formations. The concentration of the C-terminal of FATZ-3 (81-251 aa) was measured at 280nm then this value was divided by the extension coefficient of the protein. CD measurements were performed on a Pistar-180 spectrometer (Applied photo physics) using a 0.5mm path length cuvette (QS) with a protein concentration of 3.6 μM. Wavelength spectra were obtained by averaging five scans at 20^{o}C recorded at 0.5nm intervals from 180 to 360 nm at a rate of 45 nm min-1 and a bandwidth of 2.0 nm. (number of samples 50,000; sample period 25.0 microseconds). Using 23 reference proteins, quantitative determination of secondary structure elements was achieved using the CDNN (CD Spectroscopy Deconvolution) program.

2.12.5 Stura Footprint screens

"Stura footprint screen" is a simple test that defines the individual pattern of solubility for a given protein with a range of precipitants, the method was described by Enrico Stura (Stura et al., 1994). The methodology of the test depends on mixing different

concentrations of the desired protein with different concentrations of precipitants, then checking at which conditions the protein will start to precipitate. The condition where the protein will start to precipitate gives an indication of the optimum crystallization conditions. The stura footprint screening kit used was obtained from Molecular Dimensions. C-term FATZ-3 (81-251aa) was used at a concentration of 10mg/ml with 6 different conditions of the kit. These were the recommended starting conditions, especially if the protein sample was limited (as was the case the C-terminal FATZ-3 protein). The 6 recommended precipitants were used with the C-terminal FATZ-3 (81-251aa) protein by mixing 1ul of each precipitant with 1ul of the protein (10mg/ml), then immediately checking under the microscope for the formation of any precipitates. The best condition was obtained using PEG plus 0.2M imidazole malate pH 7.

2.12.6 Protein crystallization

The protein crystallization was performed by the "sitting drop technique" using three commercial crystallization kits The JCSG+ Suite (QIAGEN), the JBScreen 1, 2, 3 and 4 (JENA BIOSCINCE) and the PACT premier-HT96 MD1-36 (Molecular Dimension Limited). The mixing of the protein-precipitants was performed using the nanodrop robot. Two different concentrations of the protein were mixed with each concentration of the precipitant (0.1 ul and 0.2 ul of the protein with 0.1 ul of the precipitant). Approximately 300 conditions were used and the drops were then incubated at 22°C.

2.13 Transfections and co-immunoprecipitations

Sub-confluent COS-7 cells (7.5 x 10^5 cells) were seeded onto 100 mm plates (Falcon) and transfected with the following expression vectors (2 μg) Ankrd2-c-myc-pCMV, pcDNA3 and FATZ-3-FLAG-pCMV using the FuGENE 6 reagent (Roche) as

described in the manufacturer's protocol. Then 48 hr after transfection cells were harvested and lysed in 300 µl of E1A buffer (50 mM Hepes pH 7, 250 mM NaCl, 0.1 % v/v NP40 and protease inhibitors (Complete-EDTA free, Roche). Samples were briefly sonicated (10 seconds) at maximum power and then centrifuged for 10 minutes at 14,000 rpm at 4°C to remove cell debris. Supernatants were recovered and the protein concentration determined using the Biorad Protein Assay (Biorad). Extracts were subjected to SDS-PAGE and blotted onto a PDVF membrane to be tested for the presence of the desired protein products, using appropriate antibodies. Tagged proteins were immunoprecipitated from the extracts by the addition of specific antibodies for 2 hours at 4°C. Then protein A-Sepharose (GE Healthcare) was added and samples kept in agitation for 1 hour at 4°C. After five washings in E1A buffer the beads were centrifuged and following the addition of protein sample buffer, boiled 5 min and subjected to SDS-PAGE and then western blotting. The antibodies used for immunoprecipitation were anti c-myc clone 9E10 mouse monoclonal ascites fluid (M5546, SIGMA) and anti FLAG (M2), F3165 mouse monoclonal antibody (SIGMA).

2.14 Western blotting

Protein extracts or complexes from immunoprecipitations were separated by SDS-PAGE and then blotted onto Immobilon-P membrane (Millipore) to perform western blotting. The transfer of protein samples from the gel onto the membrane was done in a blotting apparatus using a constant voltage of 20 V overnight, the transfer buffer contained 20 % methanol and 10 % Tris-glycine.

The membrane was blocked for at least 1 hour in a solution of 10 % low fat milk in PBS containing 0.05 % Tween-20. The primary antibodies were diluted in 5 % low fat milk in PBS with 0.05 % Tween-20 and incubated for at least 90 minutes with gentle mixing.

The secondary antibodies were diluted in 5% low fat milk in PBS with 0.05% Tween 20 and incubated 45 minutes with agitation. Both Alkaline Phosphatase (AP)- and Horseradish Peroxidase (HRP)- conjugated secondary antibodies were used, according to the detection method employed, NBT/BCIP colorimetric assay or ECL respectively.

2.15 Primers used for this study:

FATZ-3 primers

Primer name	Primer sequnce	TM
Rcen-FATZ-3	TATAAGCTTCTAATCGCTCTGGTAGTC	62.8°C
Rev Ab FATZ-3	TATAAGCTTCTACAGGGCGCTGGGGCTG	76°C
For Ab FATZ-3	TATGGATCCATGTTAGCAGCCAGCCAGC	76.4°C
FATZ3 F Olson 1	TATGGATCCATGATCCCCAAGGAGCAG	75.2°C
FATZ3 F Olson 2	TATGGATCCATGATGGAGGAGCTGTCAC	73.9°C
FATZ3 F Olson 3,4,5	TATGGATCCTTCCCGGCCTCACCC	76.5°C
FATZ3 F Olson 6	TATGGATCCATGCTGGCCGGAAGC	76.7°C
FATZ3 F Olson 7	TATGGATCCGCAGCCAGCCAGC	75.9°C
FATZ3 F Olson 8,9,10	TATGGATCCCTCCTCTTCCAGAAGAGG	71.5°C
FATZ3 R Olson 1,2,10	TATAAGCTTCGGGAAGATGTGGAGCTC	70.4°C
FATZ3 R Olson 3,6,8	TATAAGCTTCTACAGCTCCTCGGACTC	66.5°C
FATZ3 R Olson 5,7,9	TATAAGCTTGGGGGTGTGACTTCG	68.6°C
FATZ3 R Olson 4	TATAAGCTTCCCCACGAGGGGTCCTC	73.5°C
FATZ3 -5 R	TATAAGCTTTGGGAGGTTACGGACC	67.4℃
FATZ-3 FOR C56	GTAGGATCCATGAAGACCCCGGTGCCA	78.4°C
FATZ-3 REV C56	TAAAAGCTTCTACAGCTCCTCGGACTC	68.9°C
FATZ3F	GTTAACAAGCGGAAGCTACCA	62.9°C
FATZ3R	GTCTTGGCTCCGGATGTTACC	66.6°C
FATZ3ORFF	TATGGATCCATGATCCCCAAGGAGCAGA	76.2°C
FATZ3ORFR	TATAAGCTTCTACAGCTCCTCGGACTC	66.5°C
FATZ-3 ORF-F2	TATGGATCCATGATCCCCAAGGAGCA	75°C
FATZ-3 ORF-NSR	TATAAGCTTCAGCTCCTCGGACTCTGGC	73°C
FN-FATZ-3	TATGGATCCATGATCCCCAAGGAGCAGA	76.2°C
RN-FATZ-3	TATAAGCTTCTACCTCCTGGCGCTTCC	71°C
FC-FATZ-3	TATGGATCCATGGGCCGAAGTCACACC	77.6°C
RC-FATZ-3	TATAAGCTTCTACAGCTCCTCGGAC	64.6°C
Fcen-FATZ-3	TATGGATCCATGAAGGTGACTGGAAC	69.5°C

FATZ-1 primers

Primer name	Primer sequnce	TM
FATZ-1 FOR C56	GTTGGATTCATGAAGTTTGACCTGG	68.2°C
FATZ-1 REV C56	GTTAAGCTTTCACAGCTCCTCTGTTTG	67.7°C
FATZ-1 ORF-F	TATGGATCCATGCCGCTCTCAGGAACCCC	80.5°C
FATZ-1 ORF-NSR	TATAAGCTTCAGCTCCTCTGTTTCTC	63.9°C
FATZ1 -5 F	TATGGATCCATGCCGCTCTCAGGAACC	76.9℃
FATZ1 -5 R	TATAAGCTTTCCATCCAAGGGGATGC	70.7℃

FATZ-2 Primers

Primer name	Primer sequnce	TM
FATZ-2 FOR C56	GTTGGATCCATGTTTGAGCTATTGC	68.1°C
FATZ-2 REV C56	GCCAAGCTTTCATAGGTCTTCTGATTCTGGTA	72°C
FATZ-2 ORF-F	TATGGATCCATGCTCTCACATAATACT	64.3°C
FATZ-2 ORF-NSR	TATAAGCTTTAGGTCTTCTGATTCTGG	62.6°C
FATZ2 -5 F	TATGGATCCATGCTATCACATAATAC	61.5℃
FATZ2 -5 R	TATAAGCTTTGGTACAGTGGTATCATC	62℃

Myotilin Primers

Primer name	Primer sequnce	TM
Myotilin R Rest	TATGAATTCTTAAAGTTCTTCACTTTC	58.9°C
Myotilin F Rest	TATGGATCCATGTTTAACTACGAACG	65.3°C
Myotilin F	ATGTTTAACTACGAACGTCC	55.7°C
Myotilin R	TTAAAGTTCTTCACTTCATAG	50.4°C
Myotilin F part 1	TATGGATCCATGGCTCGCAGATTGC	74.9°C
Myotilin R part 2	TATGAATTCTGGTGGGTAAAATTTC	62.6°C
Myotilin -5 R	TATAAGCTTATAGAGTCCAGATTGAG	57.9℃
MyT 973 For	GGGCTTATGCATGTGTTGCCAAGAATAGAGCAGG	78.9℃
MyT 973 Rev	CCTGCTCTATTCTTGGCAACACATGCATAAGCCC	78.9℃

Other primers

Primer name	Primer sequnce	TM
ALP HindIII primer REV	TATAAGCTTTAAGAATGAGACCCCGCA	68.6°C
F PDZ-ZASP Bgl II	TATAGATCTTATGTCTTACAGTGTGACC	59.5°C
R PDZ-ZASP EcoRV	TATGATATCTACGCTTTGATTTCTGCAG	65.8°C
M13	CAGGAAACAGCTATGAC	50.6°C
M13/Puc Rev	AGCGGATAACAATTTCACACAGG	65.8℃

Chapter 3 RESULTS

3.1 Amplification, cloning and expression of FATZ-3

The FATZ-1 and FATZ-2 genes had previously been cloned in our laboratory (Faulkner et al., 2000). My project was to study the function of the FATZ-3 gene. The human FATZ-3 gene had previously been shown to map at locus 5q31 and contain 7 exons spanning a 19kb region. It codes for a 251 amino acid protein having a high homology to the N- and C-termini of FATZ-1 and FATZ-2 (Frey and Olson, 2002).

In order to study FATZ-3 its cDNA was amplified by RT-PCR from human skeletal muscle mRNA (Clontech) and an band of approximately 770 bp was obtained (Fig. 7)

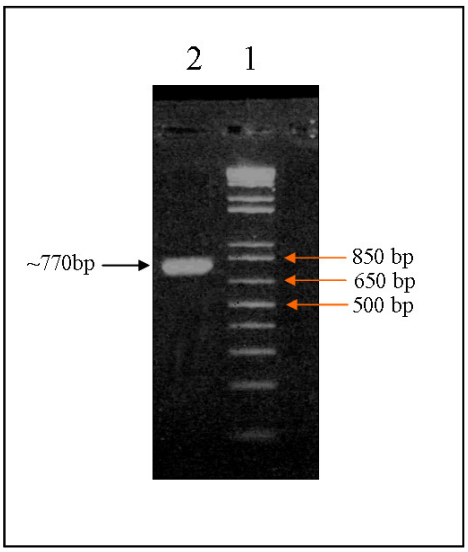

Figure 7. FATZ-3 cDNA amplified from skeletal muscle mRNA by RT-PCR and run on an agarose gel (1%). Lane 1, molecular weight marker, 1 kb plus ladder (Invitrogen); lane 2, the amplified cDNA of FATZ-3.

This amplified cDNA was then sequenced and I found no discrepancies between this sequence and the sequence of FATZ-3 in the NCBI database. The primers used to amplify the FATZ-3 cDNA had restriction sites which facilitated the cloning of this cDNA into a variety of expression vectors both prokaryotic and eukaryotic. To check the level of expression of FATZ-3 in eukaryotic cells, COS-7 cells were transfected with FATZ-3 vectors expressing either c-myc or FLAG tagged recombinant proteins (respectively pCMV-3B, pCMV-2B). The proteins from transfected cell lysates were separated by SDS-PAGE, immunoblotted and detected with antibodies against c-myc (Fig. 8 a) and FLAG (Fig 8 b).

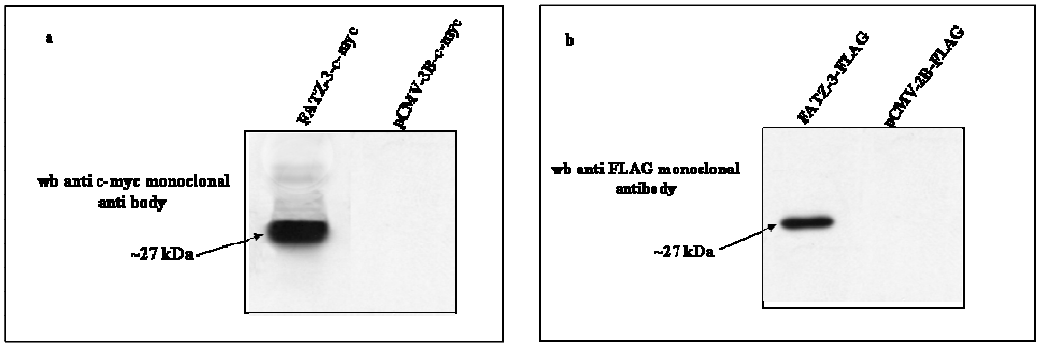

Figure 8. (**a**) and (**b**)**:** Western blots showing the recombinant FATZ-3 protein expressed in COS-7 cells and detected respectively, by anti c-myc and anti-FLAG monoclonal antibodies. 15 µg of cell lysate was loaded on the SDS PAGE gel and detected with anti-c-myc monoclonal antibody diluted 1:1000 (M5546, SIGMA) **a,** and monoclonal anti-FLAG antibody diluted 1:1000 (F 2426, SIGMA).

3.2 The FATZ family, myotilin, palladin and myopalladin share high similarity at their extreme C-termini (last 5 amino acids)

Together with Prof. Olli Carpen, University of Turku, Finland, we noted that the terminal 5 amino acids of FATZ-1 (ETEEL), FATZ-2 (ESEDL), FATZ-3 (ESEEL), myotilin (ESEEL), myopalladin (ESDEL) and palladin (ESEDL) share high similarity (Fig. 9). Notably those of FATZ-3 and myotilin are identical (ESEEL) as are those of FATZ-2 and palladin (ESEDL). This high similarity raised the question of whether these proteins could interact via their C-terminal with the same protein or proteins as well as the possibility that the C-terminal final five amino acids may represent a new binding motif involved in protein interactions.

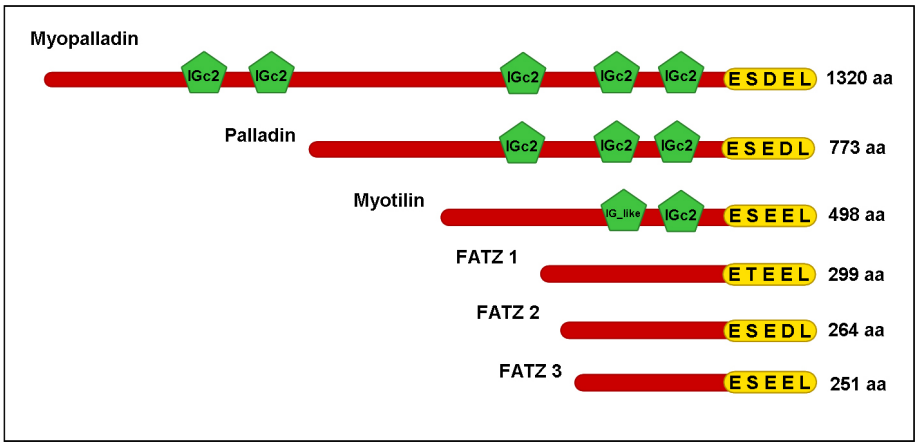

Figure 9. A schematic diagram showing the proteins of myopalladin, palladin and myotilin with their IGc2 and IG-like domains and the FATZ family of proteins. All six proteins share high homology at the last 5 amino acids of their C-terminal.

To verify if this putative binding motif was shared by other proteins a program was written by Prof. G. Valle, Genome Research Group, CRIBI, University of Padova, to extract proteins from any database with the last 5 amino acids having the motif

E[ST][DE][DE]L. The last 5 amino acids were given the following weightings: position 0 L = 2, position 1 E or D = 1, position 2 E or D = 1, position 3 S or T = 1 and position 4 E = 1. A score of 6 is given when all the criteria are met. The program was used to check the UniProt Knowledgebase Release 11.3 (UniProtKB/Swiss-Prot Release 53.3 of 10-Jul-2007 and the UniProtKB/TrEMBL Release 36.3 of 10-Jul-2007). The E[ST][DE][DE]L motif was found to be restricted in Vertebrates to the proteins of the FATZ family, myotilin, myopalladin and palladin with the exception of histidine ammonia lyase that has the final C-terminal amino acids the same as FATZ-2 and palladin (ESEDL). The data is reported in Table 1 is only for the proteins with a score of 6 corresponding to exact matches for the motif E[ST][DE][DE]L. It is notable that there are very few proteins that have exact matches: FATZ-1 (myozenin-1/ calsarcin-2), FATZ-2 (myozenin-2/calsarcin-1), FATZ-3 (myozenin-3/ calsarcin-3), myopalladin, palladin and histidine ammonia lyase. All of these proteins except histidine ammonia lyase and palladin are localized in the Z-disc of striated muscle. Palladin is an actin-binding protein involved in cytoskeletal organization in a variety of cell types and has a high identity with myopalladin which is found in the Z-disc. Therefore, with the exception of histidine ammonia lyase the proteins conserving the E[ST][DE][DE]L motif have a role in muscle or cytoskeletal structure and/or function. L-Histidine ammonia-lyase is a cytosolic enzyme catalyzing the first reaction in histidine catabolism, the nonoxidative deamination of L-histidine to trans-urocanic acid. Genetic deficiency of the enzyme, transmitted as an autosomal recessive trait, causes histidinaemia which is characterized by increased histidine and histamine as well as decreased urocanic acid in body fluids. Histidine ammonia lyase has been reported to be localized in the sarcoplasm of the muscle (Krishnamoorthy, 1977).

It had previously been shown that the FATZ family of proteins bound ZASP (Cypher/Oracle) however these interactions had not been mapped either on ZASP or on the FATZ family members (Frey and Olson, 2002). Recently in the laboratory of Prof. Olli Carpen (personal communication, unpublished results) as a result of yeast–two-hybrid experiments it was found that myotilin binds to ZASP through its C-terminal and that they co-localize in the Z-disk. Based on this data and our observations we speculated that the last 5 amino acids of the C-terminal of myotilin, myopalladin, palladin and the FATZ family could have a role in the interaction with ZASP. This hypothesis was further strengthened by the information obtained using the ELM program (a resource for predicting functional sites in eukaryotic proteins, (Puntervoll et al., 2003) which predicted that the terminal four amino acids of myotilin, myopalladin, palladin and the FATZ family constituted a binding motif for class III PDZ domain proteins: X[DE]X[IVL], where X is any amino acid.

Table 1 Results of the protein database scan for the motif **E[ST][DE][DE]L**

Score	3' end	SwissProt Entry No.	Protein
6	LDG**ETEEL**	Q9NP98	**MYOZ1_HUMAN FATZ-1 (Myozenin-1/Calsarcin-2)**
6	LDG**ETEEL**	Q1AG03	Q1AG03_CANFA Calsarcin 2 - Canis familiaris (Dog)
6	LDG**ETEEL**	Q8SQ24	MYOZ1_BOVIN Myozenin-1 - Bos taurus (Bovine)
6	LDG**ETEEL**	Q0IIE1	Q0IIE1_BOVIN MYOZ1 protein - Bos taurus (Bovine)
6	LDG**ETEEL**	Q4PS85	MYOZ1_PIG Myozenin-1 - Sus scrofa (Pig)
6	LDG**ETEEL**	Q1AG04	Q1AG04_PIG Calsarcin 2 - Sus scrofa (Pig)
6	LDG**ETEEL**	Q1AG02	Q1AG02_RABIT Calsarcin 2 - Oryctolagus cuniculus (Rabbit).
6	LDG**ETEEL**	Q9JK37	MYOZ1_MOUSE Myozenin-1 - Mus musculus (Mouse)
6	VDG**ETEEL**	Q6DIU0	Q6DIU0_XENTR Myozenin 1 - Xenopus tropicalis
6	VDG**ETEEL**	Q7ZYN8	Q7ZYN8_XENLA MGC53296 protein - Xenopus laevis
6	MDG**ETEEL**	Q7SYY0	Q7SYY0_XENLA Myoz1-prov protein - Xenopus laevis
6	FDG**ETDDL**	Q6DHF0	Q6DHF0_DANRE Zgc:92347 - Danio rerio (Zebrafish).
6	FDG**ETDDL**	Q6P0T8	Q6P0T8_DANRE Zgc:77785 - Danio rerio (Zebrafish)
6	SSE**ETDDL**	Q1JQ62	Q1JQ62_DANRE Si:ch211-238e6.5 - Danio rerio (H-L-H protein)
6	SSE**ETDDL**	Q5TZ58	Q5TZ58_DANRE Novel protein (H-L-H)

6	FDG**ETDEL**	Q4SQM4	Q4SQM4_TETNG Chromosome 17 SCAF14532, Calsarcin rel.
6	FDG**ETDDL**	Q4SV47	TETNG Chromosome undetermined SCAF13803 calsarcin rel.
6	TVP**ESEDL**	Q9NPC6	**MYOZ2_HUMAN FATZ-2 (Myozenin-2/Calsarcin-1)**
6	TVP**ESEDL**	Q5R6I2	MYOZ2_PONPY Myozenin-2 - Pongo pygmaeus (Orangutan)
6	TIP**ESEDL**	Q5E9V3	MYOZ2_BOVIN Myozenin-2 - Bos taurus (Bovine)
6	TIP**ESDDL**	Q1AG08	Q1AG08_PIG Calsarcin 1 - Sus scrofa (Pig)
6	TVP**ESDDL**	Q9JJW5	MYOZ2_MOUSE Myozenin-2 - Mus musculus (Mouse)
6	TIP**ESDDL**	Q8CE60	Q8CE60_MOUSE 10 days neonate skin cDNA, RIKEN.
6	TIP**ESDDL**	Q9D3I5	Q9D3I5_MOUSE 6 days neonate head cDNA, RIKEN
6	EIP**ESDDL**	Q8AVF9	Q8AVF9_XENLA Myoz2-prov protein - Xenopus laevis.
6	EIP**ESDDL**	Q63ZK4	Q63ZK4_XENLA LOC494787 protein - Xenopus laevis
6	EIP**ESDDL**	Q5I0T4	Q5I0T4_XENTR Myozenin 2 - Xenopus tropicalis
6	EIP**ESDDL**	Q6P5L6	Q6P5L6_DANRE Zgc:77703 - Danio rerio (Zebrafish)
6	FIP**ESDDL**	Q6P2T2	Q6P2T2_DANRE Myozenin 2 - Danio rerio (Zebrafish)
6	ALV**ESEDL**	Q7L3E0	**Q7L3E0_HUMAN Palladin protein - Homo sapiens**
6	ALV**ESEDL**	Q7L8P5	Q7L8P5_HUMAN Hypothetical protein DKFZp586L0518
6	ALV**ESED**L	Q9Y3E9	Q9Y3E9_HUMAN CGI-151 protein - Homo sapiens (Human)
6	ALV**ESEDL**	Q9UQF5	Q9UQF5_HUMAN SIH002 - Homo sapiens (Human)
6	ALV**ESEDL**	Q9Y2J6	Q9Y2J6_HUMAN KIAA0992 protein - Homo sapiens (Human)
6	ALV**ESEDL**	Q4R5Y9	Q4R5Y9_MACFA Testis cDNA, clone: QtsA-19723
6	GLV**ESEDL**	Q3MHW8	Q3MHW8_BOVIN PALLD protein - Bos taurus (Bovine)
6	GLV**ESEDL**	Q6DFX7	Q6DFX7_MOUSE Palld protein - Mus musculus (Mouse)
6	GLV**ESEDL**	A0JNZ3	A0JNZ3_MOUSE Palld protein - Mus musculus (Mouse)
6	GLV**ESEDL**	Q9ET54	Q9ET54_MOUSE Actin-associated protein palladin
6	GLV**ESEDL**	Q9CWW1	Q9CWW1_MOUSE ES cells cDNA, RIKEN full-length
6	GLV**ESEDL**	Q69ZT7	Q69ZT7_MOUSE MKIAA0992 protein - Mus musculus (Mouse)
6	GLV**ESDDL**	Q4RKT9	Q4RKT9_TETNG Chromosome 1 SCAF15025, whole genome
6	*KIP**ESEDL***	*Q4VB93*	***Q4VB93_HUMAN Histidine ammonia-lyase - Homo sapiens***
6	*TIP**ESDDL***	*P35492*	*HUTH_MOUSE Histidine ammonia-lyase - Mus musculus*
6	*TIP**ESDDL***	*P21213*	*HUTH_RAT Histidine ammonia-lyase - Rattus norvegicus.*
6	*TIP**ESDDL***	*>Q76N86*	*Q76N86_RAT Histidase - Rattus norvegicus (Rat)*
6	SVV**ESDEL**	Q86TC9	**MYPN_HUMAN Myopalladin - Homo sapiens**
6	SVV**ESDEL**	Q5DTJ9	MYPN_MOUSE Myopalladin - Mus musculus (Mouse)
6	SVV**ESDEL**	Q86TC92	MYPN_HUMAN Isoform 2 of Q86TC9 - Homo sapiens (Human)
6	NLP**ESEEL**	Q8TDC0	**MYOZ3_HUMAN FATZ-3 (Myozenin-3/Calsarcin-3)**
6	NLP**ESEEL**	Q8TDC02	MYOZ3_HUMAN Isoform 2 of Q8TDC0 - Homo sapiens
6	NLP**ESEEL**	Q08DI7	Q08DI7_BOVIN Myozenin 3 - Bos taurus (Bovine)
6	NLP**ESEEL**	Q1AG05	Q1AG05_PIG Calsarcin 3 - Sus scrofa (Pig)
6	KLP**ESEEL**	Q8R4E4	MYOZ3_MOUSE Myozenin-3 - Mus musculus (Mouse)
6	KLP**ESEEL**	Q9Z3272	SYNPO_RAT Isoform 2 of Q9Z327 - Rattus norvegicus
6	GLY**ESEEL**	Q9UBF9	**MYOTI_HUMAN Myotilin - Homo sapiens**
6	GLY**ESEEL**	Q0VCX9	Q0VCX9_BOVIN Similar to titin immunoglobulin domain protein
6	GLY**ESEEL**	Q9JIF9	MYOTI_MOUSE Myotilin - Mus musculus (Mouse)
6	GLY**ESEEL**	A0A509	A0A509_MOUSE Myotilin - Mus musculus (Mouse)

3.3 Preparation of native protein for use in AlphaScreen Experiments

In collaboration with the groups of Prof. Olli Carpen and Prof. Giorgio Valle we undertook a variety of experiments in order to test the hypothesis that the PDZ domain of the Enigma proteins ZASP, ALP and CLP-36 interact with the FATZ family of proteins, myotilin, palladin and myopalladin. One method used to detect binding was the AlphaScreen technique; the experiments were done in conjunction with our collaborators at CRIBI, University of Padova. This is an *in vitro* binding technique that can detect the interaction between two or more proteins with high level of sensitivity (Fig 10). The method is described in detail in the Material and Methods section.

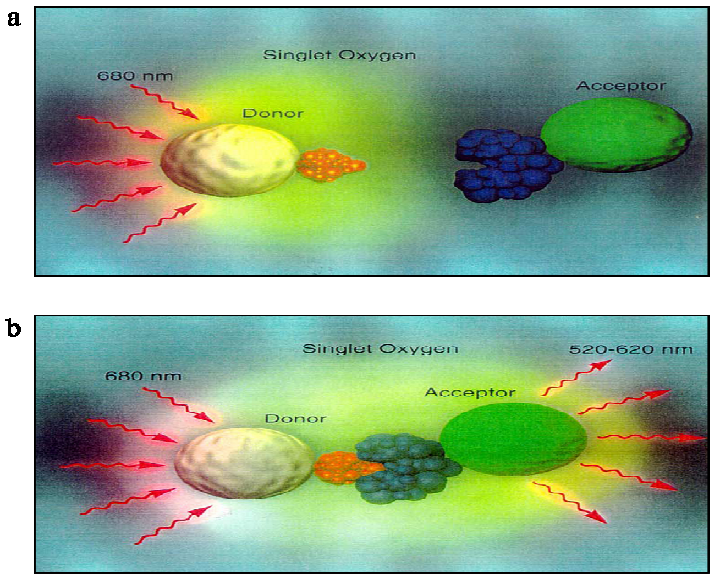

Figure 10. Diagram showing the principles of the AlphaScreen technique. When the donor beads are excited at a wavelength of 680 nm there are two possible outcomes: (**a**); there is no signal since the two proteins do not interact. (**b**); the two proteins interact and the distance between them is less than 200nm. This allows the transfer of singlet oxygen from the donor to the acceptor beads, resulting in emission from the acceptor beads at 520-620 nm (the diagrams are reproduced from the Pakard BioScience booklet "Principles of AlphaScreen").

I amplified and cloned the cDNA of the PDZ domains of ZASP, CLP-36 and ALP into prokaryotic vectors that express a His tagged recombinant protein. Figure 11 show the SDS-PAGE gel of the purification of ZASP native N-terminal His tagged PDZ protein used in the AlphaScreen, ALP and CLP-36 native His-tagged protein purifications were similar.

Also for AlphaScreen experiments I cloned, expressed and purified the native GST tagged full-length and truncated (lacking the terminal 5 amino acids) proteins of FATZ-1, FATZ-2, FATZ-3 and myotilin in bacteria (fig 12).

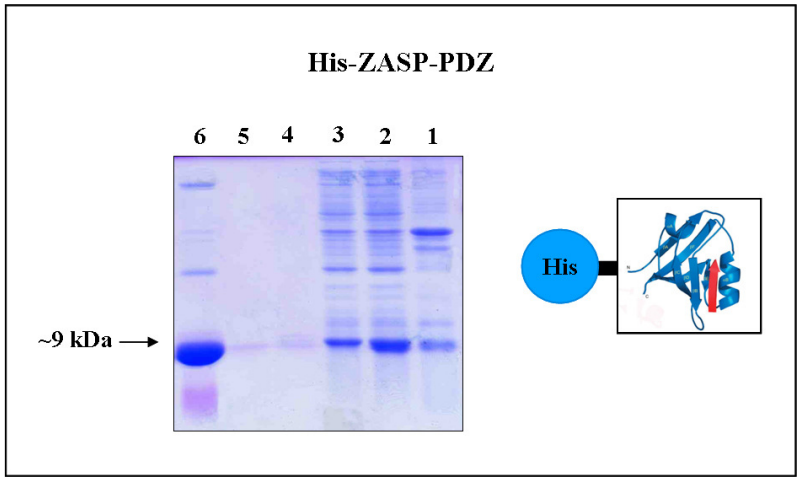

Figure 11. SDS-PAGE gel (15 %) stained with Coomassie blue showing the purification of the **ZASP His-PDZ** protein. 1) before induction with IPTG, 2) pellet (insoluble protein), 3) supernatant (soluble protein), 4) and 5) first and second washes, 6) the eluted protein (250 mM imidazole).

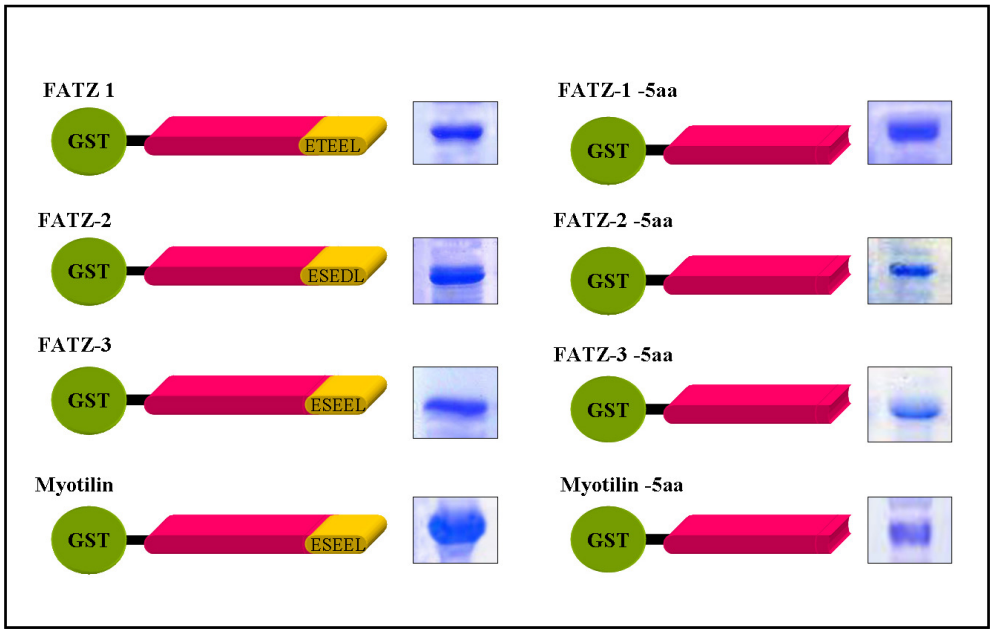

Figure 12. A schematic diagram showing the native GST tagged full-length and truncated (lacking the terminal 5 amino acids) proteins of FATZ-1, FATZ-2, FATZ-3 and myotilin produced for AlphaScreen experiments. The bands (taken from SDS-PAGE gels) close to each model show the native GST protein obtained after purification elution from glutathione resin.

3.4 *The C-terminal (last 5 amino acids) of the FATZ family and myotilin bind the PDZ domains of ZASP, ALP and CLP-36 proteins*

PDZ domains commonly bind the C-terminal of their interacting proteins. Therefore in order to check if the terminal 5 amino acids of the FATZ family, myotilin, palladin and myopalladin bind to the PDZ domains of ZASP, CLP-36 and ALP we performed binding experiments using both full-length and truncated (minus C-terminal 5 aa's) protein. The His-tagged PDZ domain proteins were bound to the donor beads and the GST tagged ligand bearing proteins to the acceptor beads. Since the proteins used in these experiments were expressed in bacteria they were not phosphorylated.

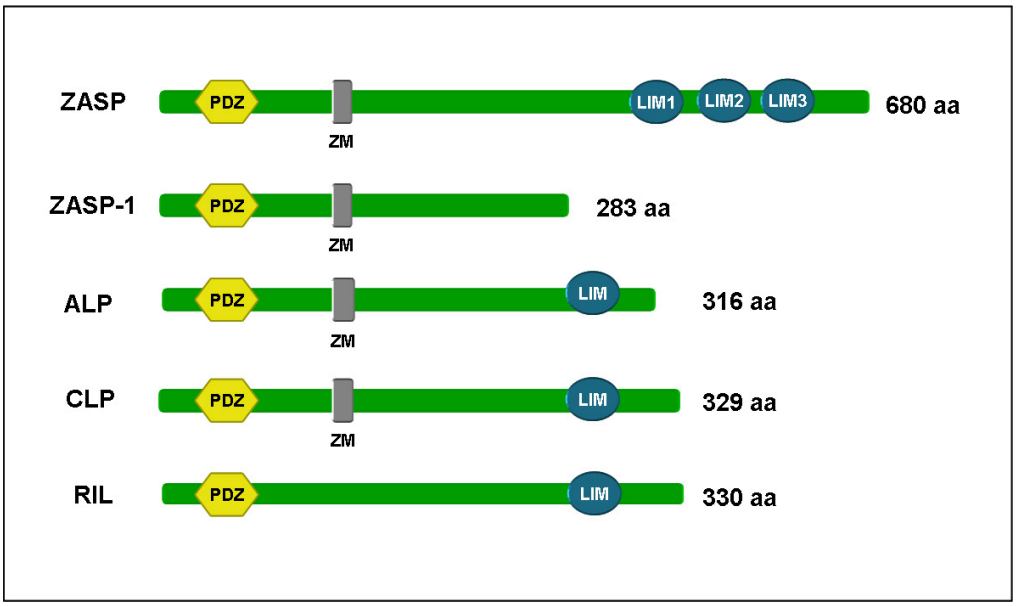

Figure 13. A schematic representation of four of the proteins of the enigma family ZASP, ALP, CLP-36 and RIL, with their different binding domains. All four proteins have a PDZ domain at their N-terminal and one or three LIM domains at the C-terminal of the protein. ZASP, ALP and CLP-36 have in common another binding motif called ZM. The ZASP-1 isoform of ZASP that lacks the LIM domains at the C-terminal was used in all of the experiments reported in this thesis.

A schematic diagram of the PDZ proteins studied can be found in Figure 13 showing that all of the proteins had single N-terminal PDZ domains and ALP, CLP-36 and RIL had single LIM domains towards the C-terminus. RIL was not used in AlphaScreen experiments but is a member of the Enigma family and detected in PDZ array experiments. The ZASP-1 isoform of ZASP was used in these experiments as it was the form detected by yeast-two- hybrid experiments to bind to myotilin (personal communication from Prof. Olli Carpen, unpublished data). All of the PDZ proteins used in this thesis with the exception of RIL had ZM motifs (fig 13).

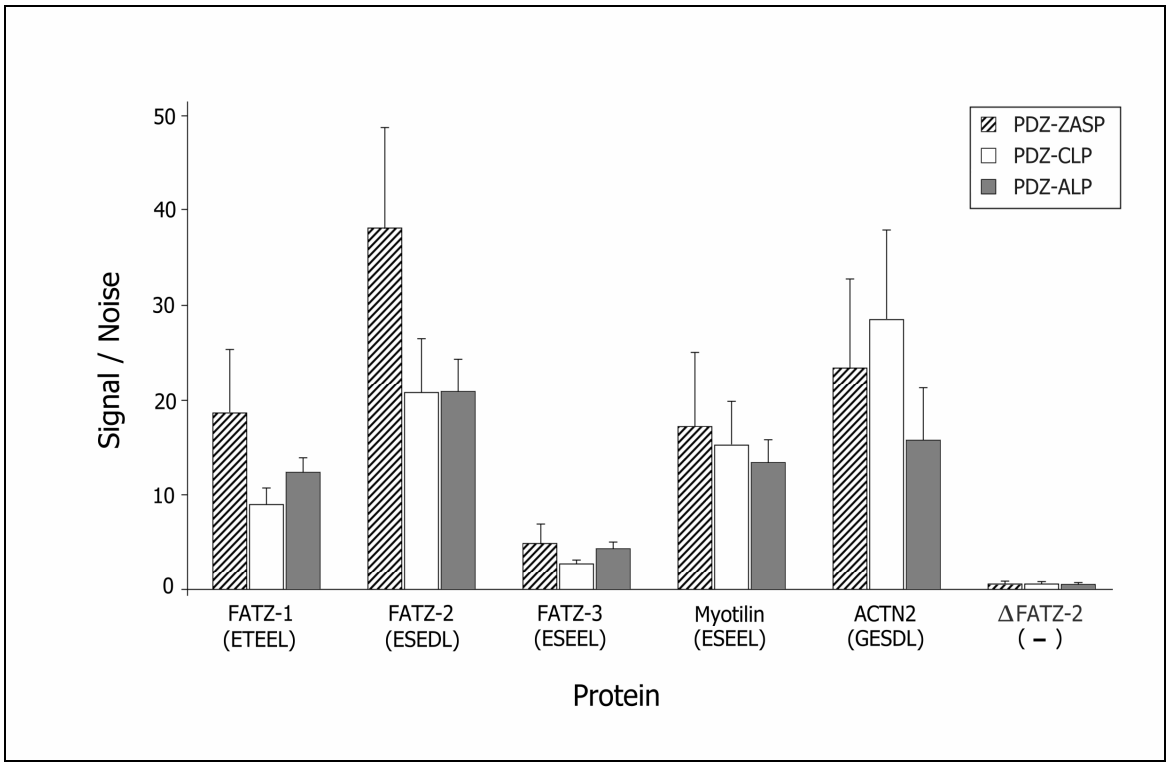

Figure 14. Results obtained from the AlphaScreen experiments using native His tagged PDZ proteins (ZASP, CLP and ALP) attached to the donor beads and native full length and truncated (minus the C-terminal 5 amino acids) GST proteins of FATZ-1, FATZ-2, FATZ-3, myotilin and α-actinin2 (ACTN2) attached to the acceptor beads. The concentration of the donor and acceptor proteins was 50 nM. The experiment was repeated at least three times and the standard deviations of the means are shown as bars at the top of the histograms.

From the results of the AlphaScreen experiments (fig 14) it is clear that all of the proteins studied (FATZ-1, FATZ-2, FATZ-3, myotilin and α-actinin2) with the exception of the truncated protein bind to the three PDZ domains (ZASP, ALP and

CLP-36). Truncated protein was produced for each of the proteins and tested but only the result for the truncated FATZ-2 protein is shown in the interests of clarity in Figure 14. All of the truncated proteins tested did not bind the PDZ domains studied. In Figure 14 it can be seen that although all of the PDZ domains were able to bind the proteins tested there was variability.

The PDZ domain of ZASP showed much stronger binding to the ligand proteins than the PDZ domains of ALP or CLP-36 with the exception of α-actinin2 had stronger binding to the PDZ domain of CLP-36. The best ligand protein for overall binding was FATZ-2 whereas FATZ-3 bound poorly to the three PDZ domains studied.

3.5 The PDZ domain of ZASP binds the IVTT full-length FATZ-3 but not truncated FATZ-3 (minus C-terminal 5 aa's)

The proteins used in the GST pulldown experiment are shown schematically in Figure 15a. In order to confirm the AlphaScreen result that FATZ-3 truncated protein is unable to bind the PDZ domain of ZASP I performed a GST pulldown *in vitro* binding assay. I used IVTT [^{35}S]-labeled FATZ-3 both full-length (251 aa) and truncated (1-246 aa) to pull down GST PDZ-ZASP and GST alone. As expected the full-length FATZ-3 but not the truncated FATZ-3 pulled down the GST PSZ-ZASP (Fig 15b). Neither protein bound strongly to GST alone.

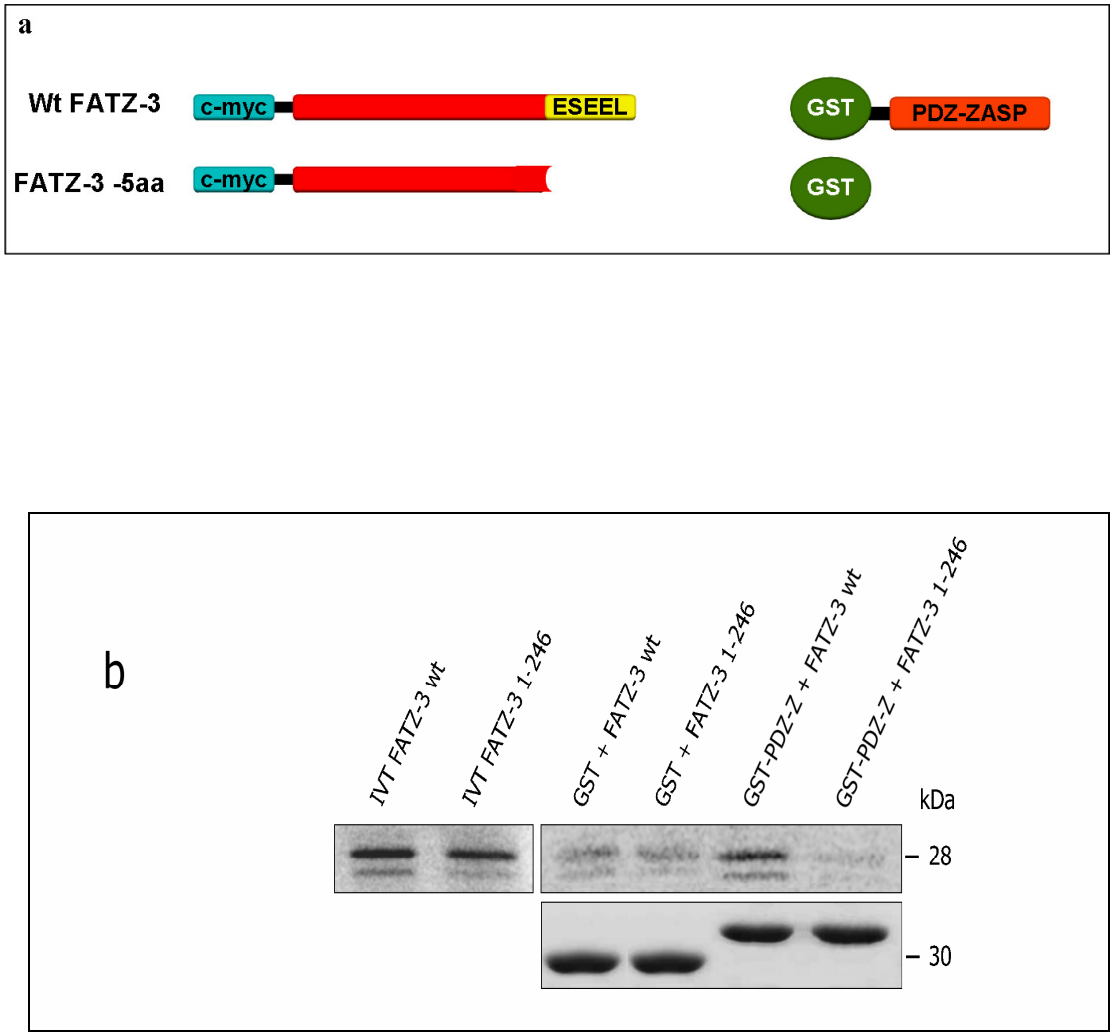

Figure 15. a). A schematic figure showing the FATZ-3 proteins both the full-length (251 aa) and the truncated minus the C-terminal 5 amino acids (246 aa). **b)** An autoradiograph of a GST pull down experiment showing that IVTT FATZ-3 full-length (wt) protein (251 aa's) binds to ZASP GST-PDZ (GST-PDZ-Z) protein whereas the FATZ-3 truncated C-terminal protein (246 aa's) does not. Neither protein bound strongly to GST alone. The first two columns show the input (50 %) of the IVTT proteins. The bottom row shows lanes from a SDS-PAGE gel stained with Coomassie blue. The lanes show the loading of the GST proteins confirming that equal amounts of ZASP GST-PDZ protein and GST protein were used in this experiment.

3.6 Peptides of the C-terminal amino acids of the FATZ family, myotilin, palladin and myopalladin bind to the PDZ domains of ZASP, ALP and CLP proteins

We designed peptides corresponding to the last 5 amino acids of the C-terminals of the proteins to be tested linked to two gamma-butyric acid (GABA) molecules that were used as non-hydrophobic linkers and biotin. These peptides were ETEEL (FATZ-1), ESEDL (FATZ-2 and palladin), ESEEL (FATZ-3 and myotilin) and ESDEL (myopalladin). It is known that the type of amino acid at position 0 is important for the binding between the ligand and the PDZ domain as changing this amino acid can either destroy or alter the binding. Therefore a peptide was designed ESEEE with the last amino acid changed from leucine (L) to glutamic acid (E) to test the specificity of binding.

The biotinylated peptides were bound to the donor beads and the His tagged PDZ proteins for ZASP, CLP-36 and ALP were bound to the acceptor beads, the experiment was performed as detailed in the Material and Methods. The PDZ domain proteins were used at a concentration of 50nM whereas the peptides were used at a concentration of 10 nM with the exceptions of ESEEE and ESDEL that were used at concentrations of 25 and 50 nm respectively. Therefore the binding seen for these peptides when compared to the others was even lower than that depicted in Figure 16.

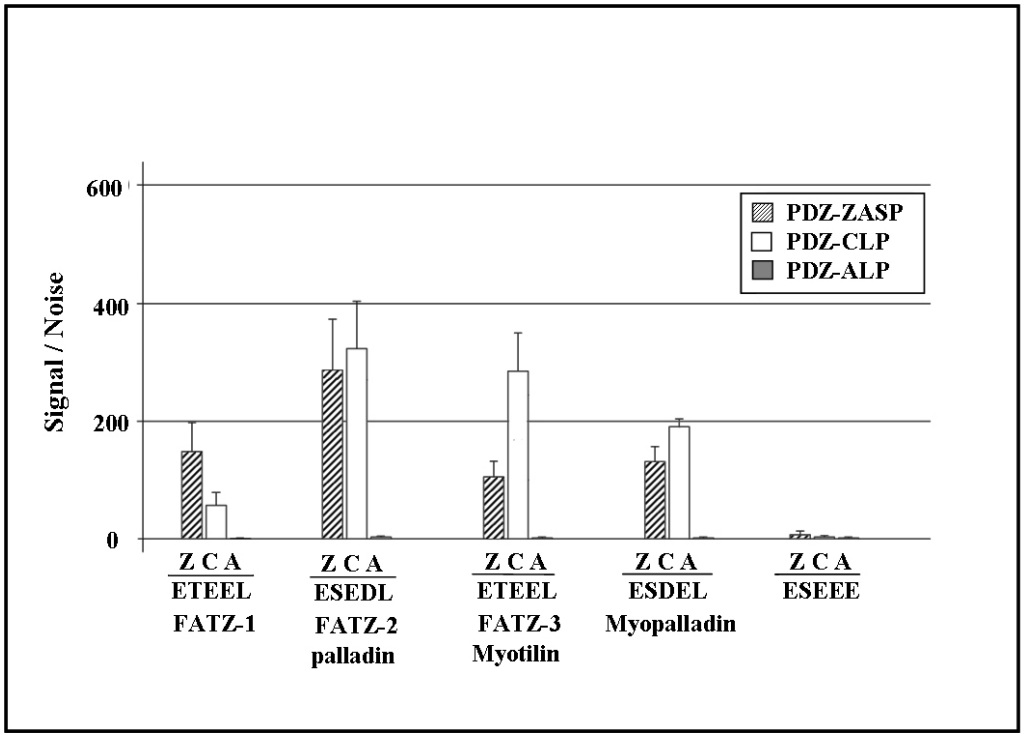

Figure 16. Results obtained from the AlphaScreen experiments using biotinylated peptides (donor) and His tagged PDZ proteins (acceptor). The peptides which correspond to last 5 amino acids of the C-terminals of FATZ-1, FATZ-2/palladin, FATZ-3/myotilin, myopalladin as well as the mutated peptide with the L changed to E were tested for binding to the PDZ domains of ZASP (Z), CLP-36 (C) and ALP (A). The experiment was repeated at least three times and the standard deviations of the mean are shown as bars at the top of the histograms.

From the results of the AlphaScreen experiments shown in Figure 16 it can be seen that all of the peptides bind to the different PDZ domain proteins with the exception of the mutated peptide (ESEEE) with the last amino acid L substituted with E. Therefore the last amino acid is crucial for the interaction with the PDZ motif of ZASP, CLP-36 and ALP. These results confirm the computer prediction that the last four amino acids of the FATZ family, myotilin, palladin and myopalladin were PDZ binding ligands.

The variation in binding is dependent both on the peptide and the PDZ domain studied. The FATZ-1 peptide would seem to bind better to the PDZ domain of ZASP whereas the FATZ-2/palladin peptide binds equally well to the PDZ domain of CLP36 and ZASP. FATZ-3/myotilin and myopalladin both bind better to the PDZ domain of CLP-36. It should be noted that both the peptides and the proteins are non-phosphorylated (fig 16).

3.7 Phosphorylation affects the binding activity of the C-terminal amino acid peptides to the PDZ domains of ZASP, CLP-36 and ALP:

To determine the influence of phosphorylation on the binding between the biotinylated peptides and the PDZ domains; peptides were designed phosphorylated on either the serine (EpSEEL, EpSEDL, EpSDEL, EpSEEE) or the Threonine (EpTEEL) residues. These phosphorylated peptides were tested for binding activity with the PDZ domains of ZASP, CLP-36 or ALP using AlphaScreen. The phosphorylated peptides were bound to the donor beads and the native His tagged PDZ domain proteins were bound to the acceptor beads. There was a significant difference in the strength of the binding between different phosphorylated peptides to the PDZ domains (fig 17)

Although there is variation in the strength of binding all the phosphorylated peptides bind well with the PDZ domain of ZASP. The strongest binding being that of the FATZ-3/myotilin peptide followed in order of decreasing strength by that of FATZ-2/palladin, FATZ-1, myopalladin respectively. The peptide mutated EpSEEE did not show any appreciable binding to the three PDZ domains used in these experiments. Only the FATZ-3/myotilin and the FATZ-2/palladin phosphorylated peptides showed appreciable binding with the CLP-36 and ALP PDZ domains. The binding to the ALP

PDZ domain was particularly weak since 5 times more peptide was used in these binding experiments than in the others. If the same concentration was used (ie 10 nM) no binding was seen.

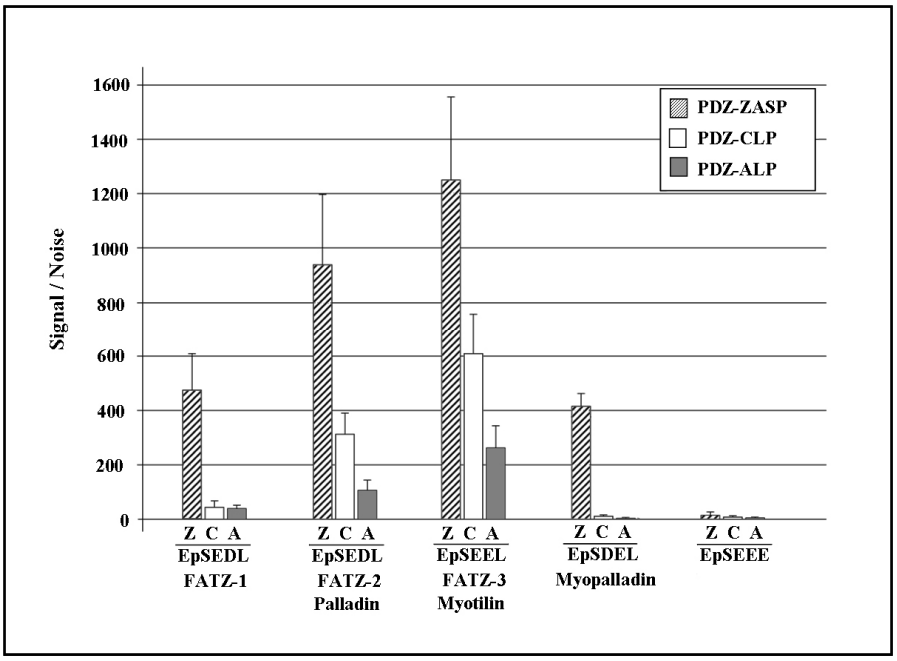

Figure 17. Results from AlphaScreen experiments showing the binding of the phosphorylated peptides with the PDZ domains of ZASP (Z), CLP (C) and ALP (A). The His tagged PDZ domain proteins were used at a concentration of 50 nM whereas the phosphorylated peptides were used at a concentration of 10 nM the exceptions to this were ESEDL and ESEEE that were used at 50 nM. The experiment was repeated at least three times and the standard deviations of the means are shown as bars at the top of the histograms.

Seen in Figure 18 is a composite diagram showing results of the AlphaScreen binding experiments for both the non-phosphorylated peptides (fig 16) and the phosphorylated peptides (fig 17). The results show the binding between the peptides and the PDZ domains of ZASP, CLP-36 and ALP. The strength of the binding interactions varied

between peptides and also PDZ domains. The mutated peptide phosphorylated (EpSEEE) or not (ESEEE) showed no binding with any of the PDZ domains. This result is in keeping with the known literature on PDZ domain interactions, namely that the last amino acid of the C-terminal ligand is crucial for the binding. Therefore we can conclude that this observation is also true for the binding of the **E[ST][DE][DE]L** ligand to the PDZ domains of ZASP, CLP-36 and ALP (fig 18). Previously, it was not known that the FATZ family, myotilin, palladin and myopalladin could bind to CLP-36 and ALP.

Mutated peptides (ESEEE, EpSEEE): Both the phosphorylated and non phosphorylated peptide showed no binding with the PDZ domains of ZASP, CLP-36 and ALP (Fig. 18).

FATZ-1 (ETEEL, EpTEEL): The phosphorylated peptide showed stronger binding to the ZASP-PDZ domain than to the PDZ domains of CLP-36 and ALP and this was also true for the non phosphorylated peptide. Therefore for the FATZ-1 ligand phosphorylation would appear to be an advantage at least for binding the PDZ domain of ZASP (fig. 18). The binding to CLP-36 although weak did not change due to phosphorylation.

FATZ-2/palladin (ESEDL, EpSEDL): The phosphorylated peptide showed stronger binding to the ZASP-PDZ domain than to the PDZ domains of CLP-36 and ALP. The non phosphorylated peptide showed the strongest binding to the CLP-36 PDZ domain. For the FATZ-2/palladin ligand phosphorylation would appear to be an advantage at least for binding the PDZ domain of ZASP (fig. 18). The binding to CLP-36 did not change due to phosphorylation. However it is notable that only the phosphorylated peptide was able to bind the PDZ domain of ALP.

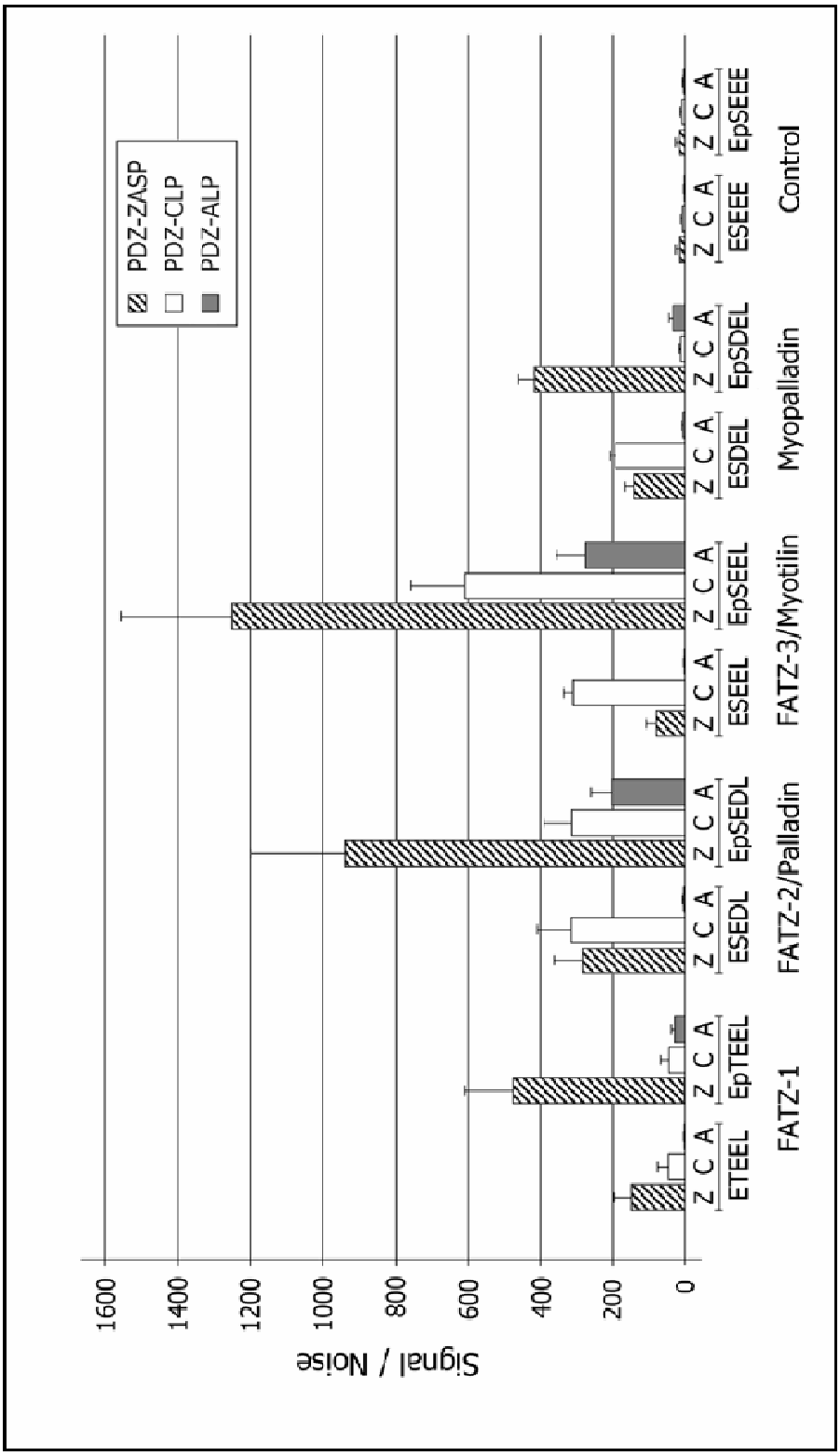

Figure 18. A composite diagram showing together the results of the AlphaScreen experiments for the bindings of both the non-phosphorylated peptides (fig 15) and the phosphorylated peptides (fig 16) with the PDZ domains ZASP (Z), CLP (C) and ALP (A). These experiments were repeated at least three times and the standard deviations of the means are shown as bars at the top of the histograms.

FATZ-3/ myotilin (ESEEL, EpSEEL): The phosphorylated peptide showed stronger binding to all three PDZ domains than the non phosphorylated peptide. It is interesting that also in this case only the phosphorylated peptide was able to bind the ALP PDZ domain. Therefore for FATZ-3/myotilin phosphorylation had positive effect on the interactions with the PDZ domains of ZASP, CLP-36 and ALP (Fig. 18).

Myopalladin (ESDEL, EpSDEL): The phosphorylated peptide showed stronger binding to the ZASP PDZ domain than the non-phosphorylated peptide. On the other hand the non-phosphorylated peptide showed stronger binding to the CLP-36 PDZ domain than the phosphorylated peptide. There was only very weak binding of the phosphorylated peptide to the ALP PDZ domain and none with the non-phosphorylated peptide. In the case of myopalladin phosphorylation had positive effect on the interaction with the PDZ domains of ZASP and ALP and negative effect on that of CLP-36 (Fig. 18).

3.8 The C-terminal FATZ-1 (CD2) competes with the binding between the phosphorylated and non phosphorylated peptides of FATZ-3/myotilin and the ZASP-1 protein:

One of the advantageous of the AlphaScreen technique is that it can be used for performing competition studies. In this competition experiment we used the C-terminal domain of the FATZ-1 protein (CD2) as competitor for the binding between the peptides phosphorylated and non-phosphorylated of FATZ-3/myotilin and the ZASP-1 protein (fig 19).

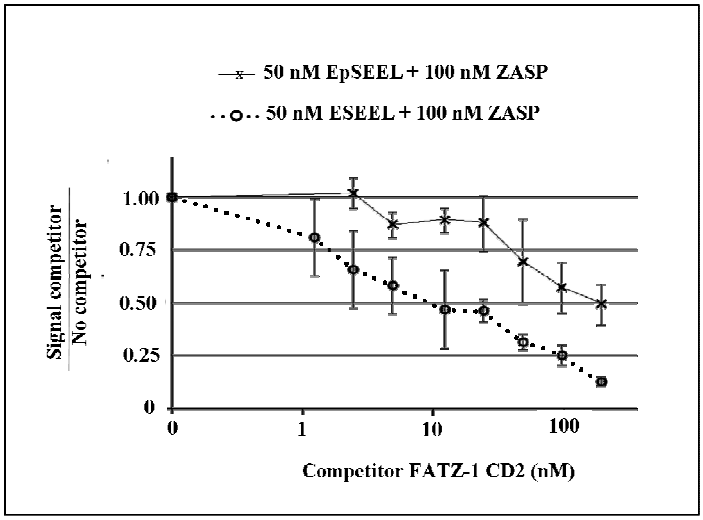

Figure 19. Results of the AlphaScreen competition assay. The phosphorylated (EpSEEL) and non-phosphorylated (ESEEL) FATZ-3/myotilin peptides were used at a concentration of 50 nM and the ZASP-1 protein at 100 nM. The strength of binding of these peptides to the ZASP-1 protein was taken as 100 % when measured without the addition of the competitor. Increasing amounts of the competitor (the C-terminal domain of the FATZ-1-CD2 protein) were added to the interaction. The standard deviation of the means were added as lines either side of the points denoting the Signal/Noise ratio.

The CD2 region of FATZ-1 is the C-terminal part of the protein comprising of amino acids 171 to 299 (Faulkner et al., 2000). The non-phosphorylated native His tagged C-terminal FATZ-1 protein (CD2) was able to compete better with the binding between the non-phosphorylated peptide and the native ZASP-1 protein than with the binding between the phosphorylated peptide and the ZASP-1. It required 10 nM of the competitor protein to knockdown 50 % of the binding strength in the case of the non-phosphorylated peptide and 100 nM in the case of the phosphorylated peptide. This correlates with what could be deduced from the strength of binding of the

phosphorylated and non-phosphorylated FATZ-3/myotilin peptides with the PDZ domain pf ZASP noted in the previous experiments (fig 18) since that of the phosphorylated peptide was stronger. Therefore this result confirms that the AlphaScreen can measure qualitatively the strength of binding of an interaction and that the full-length protein behaves in a similar manner to the PDZ domain alone. A schematic model of the AlphaScreen interactions can be seen in Figure20.

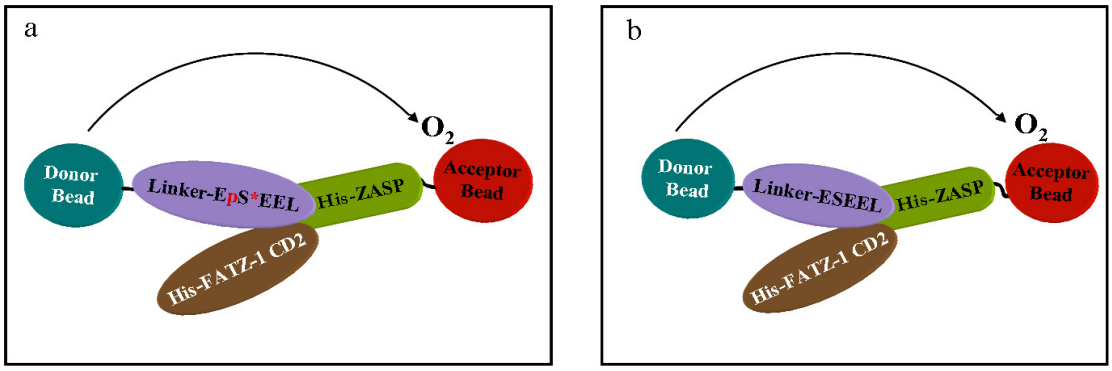

Figure 20. Schematic diagrams depicting the competition by the native His tagged FATZ-1 protein of the binding between the native ZASP-1 protein and the **a**) phosphorylated and **b**) non-phosphorylated FATZ-3/myotilin.peptides.

3.9 The ACTN2 protein competes with the binding between the phosphorylated and non-phosphorylated peptides of FATZ-3/myotilin and the ZASP-1 protein.

It is known that α-actinin2 (ACTN2) binds the PDZ domain of ZASP (Zhou et al., 1999). The final four amino acids of the C-terminal of ACTN2 constitute a binding motif for class I PDZ domain proteins: X[ST]X[VIL] where X is any amino acid. In PDZ domain nomenclature since ZASP PDZ binds ACTN2 it would be classified as a

type I PDZ domain however we have shown that it can also be classified as a type III PDZ domain. Therefore we wanted to check if ACTN2 was capable of competing the binding between the ZASP-1 protein and the phosphorylated and non-phosphorylated peptides of FATZ-3/myotilin that is an interaction with a type III ligand (fig 21).

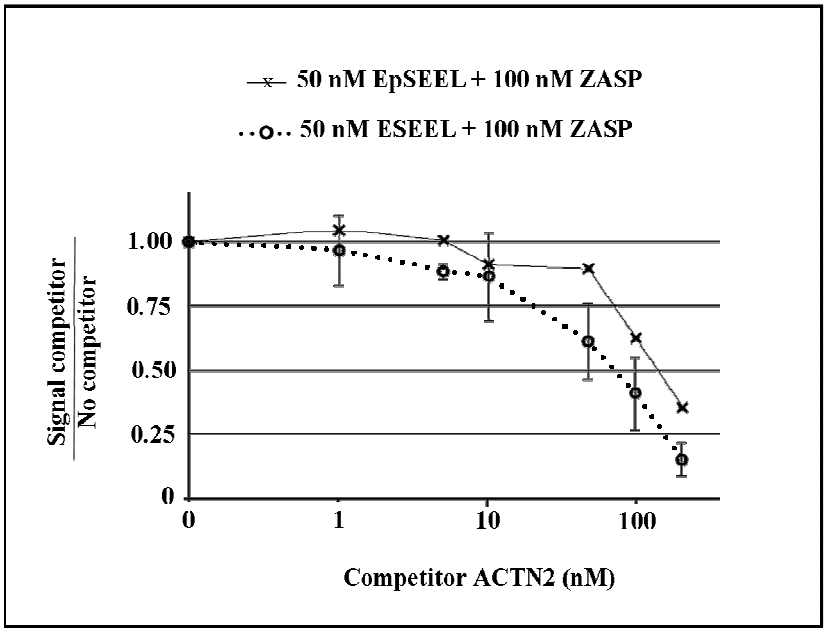

Figure 21. The competition of ACTN2 for the binding of non-phosphorylated and phosphorylated peptides of FATZ-3/myotilin with ZASP-1 protein detected using the AlphaScreen technique.

Although the difference was not as striking as with the FATZ-1 CD2 protein the non-phosphorylated native His tagged ACTN2 was able to compete better with the binding between the native ZASP-1 protein and the non phosphorylated FATZ-3/myotilin. Until a concentration 10 nM of this competitor protein there was no appreciable reduction in the binding strength. In the case of the non-phosphorylated peptide binding ZASP-1 at 100 nm concentration there was approximately a 40 % decrease in binding whereas in

the case of the phosphorylated the decrease was approximately 60 % (fig 20). Therefore the ACTN2 protein is capable of interfering with the binding between a class III PDZ domain ligand and ZASP-1. A schematic model of the AlphaScreen interactions can be seen in Figure22

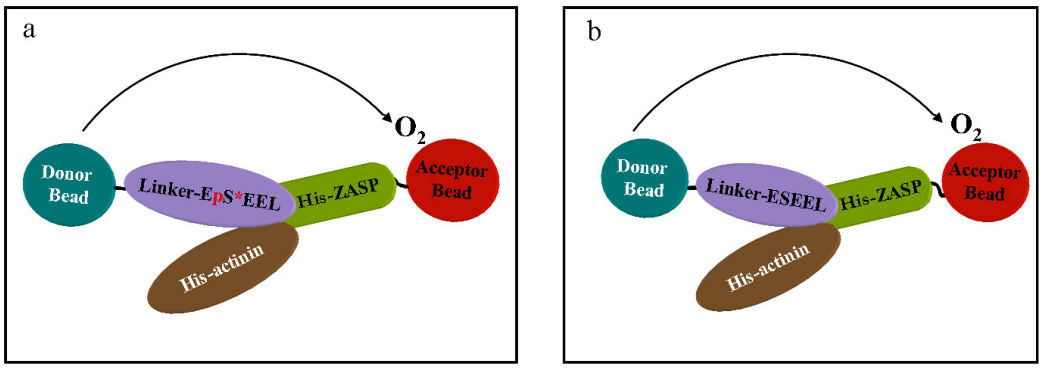

Figure 22. Schematic diagrams depicting the competition by the native His tagged ACTN2 protein of the binding between the native ZASP-1 protein and the **a**) phosphorylated and **b**) non-phosphorylated FATZ-3/myotilin.peptides.

3.10 PDZ array experiments

It was important to know if the **E[ST][DE][DE]L** motif was specific for a set of PDZ domain proteins or if it bound ubiquitously to any PDZ domain therefore as a way of testing several PDZ domains for binding to this ligand a commercial array of PDZ proteins was used (Panomics PDZ Array I). There are 28 different GST tagged PDZ domain proteins spotted in duplicate on the blot as well as positive and negative control proteins (fig 23).

A	Mint-2-D1		Mint-3-D1		Mint-3-D2		Mint-1-D1		Mint-1-D2		CSKP		Dlg-D1		Dlg1-D3		pos	
B	Dlg2-D2		Dlg4-D3		DVL1		DVL3		DVLL		GIPC		HtrA2		LIMK2		pos	
C	MPP2		NEB1		OMP25		hCLIM1		PTPH1		ZO-2-D1		hPTP1E-D1		hPTP1E-D5		pos	
D	RGS12		RIL		ZO-1-D3		ZO-2-D3		GST								pos	
E	pos		pos		pos		pos		pos		pos		pos		pos		pos	
	1	2	3	4	5	6	7	8	9	10	11	12	13	14	15	16	17	18

Figure 23. Schematic diagram of the TranSignal PDZ Domain Array I. The proteins on the array are spotted in duplicate at 100 ng. Positive controls (Histidine tagged ligands) are spotted along the row E and the columns 17 and 18, a negative control (GST protein) was spotted at position D 9 and 10 (Panomics)

.

In the PDZ array experiments I used the same biotinylated phosphorylated and non-phosphorylated peptides that we had previously used for the AlphaScreen experiments but at a concentration of 0.3 µg/ml, as well as native His tagged C-terminal FATZ-3 (81-251 aa) protein at a concentration of 15 µg. The results with the various peptides are detailed below.

3.10.1 FATZ-1 peptides bind to the PDZ domain of hCLIMI (CLP-36) and RIL

Both the phosphorylated (EpTEEL) and the non-phosphorylated (ETEEL) peptides corresponding to the last 5 amino acids of FATZ-1 were incubated with individual

membranes in order to check for interactions with PDZ domain proteins. The strength of the binding of the biotinylated ligand to the GST PDZ protein roughly correlates with the intensity of the signal detected. The phosphorylated peptide had a stronger binding to the PDZ domain of hCLIM1 (CLP-36) than the non-phosphorylated peptide (fig 24) which confirms with the result obtained using the AlphaScreen technique (fig 18). Also both peptides bound to a new PDZ domain protein, RIL (fig 24). As can be seen in Figure 24 the binding with RIL was strong and phosphorylated peptide bound better than the non-phosphorylated peptide

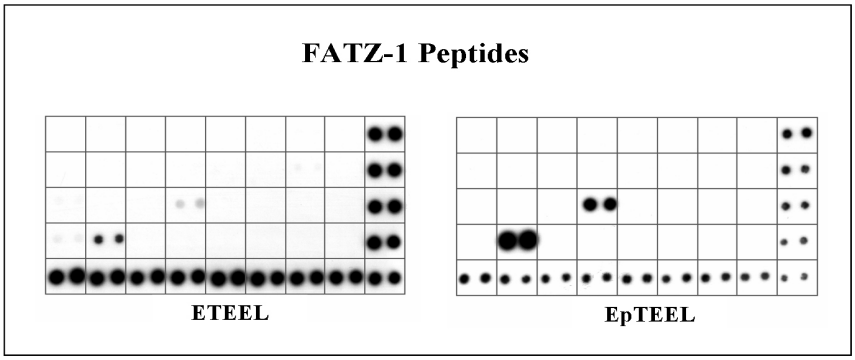

Figure 24. PDZ Array blots showing the interactions of the phosphorylated (EpTEEL) and non-phosphorylated (ETEEL) FATZ-1 peptides with the GST PDZ domain proteins on the blot. The only PDZ domain proteins positive in both blots were hCLIMI (CLP-36) and RIL.

3.10.2 FATZ-2/palladin peptides bind to the PDZ domain of hCLIMI (CLP-36) and RIL

The phosphorylated (EpSEDL) and non-phosphorylated (ESEDL) peptides of FATZ-2/palladin were individually incubated with the two membranes.

Both peptides showed interactions with the PDZ domain of hCLIM1 (CLP-36) and RIL however the non-phosphorylated peptide bound better to RIL (Fig 25). Both peptides

bound with equal strength to hCLIMI (CLP-36) confirming the AlphaScreen result (fig 18).

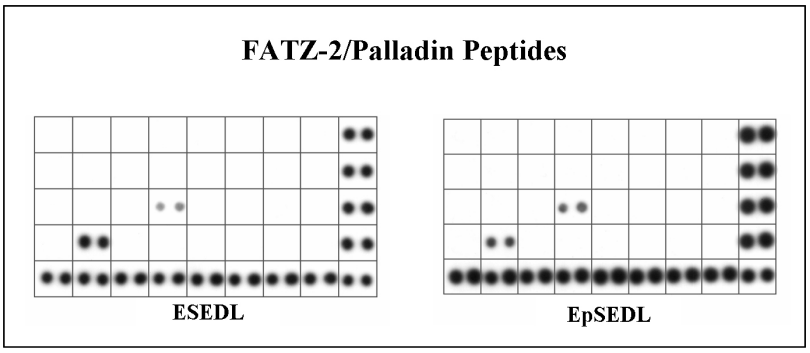

Figure 25. PDZ array blots showing the interaction of the non-phosphorylated (ESEDL) and phosphorylated (EpSEDL) FATZ-2/palladin peptides with the PDZ domain of hCLIM1 (CLP-36) and RIL.

3.10.3 FATZ-3/myotilin peptides bind to the PDZ domain of CLP and RIL

The phosphorylated (EpSEEL) and non-phosphorylated (ESEEL) peptides corresponding to the last 5 amino acids of FATZ-3/myotilin were incubated with two different membranes and showed binding to the PDZ domain proteins of hCLIM1 (CLP-36) and RIL (fig 26). In this instance the non-phosphorylated peptide bound stronger to the RIL PDZ domain protein than the phosphorylated peptide.

However inexplicably the non-phosphorylated peptide bound stronger to the hCLIM1 (CLP-36) protein this is in contradiction to the results found using the AlphaScreen. The amount of protein blotted can vary therefore the PDZ Array is less precise than the AlphaScreen were accurate concentrations of peptides and proteins can be compared.

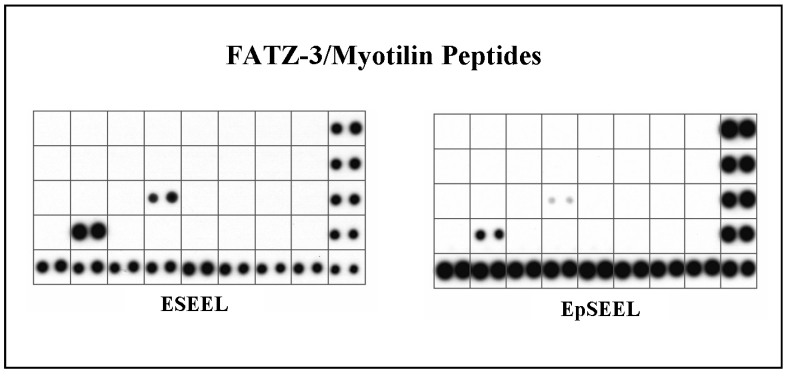

Figure 26. PDZ Array blots showing the interaction of the non-phosphorylated (ESEEL) and phosphorylated (EpSEEL) FATZ-3/myotilin peptides with the PDZ domain proteins hCLIM1 (CLP-36) and RIL.

3.10.4 Myopalladin peptides bind to the PDZ domain of CLP and RIL

The non-phosphorylated (ESDEL) myopalladin peptide bound stronger to the PDZ domain proteins hCLIM1 (CLP-36) and RIL than the phosphorylated peptide (EpSDEL) (fig 27). This result confirms that of the AlphaScreen for the non-phosphorylated myopalladin peptide (fig 18).

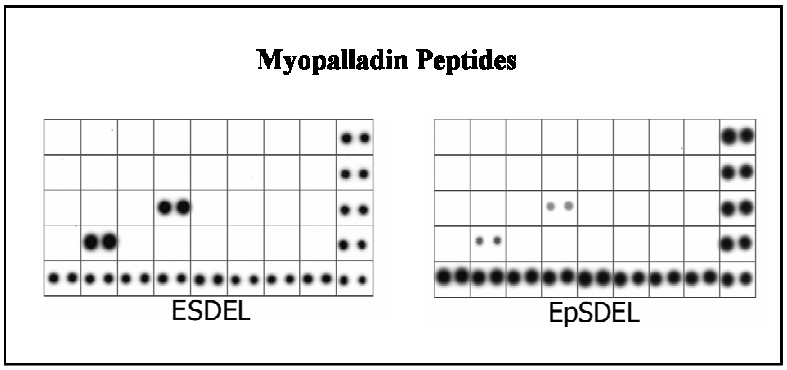

Figure 27. PDZ Array blots showing the interaction of the non-phosphorylated (ESDEL) and phosphorylated (EpSDEL) myopalladin peptides with the PDZ domain of hCLIM1 (CLP-36) and RIL.

3.10.5 The mutated peptides do not bind to the PDZ domains of hCLIM1 (CLP-36) and RIL

The phosphorylated (EpSEEE) and non-phosphorylated (ESEEE) mutated peptides were both tested for binding to the GST PDZ domain proteins. As expected both of these peptides did not show any binding with hCLIM1 (CLP-36) and RIL. However the phosphorylated peptide did interact with another the PDZ domain protein, Dlg4-D3. Thus showing that by changing the amino acid at position 0 you can destroy its binding to RIL and hCLIM1 (CLP-36) as well as changing the specificity of the binding (fig 28).

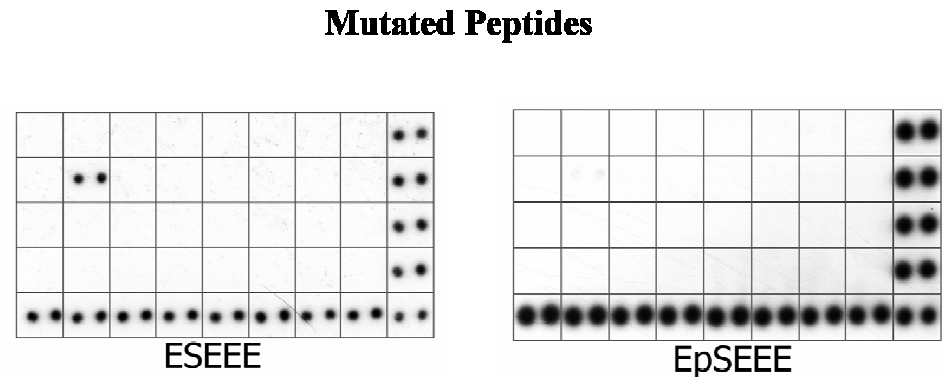

Figure 28. PDZ Array blots showing that the non-phosphorylated (ESEEE) and phosphorylated (EpSEEE) mutated peptides did not interact with the PDZ domain proteins hCLIM1 (CLP-36) and RIL. The non-phosphorylated peptide ESEEE bound to the PDZ domain of Dlg4-D3 protein.

3.10.6 The C-terminal FATZ-3 protein behaves as the non-phosphorylated FATZ-3/myotilin peptide

I produced and purified native His tagged protein of the C-terminal of FATZ-3 (81-251 aa) to check if this protein could show the same binding activity as the non-phosphorylated peptide (ESEEL). As can be seen in Figure 29 the C-terminal protein binds well to the PDZ domains of hCLIM1 (CLP-36) and RIL. The FATZ-3 protein and peptide both showed the same binding activity with these PDZ domain proteins (fig 29). This confirms that the biotinylated 5 amino acid peptides behave in a similar manner to the native His tagged protein in binding experiments.

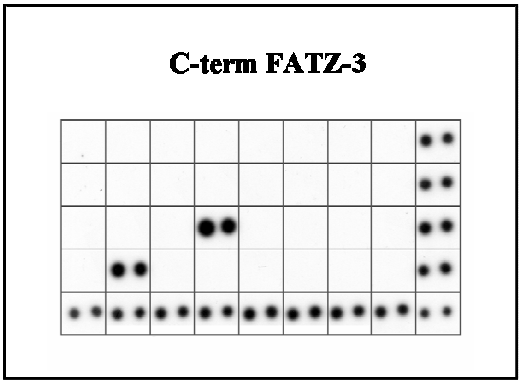

Figure 29. PDZ Array blot, showing that the native His tagged FATZ-3 C-terminal protein (~15ug/ml) interacts with the PDZ domain proteins of hCLIM1 (CLP-36) and RIL.

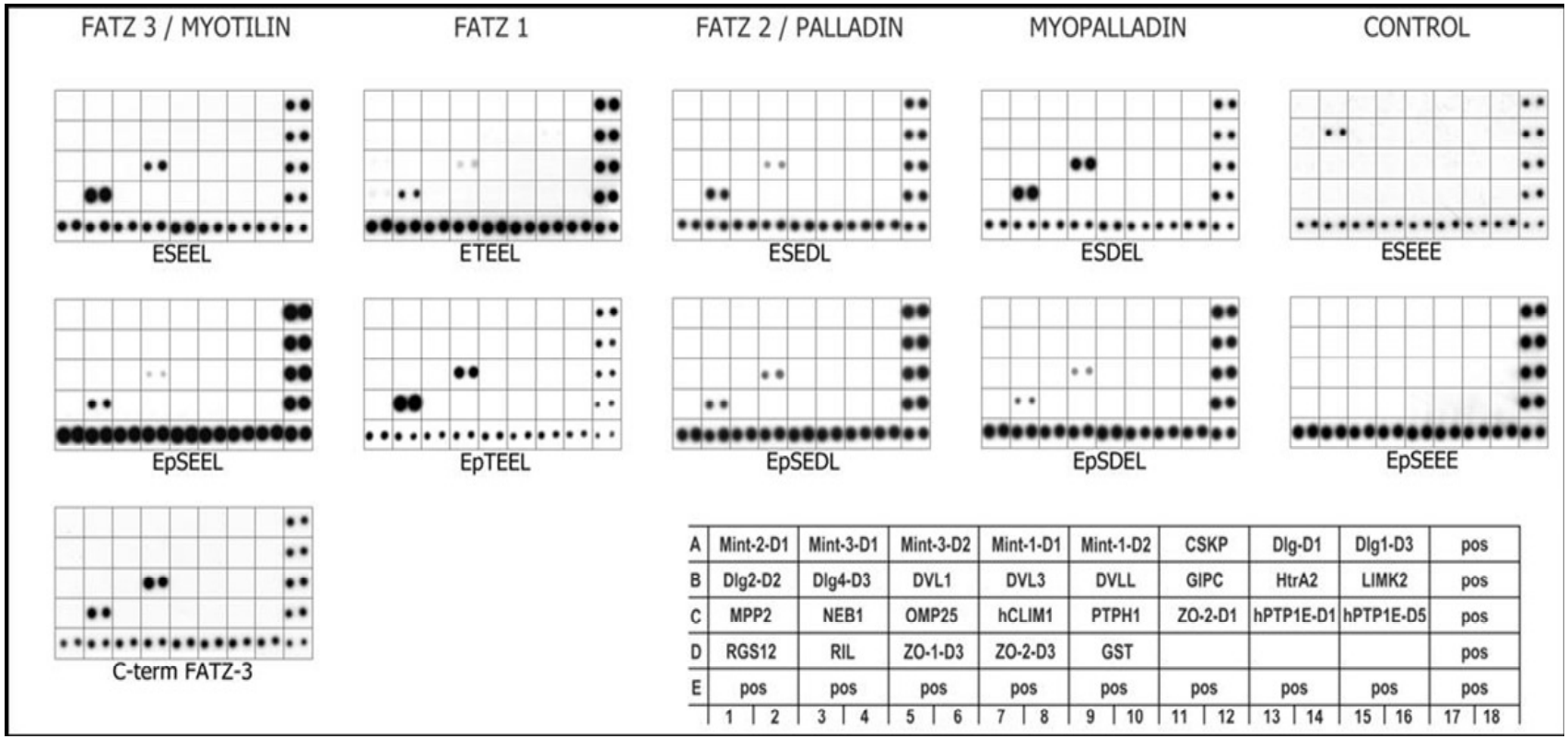

A	Mint-2-D1	Mint-3-D1	Mint-3-D2	Mint-1-D1	Mint-1-D2	CSKP	Dlg-D1	Dlg1-D3	pos
B	Dlg2-D2	Dlg4-D3	DVL1	DVL3	DVLL	GIPC	HtrA2	LIMK2	pos
C	MPP2	NEB1	OMP25	hCLIM1	PTPH1	ZO-2-D1	hPTP1E-D1	hPTP1E-D5	pos
D	RGS12	RIL	ZO-1-D3	ZO-2-D3	GST				pos
E	pos	pos	pos	pos	pos	pos	pos	pos	pos
	1 2	3 4	5 6	7 8	9 10	11 12	13 14	15 16	17 18

Figure 30. A composite figure of the PDZ Array experiments using the phosphorylated and non-phosphorylated peptides. All peptides showed interaction with the GST tagged PDZ domain proteins of hCLIM1 (CLP-36) and RIL. The exception being the non-phosphorylated mutated peptide that interacts with the PDZ domain of Dlg4-D3 protein. The C-terminal FATZ-3 protein was used at a concentration of ~15 ug/ml and the biotinylated peptides at approximately 03 ug/ml.

It can be seen in figure 30 that all of the peptides with the exception of the mutated peptides bind to the PDZ domain proteins of hCLIM1 (CLP-36) and RIL. The non-phosphorylated mutated peptide interacts with the PDZ domain of Dlg4-D3 protein. Unfortunately the proteins for ALP and ZASP were not present in these commercial Arrays therefore only the results for CLP-36 can be directly compared with the AlphaScreen results. The poor binding of the phosphorylated myopalladin peptide to CLP-36 confirms our AlphaScreen findings, as does the FATZ-2/palladin binding which was the same for both the phosphorylated and non-phosphorylated peptides. In contrast the binding of the FATZ-1 non-phosphorylated peptide was weaker in the blot than that seen by AlphaScreen were both the phosphorylated and non-phosphorylated peptides showed equal binding. The binding with the FATZ-3/myotilin peptide is also in contrast to the AlphaScreen result as the phosphorylated peptide did not bind well.

The binding of RIL to the FATZ family, myotilin , palladin and myopalladin was previously unknown although it is in keeping with the fact that the RIL belongs to the Enigma family of proteins which includes ZASP, CLP-36 and ALP.

3.11 FATZ-3 interacts with Ankrd2

During a search for new binding partners for FATZ-3 I found that Ankrd2 could bind FATZ-3. I confirmed this by co-immunoprecipitation experiments in COS-7 cells. In these experiments COS-7 cells were transfected with FLAG-tagged FATZ-3 alone or with c-myc-tagged full length Ankrd2. Cell lysates from transfected cells and non-transfected cells were immonuprecipitated with antibody against the c-myc tag, the cell lysate was subjected to SDS-PAGE, immunoblotted and then probed with antibody against the FLAG-tag. A positive band was detected in the double transfections indicating that FATZ-3 interacts with Ankrd2 since it could be detected by co-immunoprecipitation (Fig 31).

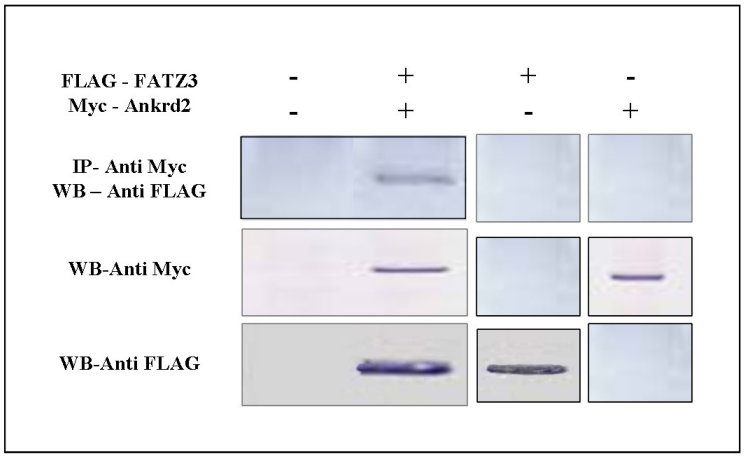

Figure 31. Co-IP of Ankrd2 and FATZ-3 transfected COS-7 cell lysates (100 µg). The cell lysates were immunoprecipitated with anti-c-myc monoclonal antibody separated by SDS-PAGE, immunoblotted and detected with anti-FLAG monoclonal antibody. Lane 1, cell lysates from non-transfected COS-7 cells; lane 2; cell lysates from COS-7 transfected with pCMV-FLAG-FATZ-3 and with pCMV-cmyc Ankrd2; lane 3, transfected with pCMV-FLAG-FATZ-3 alone; lane 4, cell lysates from COS-7 transfected with pCMV-cmyc Ankrd2 alone.

3.11.1 The N-terminal FATZ-3 binds Ankrd2

In order to determine region of FATZ-3 interacting with Ankrd2 I made two constructs of the FATZ-3 gene; an N-terminal (1-540 bp) which encodes a (1-180aa) protein and a C-terminal (241-753bp) which encodes a (81-251aa) protein. Both constructs share an overlap of 300 bp which encodes for a central region (81-180aa) of the FATZ-3 protein (fig 32a). COS-7 cells were transfected with N-terminal FLAG-tagged constructs of FATZ-3 full-length (as positive control), N-term-FATZ (1-180 aa), C-term-FATZ-3 (81-251 aa) and a c-myc tagged Ankrd2 construct as well as the vectors without inserts (negative controls). Cell lysates (70 ug) were immonuprecipitated with antibody against c-myc the then separated by SDS-PAGE, immunoblotted and probed with anti-FLAG antibody. Both full length and N-terminal FATZ-3 were able to bind to Ankrd2 as it co-immunoprecipitated with them. There was no binding of Ankrd2 with the C-terminal of FATZ-3. Therefore the binding region for Ankrd2 is the first 180 amino acids of the N-terminal of FATZ-3 (fig 32b). Western blots of cell lysates show the amount of proteins expressed in transfected cells and that there was no cross reaction of the cmyc antibody and the Flag tag and vice versa (fig 32b).

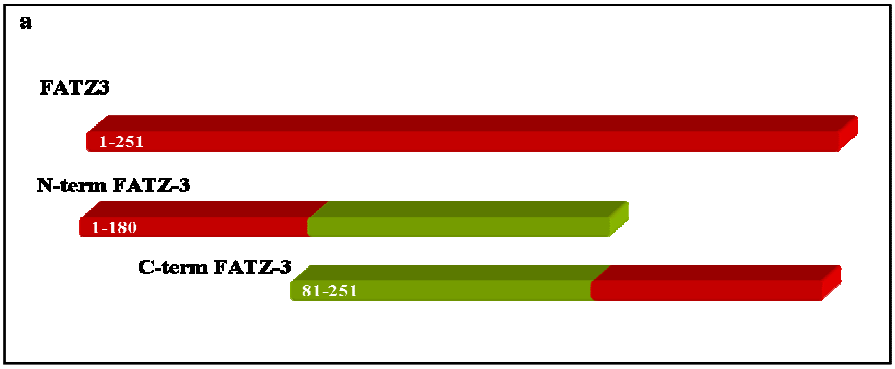

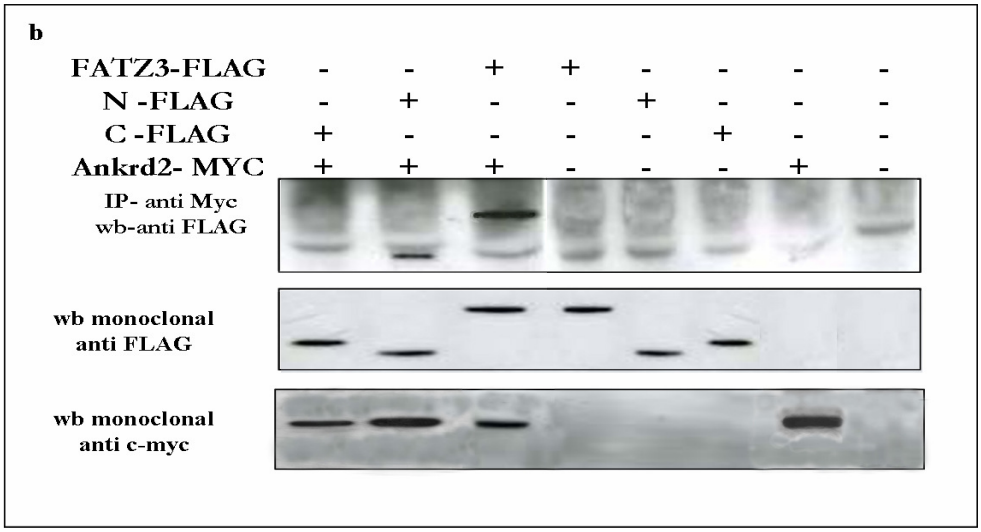

Figure 32. a) schematic diagram showing the full length FATZ-3 and the N- and C-terminal regions of FATZ-3. **b)** Co-IP of COS-7 cells transfected with pCMV-FLAG-FATZ-3, pCMV-FLAG-N-term-FATZ-3, pCMV-FLAG-C-term-FATZ-3 and pCMV-c-mycAnkrd2 as noted in the figure and immunoprecipitated with anti-myc antibody.

3.12 Expression and purification of FATZ-3 protein

The FATZ family of proteins is interesting in that apart from the motif their C-terminal that we are proposing as a PDZ domain ligand there are no other binding motifs known for these proteins. They have been shown to bind to a large variety of proteins; filamins, ACTN2, telethonin, calcineurin, myotilin, ZASP and now as demonstrated by the work in this thesis, to ALP, CLP-36 and RIL. Therefore it would be very useful to know the tertiary structure of members of this family to understand their protein-protein interactions. Therefore I undertook as part of my PhD project to obtain information on the tertiary structure of FATZ-3 and for this structural project we choose to use the approach of crystallization FATZ-3. These studies were done in collaboration with the laboratory of Prof. Kristina Carugo, University of Vienna, Austria. I prepared the purified protein and initial tests in Trieste and then went to her laboratory for 3 months to do large scale production and purification of the protein as well as the crystallization procedures outlines below. The crystals obtained were examined at the European Synchrotron Radiation Laboratory, Grenoble, France.

In order to crystallize a protein it is necessary to obtain a high concentration of purified protein (5-10 mg/ml). I spent a lot of time and effort in setting up the conditions and system for protein expression and purification mainly due to the difficulty of expressing high amounts of soluble full length FATZ-3 protein. I tried to express FATZ-3 the full length protein first as a His tagged protein and then as a GST recombinant protein using both bacterial and the Baculovirus expression systems. The protein purification trials were as follows:

3.12.1 Expression and purification of His tagged FATZ-3 full-length protein in Bacteria

The cDNA of FATZ-3 was cloned into the prokaryotic expression vector pQE30 (Qiagen) which allows the expression of a protein with a 6XHis tag at the N-terminal. *E. coli* M15 [pREP4] cells were transformed with the His-FATZ-3 construct and used for protein expression after induction with IPTG.

I made several protein production and purification trials with different all at room temperature with different concentrations of IPTG and different buffers however protein was very low. Figure 33 shows an example of a the amount of FATZ-3 obtained from purification from of a 500 ml culture of M15 cells induce with 1mM IPTG.

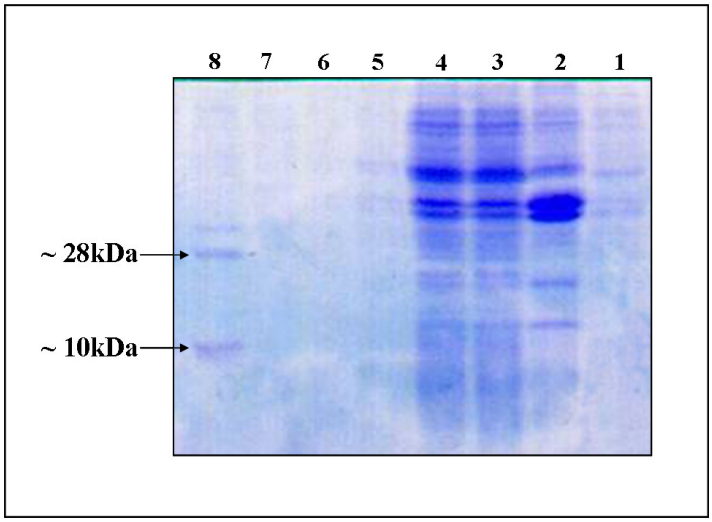

Figure 33. SDS-PAGE of His tagged FATZ-3 protein obtained from M15 cells (500ml culture) induce with 1mM IPTG: Lane1, M15 cell lysate before induction with IPTG; Lane2, pellet after induction (insoluble proteins); Lane 3, supernatant after induction (soluble proteins); Lane4, flow-through from column; Lanes 5-7, three washes; Lane8, the eluted His-FATZ-3 showing two bands, one at ~28 kD (FATZ-3) and one at ~10 kD due to degradation. The amount of soluble FATZ-3 protein recovered was very low.

3.12.2 Protein expression and purification of recombinant GST-FATZ-3 full length protein in Bacteria

Since I had difficulties expressing and purifying FATZ-3 full-length protein with an N-terminal His tag, I decided to produce FATZ-3 as a GST fusion (N-terminal) protein to try to enhance solubility. The GST-FATZ-3 construct was used to transform BL21 (DE3) pLys S bacterial cells and induced by IPTG. I made several trials with different concentrations of IPTG and different buffers; shown in Figure 34 is an example of three protein purifications with different IPTG concentrations (0.1, 0.5 and 1 mM). There was no significant difference between the three concentrations of IPTG. I obtained higher expression and solubility when FATZ-3 was expressed as a GST fusion protein. However the amount obtained was still not sufficient for protein crystallization trials (fig 34).

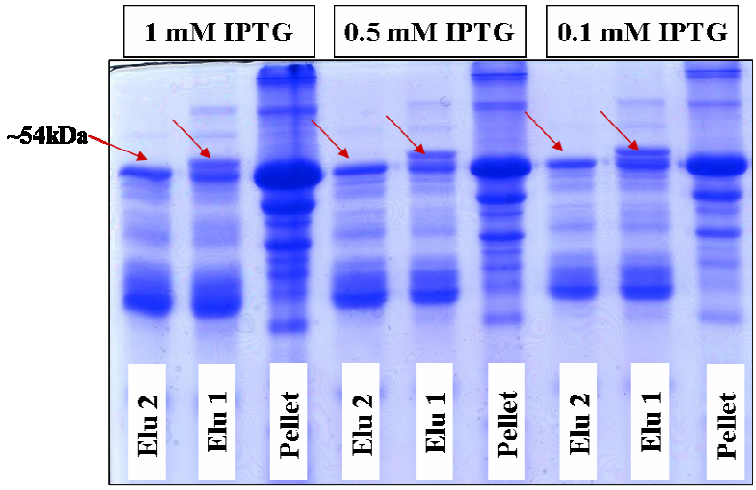

Figure 34. SDS-PAGE of the different purification trials for GST-FATZ-3. The different concentrations of IPTG used were 0.1, 0.5 and 1 mM. The GST-FATZ-3 protein was detected as a 54 kD band after SDS-PAGE. Only the eluted proteins and insoluble proteins in the pellets are shown here.

3.12.3 Protein expression and production of full-length His tagged FATZ-3 protein using the Baculovirus expression system

Since I had difficulties expressing and producing FATZ-3 in bacteria, I decided to express the protein in eukaryotic cells by using the Baculovirus expression system (Invitrogen). Full-length FATZ-3 cDNA was cloned into the pFastBacHT vector which expresses an N-terminal 6XHis tag recombinant protein. The pFastBacHT vector contains Tn7R and Tn7L which are two sequences homologous with the mini-attTn7 sequence, that is present in the baculovirus shuttle vector (bacmid 136 kb), and allows homologous recombination and thus transposition of the gene of interest into the bacmid. In order to allow the transposition of His tagged FATZ-3 into the bacmid genome the FATZ-3 pFastBacHT construct was transformed into the *E. coli* strain DH10Bac that contains the bacmid genome. After His tagged FATZ-3 was inserted into the bacmid genome, the bacmid containing FATZ-3 (1ug) was produced and then transfected into Sf9 insect cells (2 x 10^6/ml).

The baculovirus virus containing FATZ-3 (P1) was then amplified by infection in Sf9 cells (2 x 10^6/ml, MOI 0.1 to obtain a higher amount of the virus (P2). The efficiency of infection of the virus and the expression of FATZ-3 was checked by viral dose and time course experiments to determine the best conditions for FATZ-3 protein production.

3.12.3.1 Dose efficiency experiment for the P2 virus expressing His-FATZ-3 full-length protein

I performed experiments to check the efficiency of infection of the virus producing FATZ-3 and to determine the optimum amount of virus needed for protein expression.

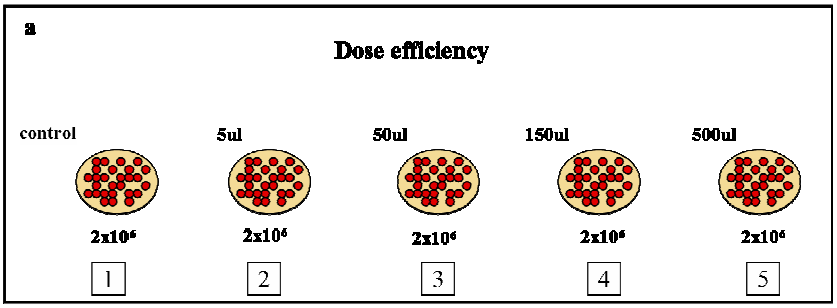

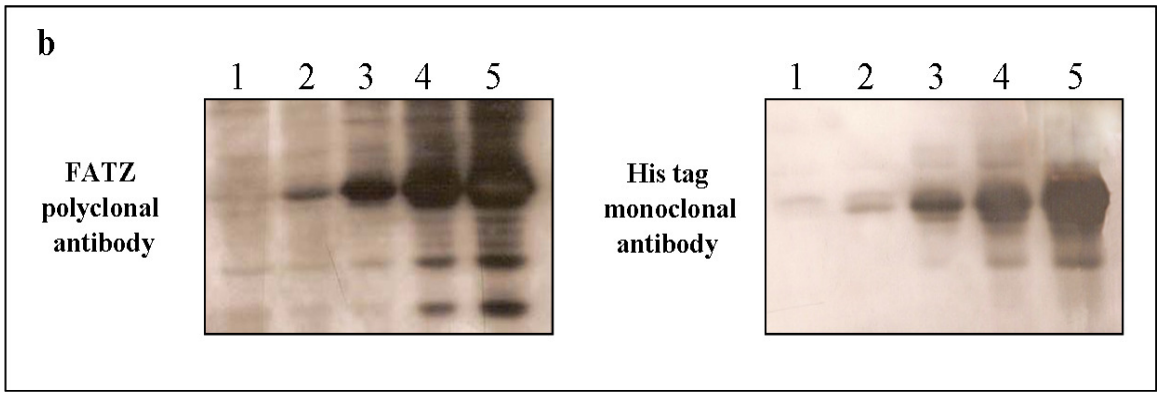

Figure 35. a) A schematic figure outlining the dose efficiency experiment. Sf9 cells were plated at $2x10^6$ cells per dish and infected with different amounts of the baculovirus expressing the full-length FATZ-3 protein. **b)** infected cell lysates (from the 5 different plates) separated by SDS-PAGE, immunoblotted and detected with monoclonal antibody to the His tag and a polyclonal antibody to FATZ-3 (a mixture of polyclonal antibody to FATZ-1 and FATZ-2 that can detect FATZ-3) to check the expression of the protein. The lane numbers correspond to the numbers in Figure 34a showing the different amounts of virus used for infection. Lane 4 shows the optimum amount of virus needed for good infection and protein production (150ul).

Sf9 cells (2 x 10^6 cells) were seeded in dishes (60 mm) and infected with different amounts of the virus (5, 50, 150 and 500 ul) plus a uninfected cells as a control (schematic diagram, fig 35a). Cells were harvested after 4 days and cell lysates were separated on two SDS-PAGE gels, blotted onto membranes and detected with antibodies against the His tag and FATZ-3 (in this case a mixture of FATZ-1 and FATZ-2 antibodies were used) to check the expression of the protein. In lane 5 the amount of the FATZ-3 protein was approximately double that in lane 4 but this result was obtained using at least 3 times more virus (500 µl of P2 virus stock) for the infection (fig 35b). Therefore the optimum amount of virus needed for good virus infection and 6XHis FATZ-3 recombinant protein production was 150 µl of the P2 stock for infection of $2x10^6$ Sf9 insect cells.

3.12.3.2 Time course experiment for the P2 virus expressing full-length His-FATZ-3 protein

I made a time course experiment to determine the best time for the expression of the His tag FATZ-3 recombinant protein. The experiment was performed by infecting Sf9 cells ($2x10^6$ cell for a 60 mm dish) with the previously determined optimum amount of baculovirus expressing FATZ-3 (150 ul) and harvesting one dish a day (schematic diagram, fig 36a). The cell lysates were then run on a SDS-PAGE gel, blotted onto a PDVF membrane and detected with anti-His antibody. I found that the optimum time of infection for FATZ-3 expression was 96 hours after infection (Fig 36b).

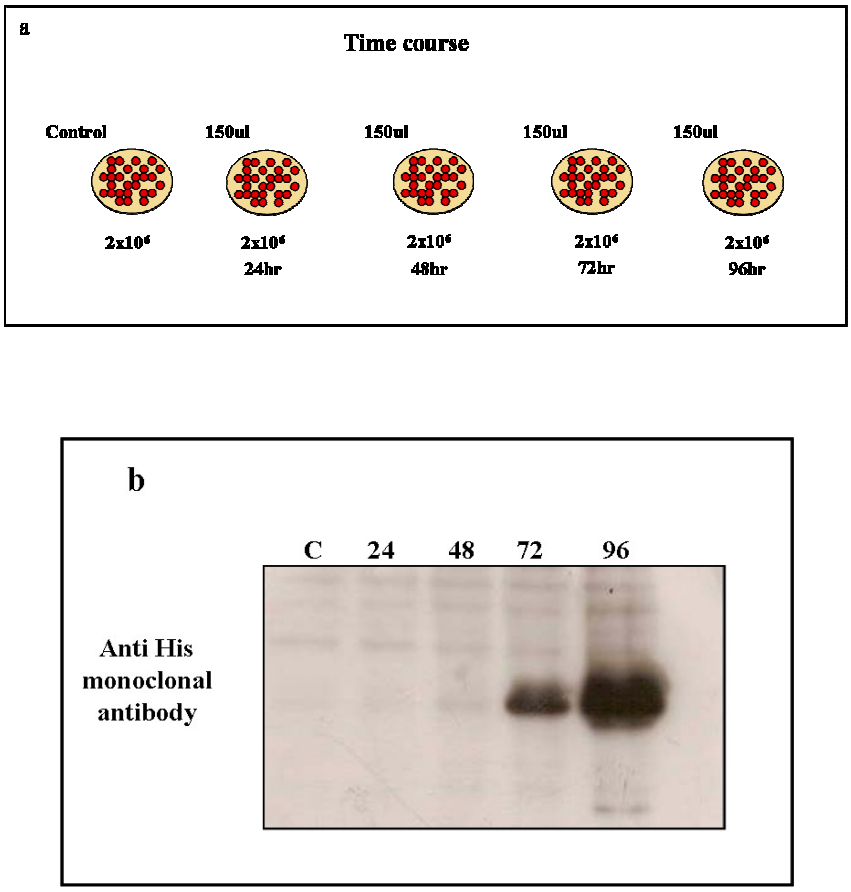

Figure 36. a) A schematic diagram outlining the time course experiment. Sf9 cells were plated at $2x10^6$ cells per dish, the cells were infected with 150ul of baculovirus and a dish was harvested every 24 hours. **b)** Sf9 cell lysates from the dishes harvested at different times were separated by SDS-PAGE, immunoblotted and detected using monoclonal anti-His antibody. The optimum expression of His tagged FATZ-3 was 96 hours or longer.

3.12.3.3 Purification of native FATZ-3 protein expressed by baculovirus in Sf9 cells

From the previous experiments (does and time course) I knew the optimum amount of virus (150ul) needed for expressing FATZ-3 and the best time to harvest the Sf9 cells (at least 4 days after infection). Therefore I started to produce the His-FATZ-3 full-length protein for purification. The details are given in the Material and Methods section

of this thesis. Briefly Sf9 cells to (200 ml, $2x10^6$ /ml) were grown in spinner flasks and infected the cells with the optimum amount of virus.

The cells lysates were lysed with buffer containing lysozyme, centrifuged, incubated with Ni-NTA resin for 2 hours at 4 °C, then washed and eluted with elution buffer containing 250 mM imidazole. The eluates were run on a SDS-PAGE gel which was then stained with Coomassie blue. In the Baculovirus system the amount of soluble native His–FATZ-3 protein obtained was higher than that obtained from bacterial expression, however still not enough for further purification for crystallization experiments (fig 37). We tried scaling up the culture volume to 1 L culture and we tried as well scaling up in bottles but both ways didn't of scaling up didn't give the right expected amount of proteins plus we faced difficulties dealing with Sf9 cells in large scales.

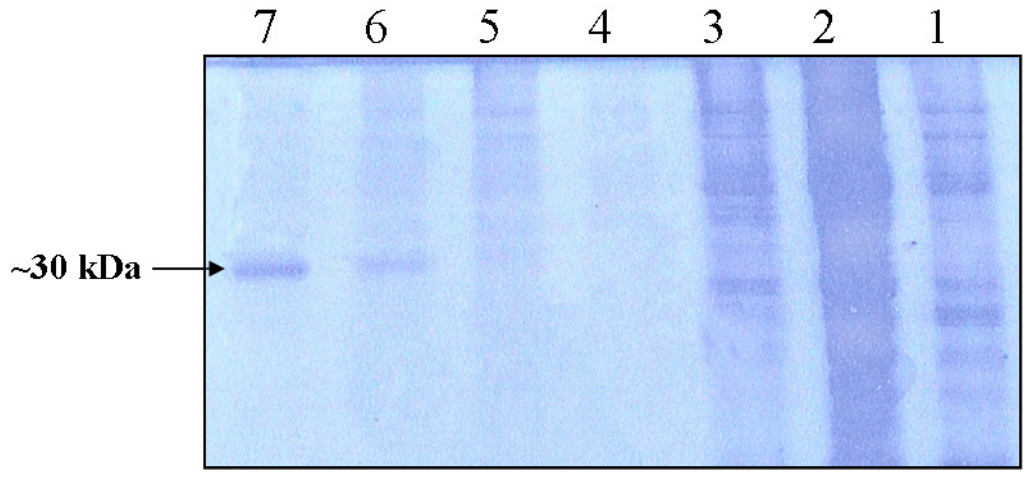

Figure 37. A SDS-PAGE gel showing His-FATZ-3 protein production and purification from a 200 ml culture of Sf9 cells. Lane 1, total cell lysate; lane 2, pellet (insoluble proteins); lane 3, flow-through from column; lanes 4-5 two different washes, lanes 6-7 first and second elutions of the His-FATZ-3 protein.

3.13 Expression and purification of C-terminal FATZ-3 protein in bacteria

Since I had a lot of difficulties expressing and producing soluble full-length FATZ-3 using both bacterial and Baculovirus systems I decided to try a different approach, namely express a shorter form rather than the full-length of the FATZ-3 protein. I found using computer predictions for FATZ-3 that by removing the first 80 amino acids the isolectric point (PI) of the protein dropped from 9.4 to 7.3. Therefore I decided to use this truncated version of the FATZ-3 protein.

3.13.1 Comparison of the expression and purification of GST and His tagged C-terminal FATZ-3

Primers were designed to amplify the last 516 bp of the FATZ-3 cDNA with restriction sites for cloning. The DNA corresponding to the C-terminal FATZ-3 was amplified by PCR and then after confirming there were no changes in the sequence it was cloned into the following prokaryotic vectors; pPROEXHTa which expresses recombinant proteins with a N-terminal His tag and contains a TEV protease cleavage site for cutting the His tag and pGEX-6P-3 which expresses a N-terminal GST protein containing a thrombin site for removing GST that can be cleaved by a prescission protease specific for thrombin. The amplified PCR fragment encodes the final 171 amino acids of the C-terminal of FATZ-3. I was interested in this C-terminal region of FATZ-3 since the C-terminal is important for the interactions with PDZ domain proteins. I used both vectors to transform the *E. coli* strain BL21-Codon Plus-RP cells. Codon bias can be a significant obstacle for efficient expression of heterologous genes in *E. coli* hosts. In GC-rich genomes, such as the mammalian, rare arginine codons (AGG or AGA) and the

proline codon (CCC) most frequently affect bacterial gene expression. BL21-CodonPlus-RP cells contain a ColE1-compatible vector with extra copies of the *argU and proL* Cam^r tRNA genes which recognize arginine and proline codons, respectively. The C-terminal of FATZ is high in proline 15.7 %. In order to compare the pPROEXHTa and pGEX-6P-3 vectors I expressed the truncated FATZ-3 protein from both. I used a 200 ml culture of bacteria and induced with 1 mM for 4 hours at room temperature. On comparing the results of the purifications of the truncated FATZ-3 protein with those of the full-length FATZ-3 protein produced in bacteria I could see that the C-terminal FATZ-3 is expressed better and is more soluble than the full-length FATZ-3. However comparing the two vectors, pPROEXHTa (fig 38a) and pGEX-6P-3 (fig 38b), there was no great difference in the production of C-terminal FATZ-3. As there was no difference between the vectors I decided to use pPROEXHTa since the His tag is very small and if necessary I could used the C-terminal FATZ-3 without removing the His tag. The His tag is less likely to interfere in structural studies of the protein than GST, since the GST is approximately 26 kD. It may be better not to cleave the tag as any cleavage involves loss of protein and the amount of soluble C-terminal FATZ-3 is not very large.

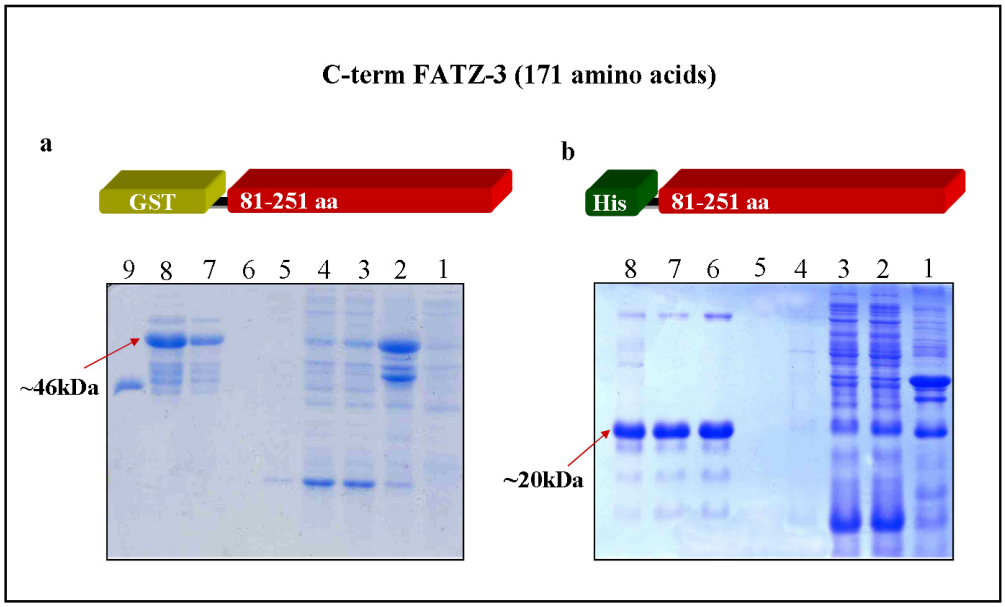

Figure 38 a) SDS-PAGE showing production of GST C-term-FATZ-3 obtained from BL21-Codon Plus-RP cells (200ml culture). Lane 1; lysate of cells before the induction with IPTG; lane 2; pellet (insoluble proteins); lane3, supernatant (soluble proteins); lane4, flow-through from column, lanes 5-6 two washes; lanes 7-8 first and second elutions respectively; lane 9, GST alone (for comparison). **b)** SDS-PAGE showing production of His C-term-FATZ-3 obtained from BL21-Codon Plus-RP cells (200ml culture); lane 1, lysate of cells before induction with IPTG; lane,2, supernatant (soluble protein), lane3, flow-through from column; lanes 4-5, two different washes; lanes 6-8, first, second and third elutions of His C-terminal FATZ-3.

3.13.2 Optimization of the purification of C-terminal FATZ-3 protein:

In order to obtain the best level of purity of native soluble C-terminal FATZ-3 I tried several different buffers for the affinity purification step varying salt and imidazole concentrations. The best concentration of salt was around 300mM NaCl in the lysis, wash and elution buffers. To find the optimum concentration of imidazole I needed to perform several purification experiments changing the concentration of imidazole in the

lysis and wash buffers in order to reach the highest purity obtainable from affinity purification with the minimum loss of protein.

Four small scale protein purification experiments were made with different concentrations of imidazole: First purification, in both lysis and wash buffers I used no imidazole; Second purification, in the lysis and wash buffers I used 3 mM and 5 mM of imidazole respectively; Third purification, in the lysis and wash buffers I used 5 mM and 10 mM of imidazole respectively; Fourth purification, in the lysis and wash buffers I used 10 mM and 20 mM of imidazole respectively. I found that the third condition (10mM imidazole lysis buffer and 20 mM in the wash buffer) was the best to obtain a good level of affinity purification for the amount of protein obtained (fig 39a).

I performed a small scale experiment to cleave the His tag from the His tag C-terminal FATZ-3 protein in order to determine the behaviour of the protein without the His tag (fig 39a). I used about 60 μg of the purified C-terminal FATZ-3 protein with 30 Units of the TEV enzyme with the addition of DTT (70 mM) in the reaction buffer, incubated overnight at 4 °C.

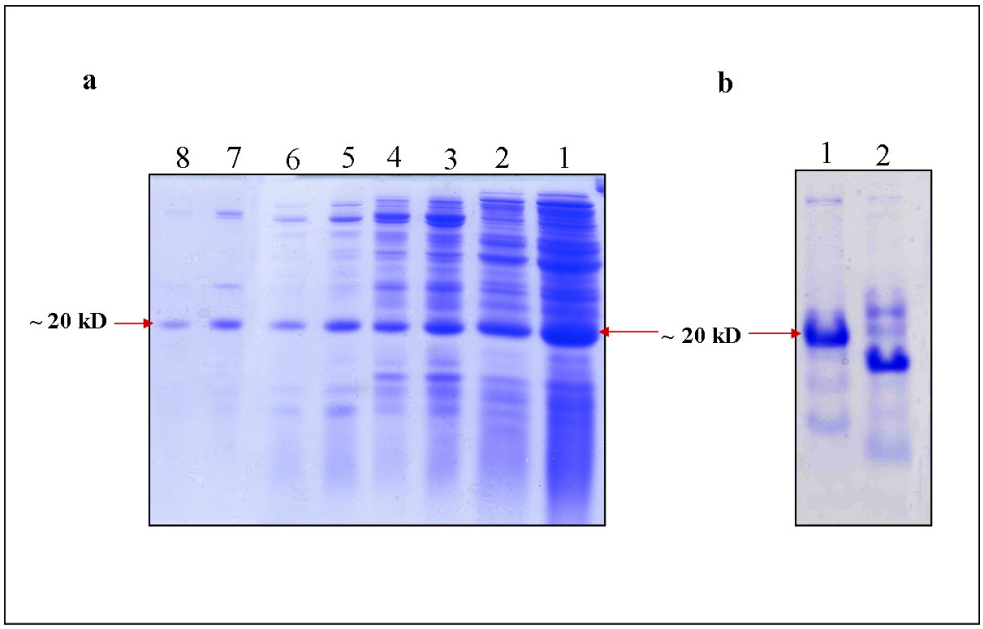

Figure 39. a) SDS-PAGE showing four different purifications using different concentrations of imidazole in the lysis and wash buffers, two elutions from each purification were loaded on the gel. Lanes 1-2, 1st and 2nd elutions from the purification using no imidazole in the lysis and wash buffers; lanes 3-4, 1st and 2nd elutions from the purification using 3 mM and 5 mM imidazole in the lysis and wash buffers respectively; lanes 4-5, 1st and 2nd elutions from the purification using 5 mM and 10 mM imidazole in the lysis and wash buffers respectively; lanes 7-8, 1st and 2nd elutions from the purification using 10 mM and 20 mM imidazole in the lysis and wash buffers respectively. **b)** SDS-PAGE the C-terminal FATZ-3 protein after cleavage of the His tag. Lane 1, His-C-terminal FATZ-3 before cleavage; lane 2, the C-terminal-FATZ-3 after cleavage of the His tag.

3.14 Medium scale production and purification of C-terminal FATZ-3 protein

Previous purification trials were made with small scale culture, volumes of 50 ml and 200 ml. I was interested to achieve a high level of protein purity and concentration for crystallization experiments therefore I increased the bacterial culture volume to 500ml. I induced the protein by adding IPTG 1 mM and incubating the culture at room temperature for 4 hours. The cells were harvested and resuspended in lysis buffer with the optimum concentrations of salt (300mM NaCl) and imidazole (10 mM), incubated on ice for 45 min. and then I purified the C-terminal FATZ-3 protein using three steps:

1 Affinity purification: after centrifuging the cell lysate, the supernatant was incubated with Ni-NTA resin for 2 hours at 4°C and then washed several times with washing buffer containing 20 mM imidazole. The protein then was eluted using an elution buffer containing 250 mM imidazole. Elutions were run on a SDS-PAGE gel and then this was stained with Coomassie to see the first level of purity.

2 Ion Exchange Chromatography: The eluted protein (after the first step) was dialysed against a buffer (KCl 75mM, TRIS 20 mM, pH 8.2) before being used in Ion exchange chromatography. The samples were then run on the mono Q column and eluted by linear gradient elution in 20 column volumes with the buffer (KCl 1M, TRIS 20 mM, pH 8.2).

Fractions were then run on a SDS-PAGE gel and stained with Coomassie blue in order to choose the right fractions with the highest purity.

3 Analytical gel filtration chromatography: Chosen fractions were concentrated and run on a Superdex 200 26/60 column for further purification. The protein eluted from the column at a molecular weight around 38 kD demonstrating that the C-terminal FATZ-3 behaves as a dimer (fig 40a). The level of purity of the C-terminal FATZ-3 was very good (fig 40 b) but the amount of protein obtained was not very high therefore I needed to scale up the protein production and purification.

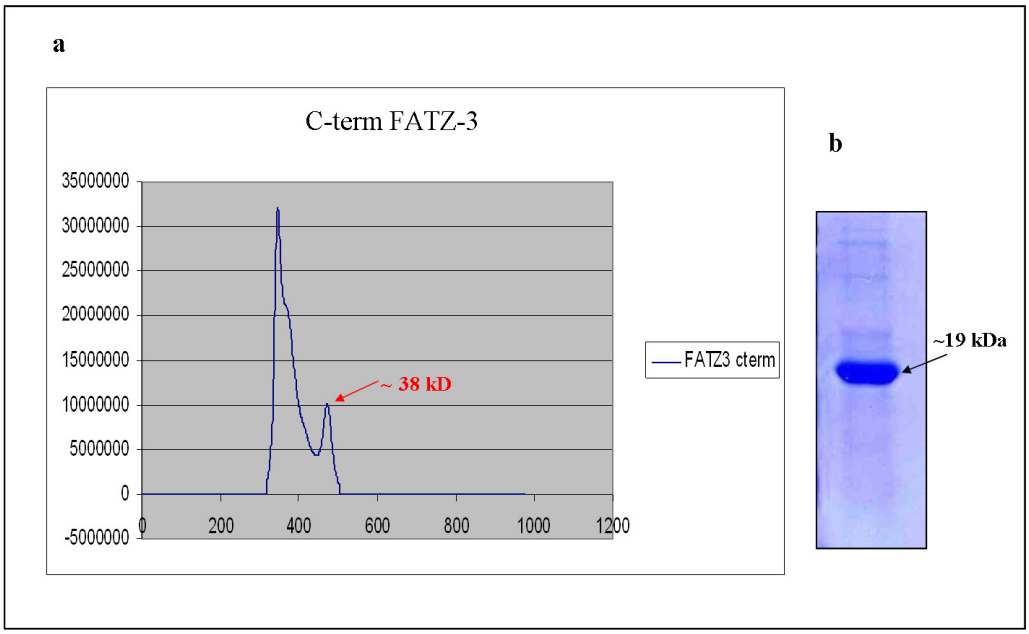

Figure 40 a) The curve of the analytical gel filtration purification, the second peak of the curve is the dimer of C-terminal FATZ-3 eluting at a molecular weight of ~38 kD. **b;** SDS-PAGE showing the protein after the three steps purification (Affinity purification, Ion Exchange Chromatography and Analytical gel filtration chromatography), the major band represents the C-terminal FATZ-3 protein after the three purification steps.

3.15 Large scale production and purification of C-terminal FATZ-3 protein

In order to obtain the optimum amount and concentration needed for protein crystallization experiments I had to scale up the protein production and purification. This part of work was done by me at laboratory of Professor Kristina Carugo, Vienna, Austria. I made several scale up trials starting from 5 L to 12 L. I faced a lot of difficulties with the protein purification when I scaled up. I tried different buffer conditions in the purification trials, until I obtained a good protocol. I had to use cationic exchange instead of ion exchange therefore I had to change the buffer from TRIS pH 8 to MES pH 6 in order to purify the protein by cationic exchange. For protein production I used a 12 L culture of bacteria induced with IPTG for 4 hours at 25°C, the cells were then harvested by centrifugation, resuspended in lysis buffer, disrupted using a French press and then centrifuged. The supernatant was then incubated with Ni-NTA resin for 2 hours, washed several times with washing buffer and eluted with elution buffer.

The eluted protein was run on a SDS-PAGE gel and stained with Coomassie blue in order to see the purity of the first step purification (fig 41 a). Eluted samples were dialysed against a buffer (KCl 1M, MES 20 mM, pH 6) before being further purified by Cation Exchange Chromatography using a Source 15S column. Fractions were run on a SDS-PAGE gel and stained with Coomassie blue in order to chose the fractions containing the best purified protein (fig 41 b). The chosen fractions where then further purified by gel size exclusion chromatography using a Superdex 200HR 16/60 column. The fractions corresponding to the molecular weight of the protein were then run on a SDS-PAGE gel and stained with Coomassie blue in order to see the level of purity and

the amount of protein obtained (Fig 41 c). The fractions were then concentrated and after concentration checked by UV at 280 nm. The amount of C-terminal FATZ-3 protein obtained was reasonable for protein crystallization trials (120 µl of protein at 10 mg/ml) (fig 41 d).

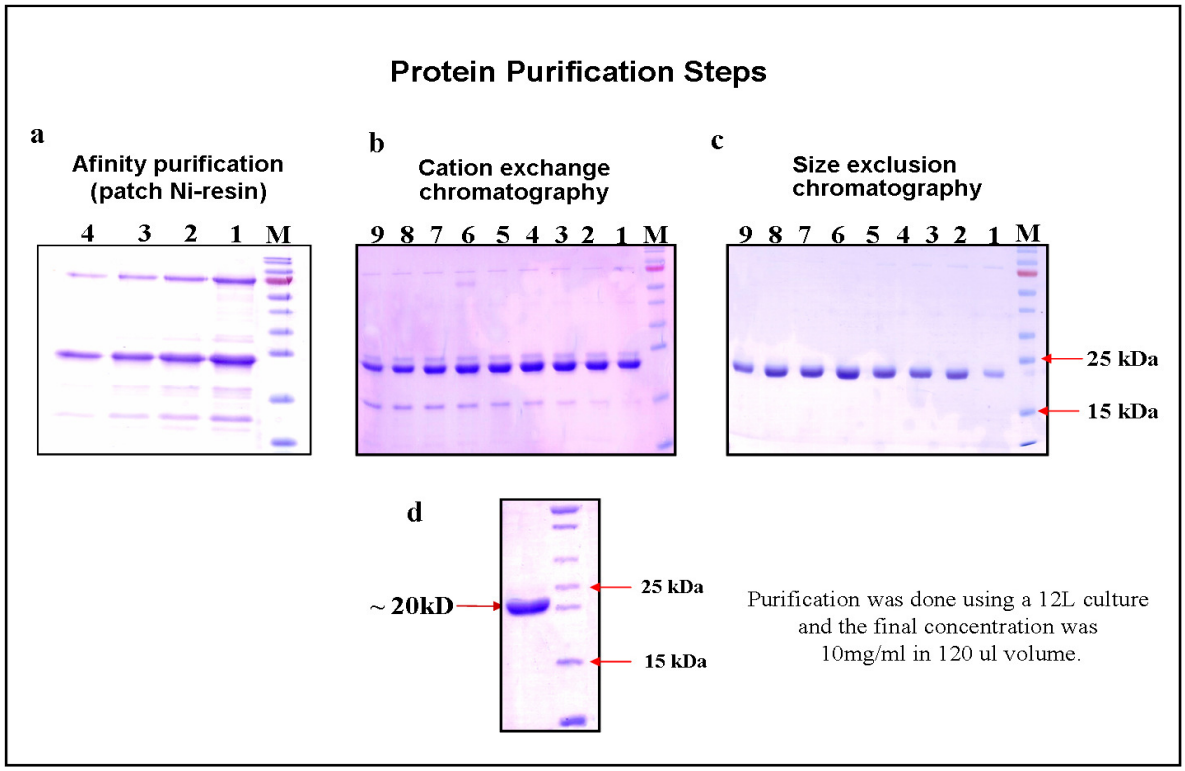

Figure 41. SDS-PAGE of the three different purification steps for the C-terminal FATZ-3 protein. **a)** M, molecular weight marker; lanes 1-4, different elutions obtained from the Affinity purification; **b)** M, molecular weight marker; lanes 1-9, chosen fractions from the cation exchange purification (eluted at the expected IP); **c)** M, molecular weight marker; lanes 1-9, chosen fractions from size exclusion chromatography (eluted at the expected molecular weight of the protein); **d)** the C-terminal FATZ-3 protein after combining together all the fractions obtained from the size exclusion chromatography purification. The concentration of the purified C-terminal FATZ-3 protein was ~10mg/ml (120 µl), this protein was used for crystallization.

3.16 Circular Dichroism (CD) shows high percentage of random coil for the C-terminal FATZ-3 (81-251aa) protein

The purified protein C-terminal FATZ-3 (81-251 aa) protein was used at a concentration of 3.6 µM for circular dichroism (CD) studies. These studies were done in order to gain information about the secondary structure of the protein. The data I obtained from the CD spectra showed that the protein contains 42.6% of random coil, 24.3 % of α-helix, 17% anti-parallel and 5.7% parallel ß-sheets. This could mean that the protein may not be very well folded and there could be difficulty to crystallize it (fig 42).

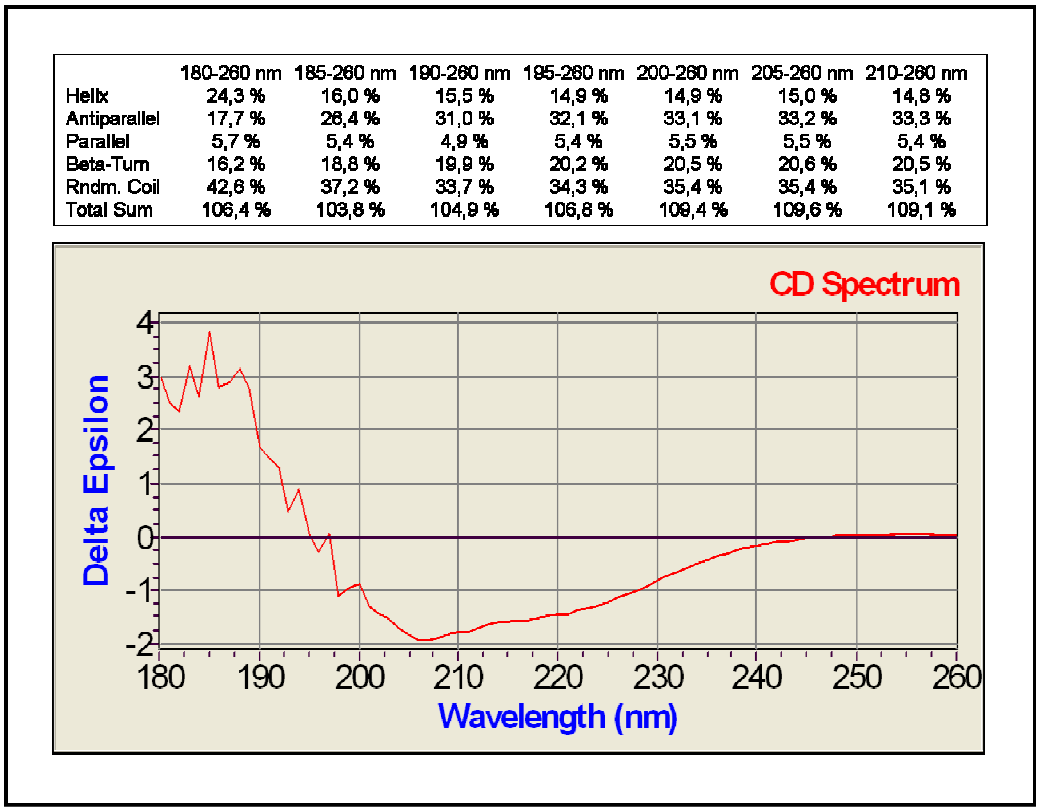

Figure 42 Circular Dichroism (CD) results showing that the C-terminal FATZ-3 protein contained a high percentage of random coil 42.6%.

3.17 Dynamic light scattering (DLS) shows a low percentage of protein polydispersity

In order to have information about the monodispersity of the protein in solution I used the purified C-terminal FATZ-3 protein at a concentration of 10mg/ml for DLS spectra.

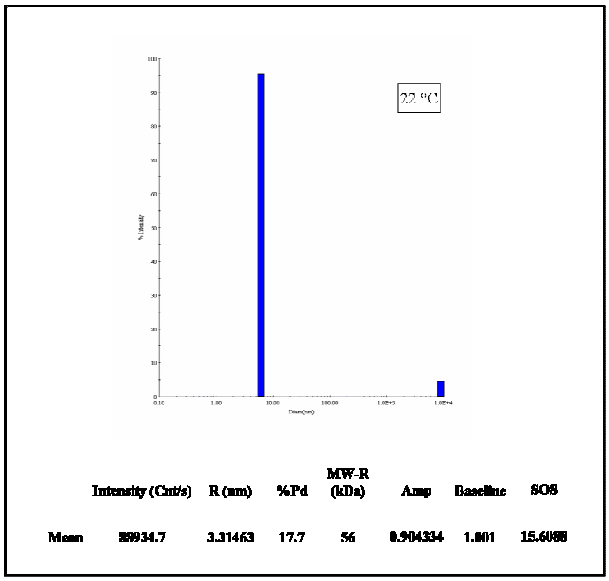

Figure 43 a). Graph of the results obtained from the Dynamic light scattering (DLS) experiment done at 22 °C showing that the C-terminal FATZ-3 protein had 17.7% of polydispersity.

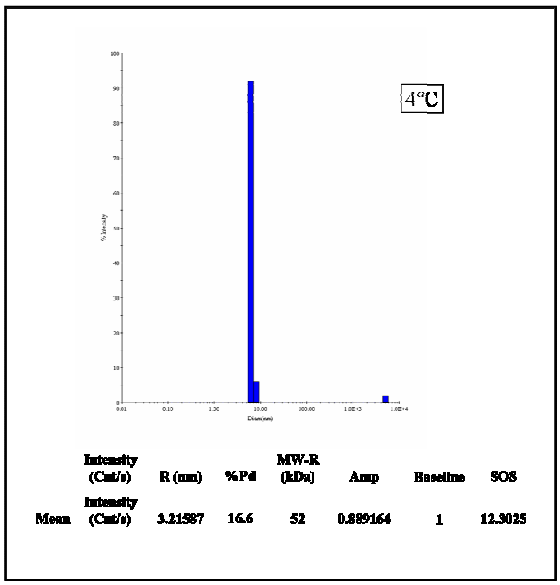

Figure 43 b). Graph of the results obtained from the Dynamic light scattering (DLS) experiment done at 4 °C showing that the C-terminal

I tested the protein sample at two different temperatures 22 °C (fig 43a) and at 4 °C (fig 43 b) in order to see the behavior of the protein at different temperatures.

The data I obtained from both temperatures showed that the protein contained a low percentage of polydispersity 17% and 16.6%, at 22 °C and 4 °C respectively: This means that the protein is homogenous in the solution.

3.18 Stura footprint screen experiment

A stura footprint screen kit was used to determine the optimum precipitants for crystallization studies and check if the concentration of the C-terminal FATZ-3 (81-251aa) protein was the best concentration for the crystallization trials. I tried eight different conditions (highlighted in Table 2) which were recommended in the kit if there was a shortage of protein. I mixed 1 ul of each precipitant with 1 ul of the C-terminal FATZ-3 protein (10mg/ml) and checked under the microscope to detect if any protein precipitates formed. I saw that the C-terminal FATZ-3 protein precipitated immediately after mixing with 0.2M imidazole malate pH 7.0, PEG4K 15% (Table 2, 2B). Therefore this is the best condition (0.2M imidazole malate pH 7.0, PEG4K 15%) to use in crystallization trials.

	1	2	3	4	5	6
	PEG 600	**PEG 4K**	**PEG 10K**	**A.S.**	**PO4**	**Citrate**
A	**15%**	**10%**	**7.5%**	**0.75M**	**0.8M**	**0.75M**
B	**24%**	**15%**	**12.5%**	**1.0M**	**1.32M**	**1.0M**
C	**33%**	**20%**	**17.5%**	**1.5M**	**1.6M**	**1.2M**
D	**42%**	**25%**	**22.5%**	**2.0M**	**2.0M**	**1.5M**
	0.2M imidazole malate pH 5.5	**0.2M imidazole malate pH 7.0**	**0.2M imidazole malate pH 8.5**	**0.15M sodium citrate pH 5.5**	**NaH2PO4 K2HPO4 pH 7.0**	**10mM sodium borate pH 8.5**

Table 2 Conditions tested for the precipitation of C-terminal FATZ-3 protein

3.19 Crystallization trials

Based on the results obtained from the stura footprint screen, I chose three crystallization kits to check the possibility of obtaining C-terminal FATZ-3 protein crystals. These kits were the JCSG+ Suite (QIAGEN), the JBScreen 1, 2, 3 and 4 (JENA BIOSCINCE) and the PACT premier-HT96 MD1-36 (Molecular Dimension Limited).

I tried around 300 crystallization conditions using the three kits. I used the vapor diffusion technique that uses sitting drops by mixing two different amounts of proteins 0.1 µl and 0.2 µl with two different amounts of the precipitants then the protein drops were then incubated at 22 °C.

The protein drops were made by a robot that forms nano drops. I started to obtain crystals after one month from the formation of the protein drops. Four crystallization conditions gave crystals from the three different kits that I used (JCSG+ Suite (QIAGEN), the JBScreen 1, 2, 3 and 4 (JENA BIOSCINCE) and the PACT premier-

HT96 MD1-36). Figure 44 shows the crystals obtained from the four different conditions. **PACT F2** (0.2M Sodium bromide, 0.1M Bis Tris propane pH 6.5, 20% w/v PEG 3350), **JENA SCREEN E2** (20% w/v PEG 4000 10% w/v 2-Propanol 100 mM HEPES Sodium Salt pH 7.5), **JCSG E6** (0.2 M Zinc acetate 0.1 M Imidazole pH 8 20% w/v PEG 3000) and **JCSG E2a** (0.2 M Sodium chloride 0.1 M Sodium cacodylate pH 6.5 2 M Ammonium sulfate). The crystals were checked by X-ray at 0.91 Å at the European Synchrotron Radiation Laboratory, Grenoble, France, unfortunately the crystals did not give a good diffraction pattern.

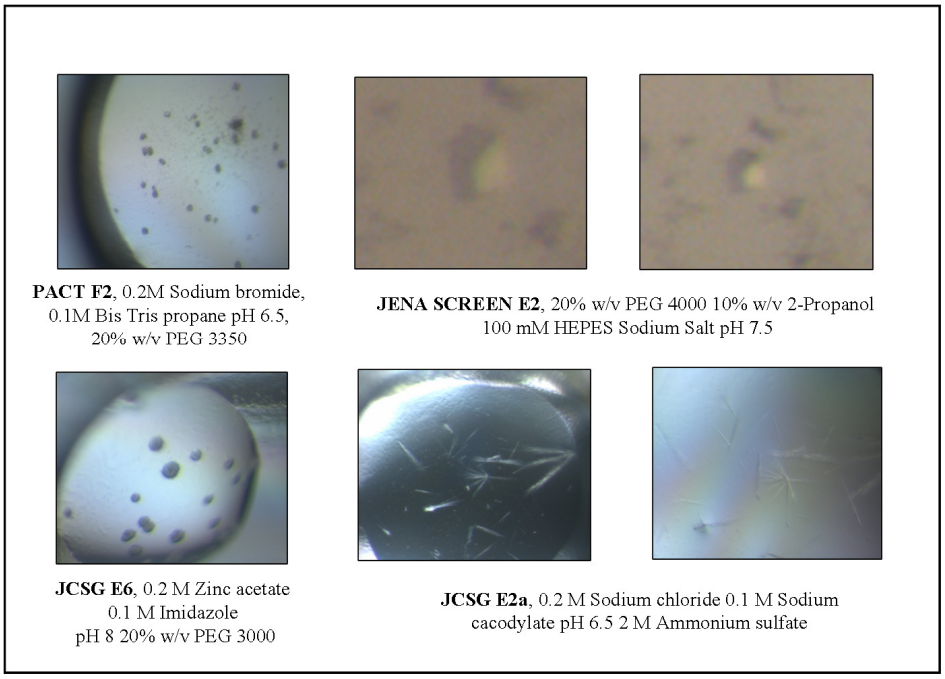

Figure 44 shows the crystals obtained from four different crystallization conditions PACT F2, JENA SCREEN E2, JCSG E6 and JCSG E2a

Chapter 4 DISCUSSION

The sarcomere is the repeating contractile unit of striated muscle. Muscle contraction occurs when actin filaments (thin filaments) slide past myosin filaments (thick filaments) towards the centre of the sarcomere. ATP plays an important role in this interaction; the binding of ATP to myosin heads reduces their affinity of binding, while the hydrolysis of ATP enhances the interaction. The contractile force of the thin and think filaments is controlled and registered by the Z-disk, which is the border line between sarcomeres. The Z-disk is an important structure of the sarcomere (Hoshijima, 2006), and is a complex of many proteins for example actin, alpha-actinin, titin, ZASP, the FATZ family, and telethonin to mention just a few. Most of the proteins that localize to the Z-disk interact with each other and mutations in Z-disk proteins can give rise to various pathological conditions such as cardiomyopathies and muscular dystrophies. Sometimes direct pathological effects can be seen as a result of the absence or alteration of proteins affecting the structure of the Z-disk. In the case of ZASP knockout mice this absence results in an unstructured Z-disk and the knock-out mice die in the first 24 hours after birth suffering from a severe congenital myopathy (Zhou et al., 2001). Several Z-disk proteins bind to other non-muscle proteins involved in cell signalling suggesting a role for the Z-disk other than purely structural.

The FATZ/Calsarcin/Myozenin family of proteins (Faulkner et al., 2000) consists of 3 members: FATZ-1, FATZ-2 and FATZ-3 that all localize in the Z-disk and show

different tissue specific expression. FATZ-1 and FATZ-3 are highly expressed in skeletal muscle fast-twitch fibres, while FATZ-2 is highly expressed in heart and slow-twitch fibres (Faulkner et al., 2000; Frey and Olson, 2002; Frey et al., 2000; Takada et al., 2001). The proteins share high homology at their N- and C-terminal and low homology in the intervening region. FATZ-3 protein shares 29% homology with FATZ-1 and shares 34% homology with FATZ-2. The members of the FATZ family of proteins interact with the same muscle proteins, such as γ-filamin, telethonin, α-actinin-2, ZASP and calcineurin (Faulkner et al., 2000; Frey and Olson, 2002; Frey et al., 2000; Takada et al., 2001) demonstrating that the FATZ family of proteins are very interactive towards other muscle proteins. All of the FATZ family members inhibit the activity of calcineurin *in vitro* and mice lacking FATZ-2 (Calsarcin-1/myozenin-2) showed a high expression of calcineurin (Frey et al., 2004; Frey and Olson, 2002; Frey et al., 2000) indicating that these proteins may be involved in modulating cell signalling. Also it is worth noting that mutations in FATZ-2 have been associated with hypertrophic cardiomyopathy (Osio et al., 2007).

Here in this thesis I report research done as part of an ongoing study on the FATZ family of proteins in order to discover the role of this family in striated muscle. The main finding of this thesis is the identification of a group of mainly striated muscle proteins, consisting of the FATZ family, myotilin, palladin and myopalladin, that selectively interact via a C-terminal motif with the PDZ domains of several Enigma proteins, ZASP, CLP-36 and ALP. These interactions were verified by several methods such as GST pulldown, *in vitro* binding using the AlphaScreen technique and PDZ Arrays. The interaction of these proteins with the Enigma family members is highly specific as verified by the restricted number of PDZ domain proteins with which their

peptide ligands will bind when given the opportunity. In fact only 2 of the 28 PDZ domain proteins on the Array bound to the peptide ligands, interestingly these were the only two Enigma family members on the Array; RIL and CLP-36 (hCLIM1). Before performing these array experiments we did not know that RIL could interact with members of the FATZ family, myotilin, palladin and myopalladin therefore RIL is another binding partner of these proteins.

Based on the work presented in this thesis we propose that the FATZ family, myotilin, palladin and myopalladin bind to members of the Enigma family of PDZ proteins via a C-terminal class III type PDZ ligand. This ligand [ST][DE][DE]L falls into the category of a class III PDZ domain binding motif (fig 45).

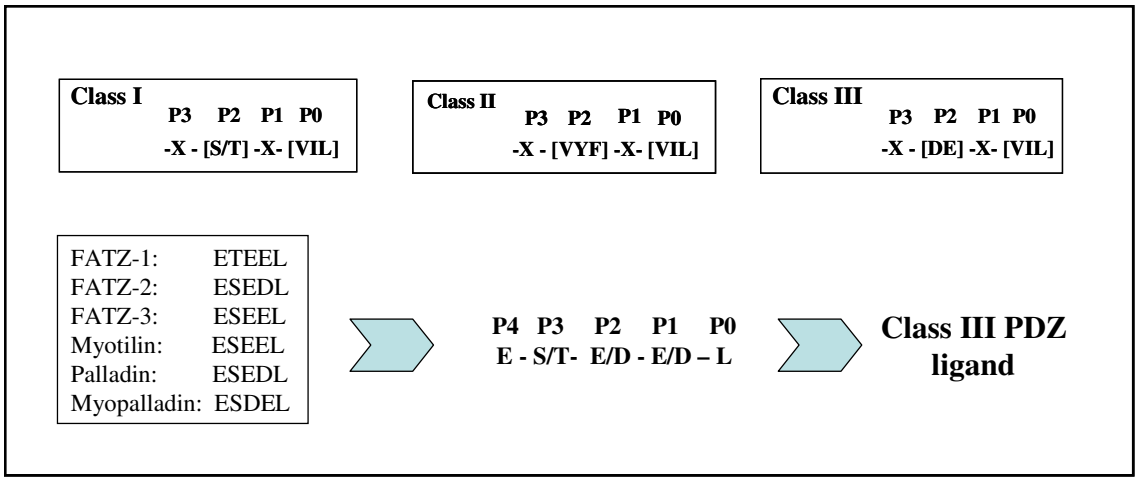

Figure 45. Showing the three motifs that represents the three classes of PDZ domains class I, class II and class III, and the last 5 amino of the FATZ family, myotilin, palladin and myopalladin which are classified as class III PDZ motif.

Initially we and our collaborators observed that the C-terminal last 5 amino acids of FATZ-3 and myotilin are identical (ESEEL), also those of FATZ-2 and palladin (ESEDL) whilst these amino acids in FATZ-1 (ETEEL) and myopalladin (ESDEL) show high similarity to those of the other members of the group. This high similarity raised the question of whether these proteins could interact with proteins via this C-terminal ligand. As mentioned in the Results section using a program written by Prof. G Valle we scanned UniProt Knowledgebase Release 11.3 for any protein having as the final amino acids of their C-terminal the motif E[ST][DE][DE]L. The amino acids were given equal weightings with the exception of the final amino acid which was given a higher weighting since it has been shown that this is the most important amino acid for the binding between PDZ domains and their ligands. We found that this motif is restricted in Vertebrates to the FATZ family, myotilin, myopalladin and palladin with the exception of histidine ammonia lyase that has the final C-terminal amino acids (ESEDL) identical to FATZ-2 and palladin (Table 2). Histidine ammonia lyase is a cytosolic involved in histidine catabolism which has been reported in striated muscle. It most probably is able to bind the PDZ domain Enigma family members but whether it does so in reality would depend on its localization whereas the FATZ family, myotilin and myopalladin are located in the Z-disk in proximity to ZASP, CLP-36 and ALP. However interactions between FATZ family, myotilin and myopalladin and RIL are unlikely to occur at least in the Z-disc since RIL is located in the brain and lung but not muscle. As the number of proteins known to interact with each other increases and multiple binding partners is the norm rather than the exception it is important to define if and where they could bind in reality. Palladin is unlike the other members in its group

primarily localized in smooth muscle and non-muscle cells such as colon where it may well interact with CLP-36.

It is important to remember that these proteins can also interact with numerous other proteins forming a vast interconnecting network. A major protein hub in this network is α-actinin. All of these proteins can bind α-actinin for example; some like RIL can bind the non-muscle isoforms of actinin, 1 and 4 whilst all the striated muscle proteins ZASP, the FATZ family, myopalladin, myotilin, ALP, CLP-36 and ZASP can bind the muscle isoforms of α-actinin. All of the Enigma family members binds to α-actinin through their PDZ domains or in some cases through their PDZ and LIM domain as in the case of CLP (Vallenius et al., 2000). It has been found that a mutation in the ALP-PDZ domain (L78K) abolishes the binding of the PDZ domain to α-actinin (Xia et al., 1997). Several mutations have also been made in the conserved sequence (PWGF) of the PDZ domain of ZASP in order to study its interaction with α-actinin. These mutations managed to disrupt the binding of the PDZ domain of ZASP to α-actinin, and its localization in the Z-disk (Zhou et al., 2001).

Since it is vital to understand what happens when several of these proteins meet at the same site we studied the effect of phosphorylation on binding and also did some competition experiments using the AlphaScreen technique. For the competition experiments we studied at the interaction between the ZASP-1 full-length protein and the FATZ-3/myotilin ligand both phosphorylated (EpSEEL) and not (ESEEL). We found that this PDZ class III binding could be competed by the addition of the C-terminal of FATZ-1, another ligand (class III) for the PDZ of ZASP. There was also competition when the α-actinin-2 was used as competitor but in this case much higher concentrations of the protein were needed to obtain the same effect as C-terminal

FATZ-1. Possibly due to the fact that the C-terminal ligand of α-actinin-2 (GESDL) involved in binding PDZ domains is classified as class I with the motif X[ST]X[VIL]. I have shown the last 5 amino acids instead of the last four amino acids, which is the canonical PDZ ligand motif, because we used peptides composed of 5 amino acids and we believe that the E at position 4 is not casual since it is conserved by the group of proteins (FATZ family, myotilin, palladin and myopalladin) that we are studying as ligands for PDZ binding. The PDZ ligand motifs used by the ELM program when scanning for functional sites in proteins are: class I (X[ST]X[VIL]), class II (X[VYF]X[VIL]) and class III (X[DE]X[IVL]). We confirmed the importance of the amino acid at position 0 by mutating L to E and thus eliminating the binding to the PDZ domain of the members of the Enigma family (ZASP, CLP-36 and ALP) that we studied.

The effect of phosphorylation on binding of the PDZ domain and ligand varied depending on which PDZ domain was used and which ligand. It was clear from experiments using the PDZ domain of ZASP that phosphorylation enhanced the binding of all of the ligands to this domain. The strongest binding was seen between the PDZ of ZASP and the phosphorylated peptide for FATZ-3/myotilin, then that for FATZ-1, myopalladin and lastly FATZ-2/palladin, in decreasing order of binding. This pattern may reflect the affinity of these ligands to bind the PDZ domain of ZASP. The effect of phosphorylation was more variable on the interactions between the PDZ domains of ALP and CLP-36. For CLP-36 the effect of phosphorylation varied greatly depending on the ligand, the phosphorylated FATZ-3/myotilin ligand (ESEEL, EpSEEL) bound better than the non-phosphorylated. There was no difference in the binding of CLP-36 to the FATZ-1 (ETEEL, EpTEEL) and the FATZ-2/palladin (ESEDL, EpSEDL) ligands

whether they were phosphorylated or not whereas the non-phosphorylated myopalladin (ESDEL, EpSDEL) and bound better than the phosphorylated. In fact it is quite striking that the phosphorylated myopalladin showed very poor binding. The ALP PDZ domain behaved in a similar way to the ZASP in that phosphorylation enhanced the binding to the ligands however only FATZ-2/palladin and FATZ-3/myotilin showed any appreciable binding. In our hands the PDZ ALP did not bind the non-phosphorylated peptide ligands this data are in contrast to the data with the full length proteins where binding was seen. PDZ domains can recognize very short C-terminal sequence motifs and the basis of this binding has been shown by X-ray crystallographic studies to be due to specific side chain interactions between the amino acids of the ligand and those of the hydrophobic pocket at the surface of the PDZ domain (Doyle et al., 1996). The four residues that reside in the carboxylate-binding loop of the Dlg PDZ domains are GLGF, in fact PDZ domains were originally named GLGF repeats (Cho et al., 1992). It is notable that all of the Enigma family members with the exception of ALP have PWGF as these four residues whereas ALP has SWGF therefore it is possible that this slight difference in binding loop residues may confer slightly different binding properties.

As a way of looking at the specificity of our C-terminal motif (E[ST][DE][DE]L) I used commercial PDZ Arrays as mentioned above. The results from these experiments showed that the interactions of our motif and the Enigma family members were specific and reflected the results obtained using the AlphaScreen experiments; the only protein common to both systems was CLP-36 (hCLIM1 in the arrays). Both phosphorylated and non-phosphorylated peptides were used as probes in the Arrays and in agreement with the AlphaScreen results the phosphorylated myopalladin peptide binds poorly to CLP-36. Also for the phosphorylated and non-phosphorylated peptides of FATZ-2/palladin

binding the results obtained in both systems were the similar. The main contrast was the binding with the FATZ-3/myotilin peptide as the phosphorylated peptide did not bind well. This discrepancy could be due to variability in the amount of protein spotted which could vary from array to array although the company try to keep this type of variation to the minimum. Also in the Arrays the proteins spotted are GST fusion proteins therefore we are comparing bindings between peptides and on the one hand GST PDZ proteins on the other His tagged PDZ domain proteins. The binding of RIL to the FATZ family, myotilin , palladin and myopalladin was previously unknown although it is in keeping with the fact that the RIL belongs to the Enigma family of proteins which includes ZASP, CLP-36 and ALP. In theses Array experiments I also used the mutated peptide ESEEE that has the last amino acid changed from L to E. As expected the phosphorylated peptide (EpSEEE) did not bind to any of the proteins on the Array instead surprising the non-phosphorylated mutated peptide interacted with the PDZ domain of Dlg4-D3 protein. This finding confirms that changing the position 0 amino acid of the motif affects the binding. In fact the results also confirm out AlphaScreen findings that changing L to E destroys the binding to the Enigma family members as binding to both RIL and CLP-36 could not be detected.

I was also able to show by co-immunoprecipitation experiments another new binding partner for FATZ-3, namely Ankrd2. This is an interesting protein that is present both in the I–band and the nucleus (Kojic et al., 2004); it is a member of the MARP family and is thought to be involved in muscle stress response pathways. In a recent paper (Tsukamoto et al., 2007) histological studies on the gastrocnemius muscle were done to determine whether nuclear accumulation of Ankrd2 occurs on muscle injury, in this case the authors used cardiotoxin or contact with dry ice to produce muscle injury. They

found that Ankrd2 accumulated in the nuclei of my fibres adjacent to severely damaged myofibres after muscle injury. They also found that Ankrd2 localized in euchromatin where genes are transcriptionally activated further confirming the hypothesis of Kojic and colleagues (Kojic et al., 2004) that Ankrd2 may translocate from the I-band to the nucleus in response to muscle damage and may participate in the regulation of gene expression. This opens up a lot of interesting questions and future experiments since I was able to map the binding of Ankrd2 to the N-terminal region of FATZ-3 (1-180 aa). This region of FATZ-3 is the known binding site for calcineurin, γ-filamin, α-actinin and telethonin (Frey and Olson, 2002).

In parallel with the project that I was involved in on the FATZ family, myotilin and myopalladin studying their interactions with other proteins I was also trying different approaches to express and purify FATZ-3 protein for crystallization experiments in order to get some structural information about that protein. As can be seen in the Results section of this thesis I faced a lot of difficulties expressing and producing FATZ-3 full-length protein in bacteria. Difficulties expressing and producing human proteins in bacteria are quite common and can be due to codon difference between human and bacterial proteins. For this reason I tried to produce and purify the FATZ-3 full-length protein in the Baculovirus system. In this system the expression and production of the protein was better but the yield was still not enough for crystallization studies. I tried scaling up the protein production in Sf9 insect cells but the amount of protein obtained was not sufficient. I also faced problems due to the inherent difficulties of working with large volumes of eukaryotic cells. Trying a different approach I managed to get higher amounts of His tagged protein expressed and purified when I removed the first 80 amino acid of the FATZ-3 protein producing only the truncated C-terminal FATZ-3

(80-251 aa) in bacteria. I then went to the laboratory of Prof. Kristina Carugo at the University of Vienna where I was able to do large scale production of the truncated FATZ-3 protein as detailed in the Results section.

When I obtained the purified protein I undertook some preliminary experiments such as circular dichroism and dynamic light scattering to obtain information on FATZ-3. The circular dichroism data I obtained showed that the purified C-terminal region of the FATZ-3 has a high percentage (42%) of random coil meaning that the protein may not be well folded and that this may case problems preventing crystallization. Nevertheless the dynamic light scattering showed that the percentage of polydispersity was low, which indicated that the protein was homogenous in solution, this could help to obtain a better quality of crystals.

The purified protein was spotted using a nanodroper robot. This method gives the possibility of trying many different conditions that were very good in my case since I had a small amount of the purified protein (120ul) with a concentration of 10 mg/ml. I started to obtain crystals 1 month after setting up the protein drops, unfortunately all the crystals I obtained where too small to give good diffraction. Despite the fact that the crystals obtained did not give good diffraction, I managed to find the right conditions for crystallizing the C-terminal of the FATZ-3 protein. Although the C-terminal of FATZ-3 contained a high percentage of random coils, this percentage did not prevent the protein from crystallizing. Studies on this part of the project are still on going and it should be possible to obtain larger crystals by spotting bigger drops using the conditions that resulted in crystal formation and larger crystals will be produced that can give good diffraction.

Another approach would be to co-transform the bacterial cells with two vectors; one is expressing the FATZ-3 protein and the other expressing the PDZ domain of the ZASP protein. This should allow us to build a complex between both proteins and to try to crystallize that complex in order to have more information about how the FATZ-3 protein binds to the PDZ domain. It is known from previous studies how the a ligand interacts with the PDZ domain of ZASP (Au et al., 2004) therefore working with a complex of full-length and/or C-terminal FATZ-3 with ZASP-1 full-length or only its PDZ domain could give more information about the general structure of the proteins and what if any structural changes occur when they interact. This is one of a future project that I would like to do.

The results that I and my collaborators obtained from these studies gave us more information about the FATZ family, myotilin and myopalladin. Even though the FATZ family members interact with the same proteins, their sites of interaction vary from one protein to another; for example FATZ-1 and FATZ-2 bind to α-actinin in a region close to the C-terminal (Faulkner et al., 2000; Frey et al., 2000) instead the FATZ-3 has two binding sites for α-actinin one close to the N-terminal (50-67 aa) and the other is close to the C-terminal (186-207 aa) (Frey and Olson, 2002). As noted the FATZ family members bind several different proteins however this PDZ motif is the first canonical binding motif reported for the family.

PDZ domains were first classified by (Songyang et al., 1997), the classification depended on the sequence of the ligand or the last amino acids of the polypeptide; position 0 and position 2 play a very important role in this classification. Depending on the ligand sequence there are three classes of PDZ domains. Class I which binds to sequence ligand X-[S/T]-X-Φ (where Φ is any hydrophobic amino acid and X is any

amino acid), class II which binds to ligand sequence (Songyang et al., 1997) and class III which binds to ligand sequence -X-[D/E/K/R]- Φ (Stricker et al., 1997). The motif that the FATZ family, myotilin, palladin and myopalladin shares is E[ST][DE][DE]L, which based on the classification of (Songyang et al., 1997) belongs to the PDZ domain class III. We have demonstrated that this motif binds to the PDZ domain of four proteins from the Enigma family ZASP, ALP, CLP-36 and RIL. Surprisingly, since the PDZ domain of ZASP is a typical class I PDZ domain (Au et al., 2004), here our motif is classified as class III but still binds to the class I PDZ domain of ZASP. This has been found previously with the syntenin protein, a 32kDa protein that interacts with many cell membrane receptors and contains two PDZ domains, the PDZI domain is able to bind peptides from class I and III, while the PDZ2 domain is able to bind peptides from classes I and II (Kang et al., 2003). We have a class III motif and that binds to the class I PDZ domain of ZASP which taken with the data on syntenin would suggest that the classification of the PDZ domains still needs further studies in order to be more defined and precise. It is known that ligands which bind to PDZ domains can contain a serine, threonine or tyrosine at the position 2 or 3 of the ligand (Cohen et al., 1996); we have a serine at the position 3 of the peptide(E[ST][DE][DE]L. The phosphorylated peptides showed stronger binding to the ZASP PDZ domain than the non-phosphorylated indicating that the phosphorylation had a positive effect on the binding with the PDZ domains. It is known that phosphorylation can reduce the binding affinity or even block binding between two proteins, for example phosphorylation of the myosin heads reduces the binding affinity of myosin towards actin which helps it slide along actin. Also phosphorylation by the PKA kinase of the amino acid at position 2 of the C-terminus of the inward rectifier K channel (Kir 2.3) protein resulted in disruption of the

binding of this protein with the PDZ domain of PSD95 (Cohen et al., 1996). On the other hand it has also been noted that phosphorylation can increase the binding of the ligand to the PDZ domains, an example of this is the phosphorylation of the C-terminal peptide of the mitochondrial ribosomal protein, MRP2, increased its binding to the three different PDZ-containing proteins PDZK1 (PDZ domain containing-protein), IKEPP (intestinal and kidney enriched PDZ protein) and EBP50 (ezrin-radixin-moesin binding phosphoprotein-50) (Hegedus et al., 2003). This is what happens in the interactions of the phosphorylated peptides (FATZ family, myotilin, palladin and myopalladin) with the PDZ domain of ZASP, phosphorylation enhances the binding.

It is known that ligands which bind to PDZ domains can contain a serine, threonine or tyrosine at the position 2 or 3 of the ligand (Cohen et al., 1996); we have a serine at the position 3 of the peptide(E[ST][DE][DE]L. The phosphorylated peptides showed stronger binding to the ZASP PDZ domain than the non-phosphorylated indicating that the phosphorylation had a positive effect on the binding with the PDZ domains.

A personal view and a very speculative hypothesis of mine is the following. The E[ST][DE][DE] motif common to the last 5 amino acids of the C-terminal of the proteins of the FATZ family, myotilin, palladin and myopalladin can allow them to be classified as a group of PDZ binding proteins which specifically bind to the PDZ domains of the Enigma family; phosphorylation of the serine or threonine at the third position of the peptide affected the binding to these PDZ domains. It is known that phosphorylation can reduce the affinity of interactions; a common example of this is the phosphorylation of the myosin heads which results in a reduction in the binding strength of the myosin head to actin leading to movement of the myosin head along actin. The effect of phosphorylation on an interaction could depend on the purpose of the

interaction; in the case of myosin it is needed to release the myosin in order to achieve movements which results in the contraction. In the case of the binding of the FATZ family, myotilin and myopalladin to ZASP, phosphorylation may be needed to strengthen their interactions to obtain higher stability of the Z-disk during contraction of the sarcomere. These proteins can still bind without phosphorylation, the phosphorylation only increases the binding so maybe these proteins only get phosphorylated when the sarcomere is contracting and dephosphorylated when the muscle is relaxed.

PDZ domains usually work as adaptors in connecting proteins together and localizing signalling proteins to different locations in the cell, they also play an important role in cell signalling which means that the FATZ family, myosin and myopalladin may act not only as muscle proteins involved in Z-disk structure but they may also be indirectly involved in cell signalling. This is not so strange since the FATZ family members have been shown to bind calcineurin and control its expression (Frey and Olson, 2002).

Chapter 5 CONCLUSIONS

The main finding of this thesis is the identification of a group of mainly striated muscle proteins, consisting of the FATZ family, myotilin, palladin and myopalladin, that selectively interact via a C-terminal motif with the PDZ domains of several Enigma proteins, ZASP, CLP-36 and ALP. These interactions were verified by several methods such as Co-IP, *in vitro* binding using the AlphaScreen technique and PDZ Arrays. The interaction of these proteins with the Enigma family members is highly specific as verified by the restricted number of PDZ domain proteins with which their peptide ligands will bind when given the opportunity. In fact only 2 of the 28 PDZ domain proteins on the Array bound to the peptide ligands, interestingly these were the only two Enigma family members on the Array; RIL and CLP-36 (hCLIM1). Therefore based on the results of the PDZ Array experiments RIL would appear to be a binding partner for proteins of the FATZ family, myotilin, palladin and myopalladin. Based on the work presented in this thesis we propose that the FATZ family, myotilin, palladin and myopalladin bind to members of the Enigma family of PDZ proteins via a C-terminal class III type PDZ ligand. This ligand motif [ST][DE][DE]L falls into the category of a class III PDZ domain binding motif.

I was also able to find another new binding partner for FATZ-3, namely Ankrd2, and also map its binding site to the N-terminal that is the region of FATZ-3 known to bind calcineurin, γ-filamin, α-actinin and telethonin. This is an interesting finding since Ankrd2 protein is thought to be involved in muscle stress response pathways and regulating gene expression. In fact, it is located both in the nucleus and the I band of

striated muscle cells and accumulates in the euchromatin in the nuclei of myofibres on muscle injury.

Another important object of this thesis was to study the tertiary structure FATZ-3 by using protein crystallography. After many difficulties expressing and producing native full-length FATZ-3 protein I adopted the approach of producing FATZ-3 without the N-terminal 80 amino acids. I was able to produce enough of this truncated FATZ-3 protein (171 amino acids) to do some structural studies at the laboratory of Prof. Kristina Carugo. I undertook some preliminary experiments such as circular dichroism and dynamic light scattering to obtain information on FATZ-3. The circular dichroism data I obtained showed that the purified C-terminal region of the FATZ-3 has a high percentage (42%) of random coils therefore the protein may not be well folded. The dynamic light scattering analysis showed that the percentage of polydispersity was low, indicating that the protein was homogenous in solution. I went ahead and tried about 300 crystallization conditions and started to obtain crystals after 1 month. However none of the crystals gave a good diffraction pattern when checked by X-ray nevertheless I have now defined the conditions suitable for crystal formation from purified C-terminal FATZ-3 protein.

Chapter 6 References

Arber, S., Halder, G. and Caroni, P. (1994) Muscle LIM protein, a novel essential regulator of myogenesis, promotes myogenic differentiation. *Cell*, **79**, 221-231.

Arber, S., Hunter, J.J., Ross, J., Jr., Hongo, M., Sansig, G., Borg, J., Perriard, J.C., Chien, K.R. and Caroni, P. (1997) MLP-deficient mice exhibit a disruption of cardiac cytoarchitectural organization, dilated cardiomyopathy, and heart failure. *Cell*, **88**, 393-403.

Arola, A.M., Sanchez, X., Murphy, R.T., Hasle, E., Li, H., Elliott, P.M., McKenna, W.J., Towbin, J.A. and Bowles, N.E. (2007) Mutations in PDLIM3 and MYOZ1 encoding myocyte Z line proteins are infrequently found in idiopathic dilated cardiomyopathy. *Mol Genet Metab*.

Au, Y., Atkinson, R.A., Guerrini, R., Kelly, G., Joseph, C., Martin, S.R., Muskett, F.W., Pallavicini, A., Faulkner, G. and Pastore, A. (2004) Solution structure of ZASP PDZ domain; implications for sarcomere ultrastructure and enigma family redundancy. *Structure*, **12**, 611-622.

Bang, M.L., Centner, T., Fornoff, F., Geach, A.J., Gotthardt, M., McNabb, M., Witt, C.C., Labeit, D., Gregorio, C.C., Granzier, H. and Labeit, S. (2001a) The complete gene sequence of titin, expression of an unusual approximately 700-kDa titin isoform, and its interaction with obscurin identify a novel Z-line to I-band linking system. *Circ Res*, **89**, 1065-1072.

Bang, M.L., Mudry, R.E., McElhinny, A.S., Trombitas, K., Geach, A.J., Yamasaki, R., Sorimachi, H., Granzier, H., Gregorio, C.C. and Labeit, S. (2001b) Myopalladin, a novel 145-kilodalton sarcomeric protein with multiple roles in Z-disc and I-band protein assemblies. *J Cell Biol*, **153**, 413-427.

Banuelos, S., Saraste, M. and Carugo, K.D. (1998) Structural comparisons of calponin homology domains: implications for actin binding. *Structure*, **6**, 1419-1431.

Barres, R., Gonzalez, T., Le Marchand-Brustel, Y. and Tanti, J.F. (2005) The interaction between the adaptor protein APS and Enigma is involved in actin organisation. *Exp Cell Res*, **308**, 334-344.

Bashirova, A.A., Markelov, M.L., Shlykova, T.V., Levshenkova, E.V., Alibaeva, R.A. and Frolova, E.I. (1998) The human RIL gene: mapping to human chromosome 5q31.1, genomic organization and alternative transcripts. *Gene*, **210**, 239-245.

Bauer, K., Kratzer, M., Otte, M., de Quintana, K.L., Hagmann, J., Arnold, G.J., Eckerskorn, C., Lottspeich, F. and Siess, W. (2000) Human CLP36, a PDZ-domain and LIM-domain protein, binds to alpha-actinin-1 and associates with actin filaments and stress fibers in activated platelets and endothelial cells. *Blood*, **96**, 4236-4245.

Beggs, A.H., Byers, T.J., Knoll, J.H., Boyce, F.M., Bruns, G.A. and Kunkel, L.M. (1992) Cloning and characterization of two human skeletal muscle alpha-actinin genes located on chromosomes 1 and 11. *J Biol Chem*, **267**, 9281-9288.

Bezprozvanny, I. and Maximov, A. (2001) Classification of PDZ domains. *FEBS Lett*, **509**, 457-462.

Blanchard, A., Ohanian, V. and Critchley, D. (1989) The structure and function of alpha-actinin. *J Muscle Res Cell Motil*, **10**, 280-289.

Borrello, M.G., Mercalli, E., Perego, C., Degl'Innocenti, D., Ghizzoni, S., Arighi, E., Eroini, B., Rizzetti, M.G. and Pierotti, M.A. (2002) Differential interaction of Enigma protein with the two RET isoforms. *Biochem Biophys Res Commun*, **296**, 515-522.

Bos, J.M., Poley, R.N., Ny, M., Tester, D.J., Xu, X., Vatta, M., Towbin, J.A., Gersh, B.J., Ommen, S.R. and Ackerman, M.J. (2006) Genotype-phenotype relationships involving hypertrophic cardiomyopathy-associated mutations in titin, muscle LIM protein, and telethonin. *Mol Genet Metab*, **88**, 78-85.

Boumber, Y.A., Kondo, Y., Chen, X., Shen, L., Gharibyan, V., Konishi, K., Estey, E., Kantarjian, H., Garcia-Manero, G. and Issa, J.P. (2007) RIL, a LIM gene on 5q31, is silenced by methylation in cancer and sensitizes cancer cells to apoptosis. *Cancer Res*, **67**, 1997-2005.

Casella, J.F., Craig, S.W., Maack, D.J. and Brown, A.E. (1987) Cap Z(36/32), a barbed end actin-capping protein, is a component of the Z-line of skeletal muscle. *J Cell Biol*, **105**, 371-379.

Centner, T., Yano, J., Kimura, E., McElhinny, A.S., Pelin, K., Witt, C.C., Bang, M.L., Trombitas, K., Granzier, H., Gregorio, C.C., Sorimachi, H. and Labeit, S. (2001) Identification of muscle specific ring finger proteins as potential regulators of the titin kinase domain. *J Mol Biol*, **306**, 717-726.

Chakarova, C., Wehnert, M.S., Uhl, K., Sakthivel, S., Vosberg, H.P., van der Ven, P.F. and Furst, D.O. (2000) Genomic structure and fine mapping of the two human filamin gene paralogues FLNB and FLNC and comparative analysis of the filamin gene family. *Hum Genet*, **107**, 597-611.

Cho, K.O., Hunt, C.A. and Kennedy, M.B. (1992) The rat brain postsynaptic density fraction contains a homolog of the Drosophila discs-large tumor suppressor protein. *Neuron*, **9**, 929-942.

Christopherson, K.S., Hillier, B.J., Lim, W.A. and Bredt, D.S. (1999) PSD-95 assembles a ternary complex with the N-methyl-D-aspartic acid receptor and a bivalent neuronal NO synthase PDZ domain. *J Biol Chem*, **274**, 27467-27473.

Clark, K.A., McElhinny, A.S., Beckerle, M.C. and Gregorio, C.C. (2002) Striated muscle cytoarchitecture: an intricate web of form and function. *Annu Rev Cell Dev Biol*, **18**, 637-706.

Cohen, N.A., Brenman, J.E., Snyder, S.H. and Bredt, D.S. (1996) Binding of the inward rectifier K+ channel Kir 2.3 to PSD-95 is regulated by protein kinase A phosphorylation. *Neuron*, **17**, 759-767.

Cooke, R. 1995. Seventh biophysics discussion - molecular motors: structure, mechanics and energy transduction. *Biophys J Suppl*. 68:382-385.

Craig, R., and R. Padron. 2004. Molecular structure of the sarcomere. *In* Myology. Vol. 1. A.G. Engel and C. Franzini-Armstrong, editors. McGraw-Hill, Philadelphia.

Cuppen, E., Gerrits, H., Pepers, B., Wieringa, B. and Hendriks, W. (1998) PDZ motifs in PTP-BL and RIL bind to internal protein segments in the LIM domain protein RIL. *Mol Biol Cell*, **9**, 671-683.

Davies, P.J., Wallach, D., Willingham, M.C., Pastan, I., Yamaguchi, M. and Robson, R.M. (1978) Filamin-actin interaction. Dissociation of binding from gelation by Ca2+-activated proteolysis. *J Biol Chem*, **253**, 4036-4042.

Djinovic-Carugo, K., Gautel, M., Ylanne, J. and Young, P. (2002) The spectrin repeat: a structural platform for cytoskeletal protein assemblies. *FEBS Lett*, **513**, 119-123.

Doyle, D.A., Lee, A., Lewis, J., Kim, E., Sheng, M. and MacKinnon, R. (1996) Crystal structures of a complexed and peptide-free membrane protein-binding domain: molecular basis of peptide recognition by PDZ. *Cell*, **85**, 1067-1076.

Ebashi, S. and Ebashi, F. (1964) A New Protein Factor Promoting Contraction Of Actomyosin. *Nature*, **203**, 645-646.

Ecarnot-Laubriet, A., De Luca, K., Vandroux, D., Moisant, M., Bernard, C., Assem, M., Rochette, L. and Teyssier, J.R. (2000) Downregulation and nuclear relocation of MLP during the progression of right ventricular hypertrophy induced by chronic pressure overload. *J Mol Cell Cardiol*, **32**, 2385-2395.

Edwards, A.S. and Scott, J.D. (2000) A-kinase anchoring proteins: protein kinase A and beyond. *Curr Opin Cell Biol*, **12**, 217-221.

Ehler, E., Horowits, R., Zuppinger, C., Price, R.L., Perriard, E., Leu, M., Caroni, P., Sussman, M., Eppenberger, H.M. and Perriard, J.C. (2001) Alterations at the intercalated disk associated with the absence of muscle LIM protein. *J Cell Biol*, **153**, 763-772.

Faulkner, G., Pallavicini, A., Comelli, A., Salamon, M., Bortoletto, G., Ievolella, C., Trevisan, S., Kojic, S., Dalla Vecchia, F., Laveder, P., Valle, G. and Lanfranchi, G. (2000) FATZ, a filamin-, actinin-, and telethonin-binding protein of the Z-disc of skeletal muscle. *J Biol Chem*, **275**, 41234-41242.

Faulkner, G., Pallavicini, A., Formentin, E., Comelli, A., Ievolella, C., Trevisan, S., Bortoletto, G., Scannapieco, P., Salamon, M., Mouly, V., Valle, G. and Lanfranchi, G. (1999) ZASP: a new Z-band alternatively spliced PDZ-motif protein. *J Cell Biol*, **146**, 465-475.

Frank, D., Kuhn, C., Katus, H.A. and Frey, N. (2006) The sarcomeric Z-disc: a nodal point in signalling and disease. *J Mol Med*, **84**, 446-468.

Frey, N., Barrientos, T., Shelton, J.M., Frank, D., Rutten, H., Gehring, D., Kuhn, C., Lutz, M., Rothermel, B., Bassel-Duby, R., Richardson, J.A., Katus, H.A., Hill, J.A. and Olson, E.N. (2004) Mice lacking calsarcin-1 are sensitized to calcineurin signaling and show accelerated cardiomyopathy in response to pathological biomechanical stress. *Nat Med*, **10**, 1336-1343.

Frey, N. and Olson, E.N. (2002) Calsarcin-3, a novel skeletal muscle-specific member of the calsarcin family, interacts with multiple Z-disc proteins. *J Biol Chem*, **277**, 13998-14004.

Frey, N., Richardson, J.A. and Olson, E.N. (2000) Calsarcins, a novel family of sarcomeric calcineurin-binding proteins. *Proc Natl Acad Sci U S A*, **97**, 14632-14637.

Furukawa, T., Ono, Y., Tsuchiya, H., Katayama, Y., Bang, M.L., Labeit, D., Labeit, S., Inagaki, N. and Gregorio, C.C. (2001) Specific interaction of the potassium channel beta-subunit minK with the sarcomeric protein T-cap suggests a T-tubule-myofibril linking system. *J Mol Biol*, **313**, 775-784.

Fyrberg, C., Ketchum, A., Ball, E. and Fyrberg, E. (1998) Characterization of lethal Drosophila melanogaster alpha-actinin mutants. *Biochem Genet*, **36**, 299-310.

Fyrberg, E., Kelly, M., Ball, E., Fyrberg, C. and Reedy, M.C. (1990) Molecular genetics of Drosophila alpha-actinin: mutant alleles disrupt Z disc integrity and muscle insertions. *J Cell Biol*, **110**, 1999-2011.

Gautel, M. and Goulding, D. (1996) A molecular map of titin/connectin elasticity reveals two different mechanisms acting in series. *FEBS Lett*, **385**, 11-14.

Gimona, M., Djinovic-Carugo, K., Kranewitter, W.J. and Winder, S.J. (2002) Functional plasticity of CH domains. *FEBS Lett*, **513**, 98-106.

Gontier, Y., Taivainen, A., Fontao, L., Sonnenberg, A., van der Flier, A., Carpen, O., Faulkner, G. and Borradori, L. (2005) The Z-disc proteins myotilin and FATZ-1 interact with each other and are connected to the sarcolemma via muscle-specific filamins. *J Cell Sci*, **118**, 3739-3749.

Gorlin, J.B., Yamin, R., Egan, S., Stewart, M., Stossel, T.P., Kwiatkowski, D.J. and Hartwig, J.H. (1990) Human endothelial actin-binding protein (ABP-280, nonmuscle filamin): a molecular leaf spring. *J Cell Biol*, **111**, 1089-1105.

Granzier, H.L. and Labeit, S. (2004) The giant protein titin: a major player in myocardial mechanics, signaling, and disease. *Circ Res*, **94**, 284-295.

Gregorio, C.C., Trombitas, K., Centner, T., Kolmerer, B., Stier, G., Kunke, K., Suzuki, K., Obermayr, F., Herrmann, B., Granzier, H., Sorimachi, H. and Labeit, S. (1998) The NH2 terminus of titin spans the Z-disc: its interaction with a novel 19-kD ligand (T-cap) is required for sarcomeric integrity. *J Cell Biol*, **143**, 1013-1027.

Griggs, R., Vihola, A., Hackman, P., Talvinen, K., Haravuori, H., Faulkner, G., Eymard, B., Richard, I., Selcen, D., Engel, A., Carpen, O. and Udd, B. (2007) Zaspopathy in a large classic late-onset distal myopathy family. *Brain*.

Grootjans, J.J., Reekmans, G., Ceulemans, H. and David, G. (2000) Syntenin-syndecan binding requires syndecan-synteny and the co-operation of both PDZ domains of syntenin. *J Biol Chem*, **275**, 19933-19941.

Guy, P.M., Kenny, D.A. and Gill, G.N. (1999) The PDZ domain of the LIM protein enigma binds to beta-tropomyosin. *Mol Biol Cell*, **10**, 1973-1984.

Hance, J.E., Fu, S.Y., Watkins, S.C., Beggs, A.H. and Michalak, M. (1999) alpha-actinin-2 is a new component of the dystrophin-glycoprotein complex. *Arch Biochem Biophys*, **365**, 216-222.

Harris, B.Z. and Lim, W.A. (2001) Mechanism and role of PDZ domains in signaling complex assembly. *J Cell Sci*, **114**, 3219-3231.

Harrison, S.C. (1996) Peptide-surface association: the case of PDZ and PTB domains. *Cell*, **86**, 341-343.

Hartwig, J.H. and Stossel, T.P. (1981) Structure of macrophage actin-binding protein molecules in solution and interacting with actin filaments. *J Mol Biol*, **145**, 563-581.

Hauser, M.A., Conde, C.B., Kowaljow, V., Zeppa, G., Taratuto, A.L., Torian, U.M., Vance, J., Pericak-Vance, M.A., Speer, M.C. and Rosa, A.L. (2002) myotilin Mutation found in second pedigree with LGMD1A. *Am J Hum Genet*, **71**, 1428-1432.

Hauser, M.A., Horrigan, S.K., Salmikangas, P., Torian, U.M., Viles, K.D., Dancel, R., Tim, R.W., Taivainen, A., Bartoloni, L., Gilchrist, J.M., Stajich, J.M., Gaskell, P.C., Gilbert, J.R., Vance, J.M., Pericak-Vance, M.A., Carpen, O., Westbrook, C.A. and Speer, M.C. (2000) Myotilin is mutated in limb girdle muscular dystrophy 1A. *Hum Mol Genet*, **9**, 2141-2147.

Haworth, R.S., Cuello, F., Herron, T.J., Franzen, G., Kentish, J.C., Gautel, M. and Avkiran, M. (2004) Protein kinase D is a novel mediator of cardiac troponin I phosphorylation and regulates myofilament function. *Circ Res*, **95**, 1091-1099.

Hayashi, T., Arimura, T., Itoh-Satoh, M., Ueda, K., Hohda, S., Inagaki, N., Takahashi, M., Hori, H., Yasunami, M., Nishi, H., Koga, Y., Nakamura, H., Matsuzaki, M., Choi, B.Y., Bae, S.W., You, C.W., Han, K.H., Park, J.E., Knoll, R., Hoshijima, M., Chien, K.R. and Kimura, A. (2004) Tcap gene mutations in hypertrophic cardiomyopathy and dilated cardiomyopathy. *J Am Coll Cardiol*, **44**, 2192-2201.

Hegedus, T., Sessler, T., Scott, R., Thelin, W., Bakos, E., Varadi, A., Szabo, K., Homolya, L., Milgram, S.L. and Sarkadi, B. (2003) C-terminal phosphorylation of MRP2 modulates its interaction with PDZ proteins. *Biochem Biophys Res Commun*, **302**, 454-461.

Henderson, J.R., Pomies, P., Auffray, C. and Beckerle, M.C. (2003) ALP and MLP distribution during myofibrillogenesis in cultured cardiomyocytes. *Cell Motil Cytoskeleton*, **54**, 254-265.

Himmel, M., Van Der Ven, P.F., Stocklein, W. and Furst, D.O. (2003) The limits of promiscuity: isoform-specific dimerization of filamins. *Biochemistry*, **42**, 430-439.

Holtzer, H., Hijikata, T., Lin, Z.X., Zhang, Z.Q., Holtzer, S., Protasi, F., Franzini-Armstrong, C. and Sweeney, H.L. (1997) Independent assembly of 1.6 microns long bipolar MHC filaments and I-Z-I bodies. *Cell Struct Funct*, **22**, 83-93.

Honda, K., Yamada, T., Endo, R., Ino, Y., Gotoh, M., Tsuda, H., Yamada, Y., Chiba, H. and Hirohashi, S. (1998) Actinin-4, a novel actin-bundling protein associated with cell motility and cancer invasion. *J Cell Biol*, **140**, 1383-1393.

Hoshijima, M. (2006) Mechanical stress-strain sensors embedded in cardiac cytoskeleton: Z disk, titin, and associated structures. *Am J Physiol Heart Circ Physiol*, **290**, H1313-1325.

Huang, C., Zhou, Q., Liang, P., Hollander, M.S., Sheikh, F., Li, X., Greaser, M., Shelton, G.D., Evans, S. and Chen, J. (2003) Characterization and in vivo functional analysis of splice variants of cypher. *J Biol Chem*, **278**, 7360-7365.

Hung, A.Y. and Sheng, M. (2002) PDZ domains: structural modules for protein complex assembly. *J Biol Chem*, **277**, 5699-5702.

Huxley, A.F. and Niedergerke, R. (1954) Structural changes in muscle during contraction; interference microscopy of living muscle fibres. *Nature*, **173**, 971-973.

Huxley, H. and Hanson, J. (1954) Changes in the cross-striations of muscle during contraction and stretch and their structural interpretation. *Nature*, **173**, 973-976.

Ilkovski, B., Cooper, S.T., Nowak, K., Ryan, M.M., Yang, N., Schnell, C., Durling, H.J., Roddick, L.G., Wilkinson, I., Kornberg, A.J., Collins, K.J., Wallace, G., Gunning, P., Hardeman, E.C., Laing, N.G. and North, K.N. (2001) Nemaline myopathy caused by mutations in the muscle alpha-skeletal-actin gene. *Am J Hum Genet*, **68**, 1333-1343.

Itoh-Satoh, M., Hayashi, T., Nishi, H., Koga, Y., Arimura, T., Koyanagi, T., Takahashi, M., Hohda, S., Ueda, K., Nouchi, T., Hiroe, M., Marumo, F., Imaizumi, T., Yasunami, M. and Kimura, A. (2002) Titin mutations as the molecular basis for dilated cardiomyopathy. *Biochem Biophys Res Commun*, **291**, 385-393.

Jelen, F., Oleksy, A., Smietana, K. and Otlewski, J. (2003) PDZ domains - common players in the cell signaling. *Acta Biochim Pol*, **50**, 985-1017.

Jeyaseelan, R., Poizat, C., Baker, R.K., Abdishoo, S., Isterabadi, L.B., Lyons, G.E. and Kedes, L. (1997) A novel cardiac-restricted target for doxorubicin. CARP, a nuclear modulator of gene expression in cardiac progenitor cells and cardiomyocytes. *J Biol Chem*, **272**, 22800-22808.

Kang, B.S., Cooper, D.R., Jelen, F., Devedjiev, Y., Derewenda, U., Dauter, Z., Otlewski, J. and Derewenda, Z.S. (2003) PDZ tandem of human syntenin: crystal structure and functional properties. *Structure*, **11**, 459-468.

Kemp, T.J., Sadusky, T.J., Saltisi, F., Carey, N., Moss, J., Yang, S.Y., Sassoon, D.A., Goldspink, G. and Coulton, G.R. (2000) Identification of Ankrd2, a novel skeletal muscle gene coding for a stretch-responsive ankyrin-repeat protein. *Genomics*, **66**, 229-241.

Kiess, M., Scharm, B., Aguzzi, A., Hajnal, A., Klemenz, R., Schwarte-Waldhoff, I. and Schafer, R. (1995) Expression of ril, a novel LIM domain gene, is down-regulated in Hras-transformed cells and restored in phenotypic revertants. *Oncogene*, **10**, 61-68.

Kim, E., Niethammer, M., Rothschild, A., Jan, Y.N. and Sheng, M. (1995) Clustering of Shaker-type K+ channels by interaction with a family of membrane-associated guanylate kinases. *Nature*, **378**, 85-88.

Klaavuniemi, T., Kelloniemi, A. and Ylanne, J. (2004) The ZASP-like motif in actinin-associated LIM protein is required for interaction with the alpha-actinin rod and for targeting to the muscle Z-line. *J Biol Chem*, **279**, 26402-26410.

Klaavuniemi, T. and Ylanne, J. (2006) Zasp/Cypher internal ZM-motif containing fragments are sufficient to co-localize with alpha-actinin--analysis of patient mutations. *Exp Cell Res*, **312**, 1299-1311.

Knoll, T., Michel, M.S., Cueva-Martinez, A., Spahn, M., Bross, S., Alken, P. and Kohrmann, K.U. (2002) Evaluation of superficial papillary ablation by endoscopic lasers in an ex vivo kidney model. *J Endourol*, **16**, 195-200.

Kojic, S., Medeot, E., Guccione, E., Krmac, H., Zara, I., Martinelli, V., Valle, G. and Faulkner, G. (2004) The Ankrd2 protein, a link between the sarcomere and the nucleus in skeletal muscle. *J Mol Biol*, **339**, 313-325.

Kong, Y., Flick, M.J., Kudla, A.J. and Konieczny, S.F. (1997) Muscle LIM protein promotes myogenesis by enhancing the activity of MyoD. *Mol Cell Biol*, **17**, 4750-4760.

Kontrogianni-Konstantopoulos, A. and Bloch, R.J. (2003) The hydrophilic domain of small ankyrin-1 interacts with the two N-terminal immunoglobulin domains of titin. *J Biol Chem*, **278**, 3985-3991.

Kotaka, M., Kostin, S., Ngai, S., Chan, K., Lau, Y., Lee, S.M., Li, H., Ng, E.K., Schaper, J., Tsui, S.K., Fung, K., Lee, C. and Waye, M.M. (2000) Interaction of hCLIM1, an enigma family protein, with alpha-actinin 2. *J Cell Biochem*, **78**, 558-565.

Kotaka, M., Lau, Y.M., Cheung, K.K., Lee, S.M., Li, H.Y., Chan, W.Y., Fung, K.P., Lee, C.Y., Waye, M.M. and Tsui, S.K. (2001) Elfin is expressed during early heart development. *J Cell Biochem*, **83**, 463-472.

Kotaka, M., Ngai, S.M., Garcia-Barcelo, M., Tsui, S.K., Fung, K.P., Lee, C.Y. and Waye, M.M. (1999) Characterization of the human 36-kDa carboxyl terminal LIM domain protein (hCLIM1). *J Cell Biochem*, **72**, 279-285.

Kozlov, G., Gehring, K. and Ekiel, I. (2000) Solution structure of the PDZ2 domain from human phosphatase hPTP1E and its interactions with C-terminal peptides from the Fas receptor. *Biochemistry*, **39**, 2572-2580.

Krishnamoorthy, R.V. (1977) Increased histaminase activity in the atrophic muscle of denervated frog. *Enzyme*, **22**, 73-79.

Kruger, M., Wright, J. and Wang, K. (1991) Nebulin as a length regulator of thin filaments of vertebrate skeletal muscles: correlation of thin filament length, nebulin size, and epitope profile. *J Cell Biol*, **115**, 97-107.

Kuo, H., Chen, J., Ruiz-Lozano, P., Zou, Y., Nemer, M. and Chien, K.R. (1999) Control of segmental expression of the cardiac-restricted ankyrin repeat protein gene by distinct regulatory pathways in murine cardiogenesis. *Development*, **126**, 4223-4234.

Kuroda, S., Tokunaga, C., Kiyohara, Y., Higuchi, O., Konishi, H., Mizuno, K., Gill, G.N. and Kikkawa, U. (1996) Protein-protein interaction of zinc finger LIM domains with protein kinase C. *J Biol Chem*, **271**, 31029-31032.

Lange, S., Xiang, F., Yakovenko, A., Vihola, A., Hackman, P., Rostkova, E., Kristensen, J., Brandmeier, B., Franzen, G., Hedberg, B., Gunnarsson, L.G., Hughes, S.M., Marchand, S., Sejersen, T., Richard, I., Edstrom, L., Ehler, E., Udd, B. and Gautel, M. (2005) The kinase domain of titin controls muscle gene expression and protein turnover. *Science*, **308**, 1599-1603.

Lazarides, E. and Granger, B.L. (1978) Fluorescent localization of membrane sites in glycerinated chicken skeletal muscle fibers and the relationship of these sites to the protein composition of the Z disc. *Proc Natl Acad Sci U S A*, **75**, 3683-3687.

Lee, E.H., Gao, M., Pinotsis, N., Wilmanns, M. and Schulten, K. (2006) Mechanical strength of the titin Z1Z2-telethonin complex. *Structure*, **14**, 497-509.

Lin, Z., Hijikata, T., Zhang, Z., Choi, J., Holtzer, S., Sweeney, H.L. and Holtzer, H. (1998) Dispensability of the actin-binding site and spectrin repeats for targeting sarcomeric alpha-actinin into maturing Z bands in vivo: implications for in vitro binding studies. *Dev Biol*, **199**, 291-308.

Luther, P.K. (1991) Three-dimensional reconstruction of a simple Z-band in fish muscle. *J Cell Biol*, **113**, 1043-1055.

Luther, P.K. (2000) Three-dimensional structure of a vertebrate muscle Z-band: implications for titin and alpha-actinin binding. *J Struct Biol*, **129**, 1-16.

Luther, P.K., Barry, J.S. and Squire, J.M. (2002) The three-dimensional structure of a vertebrate wide (slow muscle) Z-band: lessons on Z-band assembly. *J Mol Biol*, **315**, 9-20.

MacArthur, D.G. and North, K.N. (2004) A gene for speed? The evolution and function of alpha-actinin-3. *Bioessays*, **26**, 786-795.

Maestrini, E., Patrosso, C., Mancini, M., Rivella, S., Rocchi, M., Repetto, M., Villa, A., Frattini, A., Zoppe, M., Vezzoni, P. and et al. (1993) Mapping of two genes encoding isoforms of the actin binding protein ABP-280, a dystrophin like protein, to Xq28 and to chromosome 7. *Hum Mol Genet*, **2**, 761-766.

Mason, P., Bayol, S. and Loughna, P.T. (1999) The novel sarcomeric protein telethonin exhibits developmental and functional regulation. *Biochem Biophys Res Commun*, **257**, 699-703.

Mayans, O., van der Ven, P.F., Wilm, M., Mues, A., Young, P., Furst, D.O., Wilmanns, M. and Gautel, M. (1998) Structural basis for activation of the titin kinase domain during myofibrillogenesis. *Nature*, **395**, 863-869.

McElhinny, A.S., Perry, C.N., Witt, C.C., Labeit, S. and Gregorio, C.C. (2004) Muscle-specific RING finger-2 (MURF-2) is important for microtubule, intermediate filament and sarcomeric M-line maintenance in striated muscle development. *J Cell Sci*, **117**, 3175-3188.

Meerschaert, K., Bruyneel, E., De Wever, O., Vanloo, B., Boucherie, C., Bracke, M., Vandekerckhove, J. and Gettemans, J. (2007) The tandem PDZ domains of syntenin promote cell invasion. *Exp Cell Res*.

Meyer, S.C., Zuerbig, S., Cunningham, C.C., Hartwig, J.H., Bissell, T., Gardner, K. and Fox, J.E. (1997) Identification of the region in actin-binding protein that binds to the cytoplasmic domain of glycoprotein IBalpha. *J Biol Chem*, **272**, 2914-2919.

Millake, D.B., Blanchard, A.D., Patel, B. and Critchley, D.R. (1989) The cDNA sequence of a human placental alpha-actinin. *Nucleic Acids Res*, **17**, 6725.

Miller, M.K., Bang, M.L., Witt, C.C., Labeit, D., Trombitas, C., Watanabe, K., Granzier, H., McElhinny, A.S., Gregorio, C.C. and Labeit, S. (2003) The muscle ankyrin repeat proteins: CARP, ankrd2/Arpp and DARP as a family of titin filament-based stress response molecules. *J Mol Biol*, **333**, 951-964.

Millevoi, S., Trombitas, K., Kolmerer, B., Kostin, S., Schaper, J., Pelin, K., Granzier, H. and Labeit, S. (1998) Characterization of nebulette and nebulin and emerging concepts of their roles for vertebrate Z-discs. *J Mol Biol*, **282**, 111-123.

Mohapatra, B., Jimenez, S., Lin, J.H., Bowles, K.R., Coveler, K.J., Marx, J.G., Chrisco, M.A., Murphy, R.T., Lurie, P.R., Schwartz, R.J., Elliott, P.M., Vatta, M., McKenna, W., Towbin, J.A. and Bowles, N.E. (2003) Mutations in the muscle LIM protein and alpha-actinin-2 genes in dilated cardiomyopathy and endocardial fibroelastosis. *Mol Genet Metab*, **80**, 207-215.

Moncman, C.L. and Wang, K. (1995) Nebulette: a 107 kD nebulin-like protein in cardiac muscle. *Cell Motil Cytoskeleton*, **32**, 205-225.

Montell, C. (1998) TRP trapped in fly signaling web. *Curr Opin Neurobiol*, **8**, 389-397.

Montell, C. (2000) A PDZ protein ushers in new links. *Nat Genet*, **26**, 6-7.

Moreira, E.S., Wiltshire, T.J., Faulkner, G., Nilforoushan, A., Vainzof, M., Suzuki, O.T., Valle, G., Reeves, R., Zatz, M., Passos-Bueno, M.R. and Jenne, D.E. (2000) Limb-girdle muscular dystrophy type 2G is caused by mutations in the gene encoding the sarcomeric protein telethonin. *Nat Genet*, **24**, 163-166.

Moriyama, M., Tsukamoto, Y., Fujiwara, M., Kondo, G., Nakada, C., Baba, T., Ishiguro, N., Miyazaki, A., Nakamura, K., Hori, N., Sato, K., Shomori, K., Takeuchi, K., Satoh, H., Mori, S. and Ito, H. (2001) Identification of a novel human ankyrin-repeated protein homologous to CARP. *Biochem Biophys Res Commun*, **285**, 715-723.

Mues, A., van der Ven, P.F., Young, P., Furst, D.O. and Gautel, M. (1998) Two immunoglobulin-like domains of the Z-disc portion of titin interact in a conformation-dependent way with telethonin. *FEBS Lett*, **428**, 111-114.

Mykkanen, O.M., Gronholm, M., Ronty, M., Lalowski, M., Salmikangas, P., Suila, H. and Carpen, O. (2001) Characterization of human palladin, a microfilament-associated protein. *Mol Biol Cell*, **12**, 3060-3073.

Nakada, C., Oka, A., Nonaka, I., Sato, K., Mori, S., Ito, H. and Moriyama, M. (2003) Cardiac ankyrin repeat protein is preferentially induced in atrophic myofibers of congenital myopathy and spinal muscular atrophy. *Pathol Int*, **53**, 653-658.

Nakagawa, N., Hoshijima, M., Oyasu, M., Saito, N., Tanizawa, K. and Kuroda, S. (2000) ENH, containing PDZ and LIM domains, heart/skeletal muscle-specific protein, associates with cytoskeletal proteins through the PDZ domain. *Biochem Biophys Res Commun*, **272**, 505-512.

Nave, R., Furst, D.O. and Weber, K. (1990) Interaction of alpha-actinin and nebulin in vitro. Support for the existence of a fourth filament system in skeletal muscle. *FEBS Lett*, **269**, 163-166.

Nicholas, G., Thomas, M., Langley, B., Somers, W., Patel, K., Kemp, C.F., Sharma, M. and Kambadur, R. (2002) Titin-cap associates with, and regulates secretion of, Myostatin. *J Cell Physiol*, **193**, 120-131.

Niederlander, N., Fayein, N.A., Auffray, C. and Pomies, P. (2004) Characterization of a new human isoform of the enigma homolog family specifically expressed in skeletal muscle. *Biochem Biophys Res Commun*, **325**, 1304-1311.

Niethammer, M., Valtschanoff, J.G., Kapoor, T.M., Allison, D.W., Weinberg, R.J., Craig, A.M. and Sheng, M. (1998) CRIPT, a novel postsynaptic protein that binds to the third PDZ domain of PSD-95/SAP90. *Neuron*, **20**, 693-707.

North, K.N. and Beggs, A.H. (1996) Deficiency of a skeletal muscle isoform of alpha-actinin (alpha-actinin-3) in merosin-positive congenital muscular dystrophy. *Neuromuscul Disord*, **6**, 229-235.

Nowak, K.J., Wattanasirichaigoon, D., Goebel, H.H., Wilce, M., Pelin, K., Donner, K., Jacob, R.L., Hubner, C., Oexle, K., Anderson, J.R., Verity, C.M., North, K.N., Iannaccone, S.T., Muller, C.R., Nurnberg, P., Muntoni, F., Sewry, C., Hughes, I., Sutphen, R., Lacson, A.G., Swoboda, K.J., Vigneron, J., Wallgren-Pettersson, C., Beggs, A.H. and Laing, N.G. (1999) Mutations in the skeletal muscle alpha-actin gene in patients with actin myopathy and nemaline myopathy. *Nat Genet*, **23**, 208-212.

Ohtsuka, H., Yajima, H., Maruyama, K. and Kimura, S. (1997) The N-terminal Z repeat 5 of connectin/titin binds to the C-terminal region of alpha-actinin. *Biochem Biophys Res Commun*, **235**, 1-3.

Olson, J.J. (2000) Neurosurgical advances in the treatment of brain tumors. *Curr Oncol Rep*, **2**, 434-437.

Olson, T.M., Doan, T.P., Kishimoto, N.Y., Whitby, F.G., Ackerman, M.J. and Fananapazir, L. (2000) Inherited and de novo mutations in the cardiac actin gene cause hypertrophic cardiomyopathy. *J Mol Cell Cardiol*, **32**, 1687-1694.

Olson, T.M., Michels, V.V., Thibodeau, S.N., Tai, Y.S. and Keating, M.T. (1998) Actin mutations in dilated cardiomyopathy, a heritable form of heart failure. *Science*, **280**, 750-752.

Osio, A., Tan, L., Chen, S.N., Lombardi, R., Nagueh, S.F., Shete, S., Roberts, R., Willerson, J.T. and Marian, A.J. (2007) Myozenin 2 is a novel gene for human hypertrophic cardiomyopathy. *Circ Res*, **100**, 766-768.

Otey, C.A., Rachlin, A., Moza, M., Arneman, D. and Carpen, O. (2005) The palladin/myotilin/myopalladin family of actin-associated scaffolds. *Int Rev Cytol*, **246**, 31-58.

Pallavicini, A., Kojic, S., Bean, C., Vainzof, M., Salamon, M., Ievolella, C., Bortoletto, G., Pacchioni, B., Zatz, M., Lanfranchi, G., Faulkner, G. and Valle, G. (2001) Characterization of human skeletal muscle Ankrd2. *Biochem Biophys Res Commun*, **285**, 378-386.

Pallen, M.J. and Ponting, C.P. (1997) PDZ domains in bacterial proteins. *Mol Microbiol*, **26**, 411-413.

Papa, I., Astier, C., Kwiatek, O., Raynaud, F., Bonnal, C., Lebart, M.C., Roustan, C. and Benyamin, Y. (1999) Alpha actinin-CapZ, an anchoring complex for thin filaments in Z-line. *J Muscle Res Cell Motil*, **20**, 187-197.

Parast, M.M. and Otey, C.A. (2000) Characterization of palladin, a novel protein localized to stress fibers and cell adhesions. *J Cell Biol*, **150**, 643-656.

Pashmforoush, M., Pomies, P., Peterson, K.L., Kubalak, S., Ross, J., Jr., Hefti, A., Aebi, U., Beckerle, M.C. and Chien, K.R. (2001) Adult mice deficient in actinin-associated LIM-domain protein reveal a developmental pathway for right ventricular cardiomyopathy. *Nat Med*, **7**, 591-597.

Passier, R., Richardson, J.A. and Olson, E.N. (2000) Oracle, a novel PDZ-LIM domain protein expressed in heart and skeletal muscle. *Mech Dev*, **92**, 277-284.

Pinotsis, N., Petoukhov, M., Lange, S., Svergun, D., Zou, P., Gautel, M. and Wilmanns, M. (2006) Evidence for a dimeric assembly of two titin/telethonin complexes induced by the telethonin C-terminus. *J Struct Biol*, **155**, 239-250.

Popowicz, G.M., Schleicher, M., Noegel, A.A. and Holak, T.A. (2006) Filamins: promiscuous organizers of the cytoskeleton. *Trends Biochem Sci*, **31**, 411-419.

Puntervoll, P., Linding, R., Gemund, C., Chabanis-Davidson, S., Mattingsdal, M., Cameron, S., Martin, D.M., Ausiello, G., Brannetti, B., Costantini, A., Ferre, F., Maselli, V., Via, A., Cesareni, G., Diella, F., Superti-Furga, G., Wyrwicz, L., Ramu, C., McGuigan, C., Gudavalli, R., Letunic, I., Bork, P., Rychlewski, L., Kuster, B., Helmer-Citterich, M., Hunter, W.N., Aasland, R. and Gibson, T.J. (2003) ELM server: A new resource for investigating short functional sites in modular eukaryotic proteins. *Nucleic Acids Res*, **31**, 3625-3630.

Rhee, D., Sanger, J.M. and Sanger, J.W. (1994) The premyofibril: evidence for its role in myofibrillogenesis. *Cell Motil Cytoskeleton*, **28**, 1-24.

Richard, I., Broux, O., Allamand, V., Fougerousse, F., Chiannilkulchai, N., Bourg, N., Brenguier, L., Devaud, C., Pasturaud, P., Roudaut, C. and et al. (1995) Mutations in the proteolytic enzyme calpain 3 cause limb-girdle muscular dystrophy type 2A. *Cell*, **81**, 27-40.

Ronty, M., Taivainen, A., Heiska, L., Otey, C., Ehler, E., Song, W.K. and Carpen, O. (2007) Palladin interacts with SH3 domains of SPIN90 and Src and is required for Src-induced cytoskeletal remodeling. *Exp Cell Res*, **313**, 2575-2585.

Roulier, E.M., Fyrberg, C. and Fyrberg, E. (1992) Perturbations of Drosophila alpha-actinin cause muscle paralysis, weakness, and atrophy but do not confer obvious nonmuscle phenotypes. *J Cell Biol*, **116**, 911-922.

Salmikangas, P., Mykkanen, O.M., Gronholm, M., Heiska, L., Kere, J. and Carpen, O. (1999) Myotilin, a novel sarcomeric protein with two Ig-like domains, is encoded by a candidate gene for limb-girdle muscular dystrophy. *Hum Mol Genet*, **8**, 1329-1336.

Salmikangas, P., van der Ven, P.F., Lalowski, M., Taivainen, A., Zhao, F., Suila, H., Schroder, R., Lappalainen, P., Furst, D.O. and Carpen, O. (2003) Myotilin, the limb-girdle muscular dystrophy 1A (LGMD1A) protein, cross-links actin filaments and controls sarcomere assembly. *Hum Mol Genet*, **12**, 189-203.

Sanger, J.W., Ayoob, J.C., Chowrashi, P., Zurawski, D. and Sanger, J.M. (2000) Assembly of myofibrils in cardiac muscle cells. *Adv Exp Med Biol*, **481**, 89-102; discussion 103-105.

Schultheiss, T., Choi, J., Lin, Z.X., DiLullo, C., Cohen-Gould, L., Fischman, D. and Holtzer, H. (1992) A sarcomeric alpha-actinin truncated at the carboxyl end induces the breakdown of stress fibers in PtK2 cells and the formation of nemaline-like bodies and breakdown of myofibrils in myotubes. *Proc Natl Acad Sci U S A*, **89**, 9282-9286.

Schultz, J., Copley, R.R., Doerks, T., Ponting, C.P. and Bork, P. (2000) SMART: a web-based tool for the study of genetically mobile domains. *Nucleic Acids Res*, **28**, 231-234.

Schultz, J., Milpetz, F., Bork, P. and Ponting, C.P. (1998) SMART, a simple modular architecture research tool: identification of signaling domains. *Proc Natl Acad Sci U S A*, **95**, 5857-5864.

Schulz, T.W., Nakagawa, T., Licznerski, P., Pawlak, V., Kolleker, A., Rozov, A., Kim, J., Dittgen, T., Kohr, G., Sheng, M., Seeburg, P.H. and Osten, P. (2004) Actin/alpha-actinin-dependent transport of AMPA receptors in dendritic spines: role of the PDZ-LIM protein RIL. *J Neurosci*, **24**, 8584-8594.

Selcen, D. and Engel, A.G. (2004) Mutations in myotilin cause myofibrillar myopathy. *Neurology*, **62**, 1363-1371.

Sheng, M. and Sala, C. (2001) PDZ domains and the organization of supramolecular complexes. *Annu Rev Neurosci*, **24**, 1-29.

Songyang, Z., Fanning, A.S., Fu, C., Xu, J., Marfatia, S.M., Chishti, A.H., Crompton, A., Chan, A.C., Anderson, J.M. and Cantley, L.C. (1997) Recognition of unique carboxyl-terminal motifs by distinct PDZ domains. *Science*, **275**, 73-77.

Sorimachi, H., Kinbara, K., Kimura, S., Takahashi, M., Ishiura, S., Sasagawa, N., Sorimachi, N., Shimada, H., Tagawa, K., Maruyama, K. and et al. (1995) Muscle-specific calpain, p94, responsible for limb girdle muscular dystrophy type 2A, associates with connectin through IS2, a p94-specific sequence. *J Biol Chem*, **270**, 31158-31162.

Spencer, J.A., Eliazer, S., Ilaria, R.L., Jr., Richardson, J.A. and Olson, E.N. (2000) Regulation of microtubule dynamics and myogenic differentiation by MURF, a striated muscle RING-finger protein. *J Cell Biol*, **150**, 771-784.

Stossel, T.P., Condeelis, J., Cooley, L., Hartwig, J.H., Noegel, A., Schleicher, M. and Shapiro, S.S. (2001) Filamins as integrators of cell mechanics and signalling. *Nat Rev Mol Cell Biol*, **2**, 138-145.

Stricker, N.L., Christopherson, K.S., Yi, B.A., Schatz, P.J., Raab, R.W., Dawes, G., Bassett, D.E., Jr., Bredt, D.S. and Li, M. (1997) PDZ domain of neuronal nitric oxide synthase recognizes novel C-terminal peptide sequences. *Nat Biotechnol*, **15**, 336-342.

Stura, E.A., Satterthwait, A.C., Calvo, J.C., Kaslow, D.C. and Wilson, I.A. (1994) Reverse screening. *Acta Crystallogr D Biol Crystallogr*, **50**, 448-455.

Takada, F., Vander Woude, D.L., Tong, H.Q., Thompson, T.G., Watkins, S.C., Kunkel, L.M. and Beggs, A.H. (2001) Myozenin: an alpha-actinin- and gamma-filamin-binding protein of skeletal muscle Z lines. *Proc Natl Acad Sci U S A*, **98**, 1595-1600.

Takafuta, T., Wu, G., Murphy, G.F. and Shapiro, S.S. (1998) Human beta-filamin is a new protein that interacts with the cytoplasmic tail of glycoprotein Ibalpha. *J Biol Chem*, **273**, 17531-17538.

Tang, J., Taylor, D.W. and Taylor, K.A. (2001) The three-dimensional structure of alpha-actinin obtained by cryoelectron microscopy suggests a model for Ca(2+)-dependent actin binding. *J Mol Biol*, **310**, 845-858.

Te Velthuis, A.J., Isogai, T., Gerrits, L. and Bagowski, C.P. (2007) Insights into the Molecular Evolution of the PDZ/LIM Family and Identification of a Novel Conserved Protein Motif. *PLoS ONE*, **2**, e189.

Thomas, G.H., Newbern, E.C., Korte, C.C., Bales, M.A., Muse, S.V., Clark, A.G. and Kiehart, D.P. (1997) Intragenic duplication and divergence in the spectrin superfamily of proteins. *Mol Biol Evol*, **14**, 1285-1295.

Tian, L.F., Li, H.Y., Jin, B.F., Pan, X., Man, J.H., Zhang, P.J., Li, W.H., Liang, B., Liu, H., Zhao, J., Gong, W.L., Zhou, T. and Zhang, X.M. (2006) MDM2 interacts with and downregulates a sarcomeric protein, TCAP. *Biochem Biophys Res Commun*, **345**, 355-361.

Tochio, H., Zhang, Q., Mandal, P., Li, M. and Zhang, M. (1999) Solution structure of the extended neuronal nitric oxide synthase PDZ domain complexed with an associated peptide. *Nat Struct Biol*, **6**, 417-421.

Tsukamoto, Y., Senda, T., Nakano, T., Nakada, C., Hida, T., Ishiguro, N., Kondo, G., Baba, T., Sato, K., Osaki, M., Mori, S., Ito, H. and Moriyama, M. (2002) Arpp, a new homolog of carp, is preferentially expressed in type 1 skeletal muscle fibers and is markedly induced by denervation. *Lab Invest*, **82**, 645-655.

Tsunoda, S. and Zuker, C.S. (1999) The organization of INAD-signaling complexes by a multivalent PDZ domain protein in Drosophila photoreceptor cells ensures sensitivity and speed of signaling. *Cell Calcium*, **26**, 165-171.

Tyler, J.M., Anderson, J.M. and Branton, D. (1980) Structural comparison of several actin-binding macromolecules. *J Cell Biol*, **85**, 489-495.

Vaccaro, P. and Dente, L. (2002) PDZ domains: troubles in classification. *FEBS Lett*, **512**, 345-349.

Vainzof, M. and Zatz, M. (2003) Protein defects in neuromuscular diseases. *Braz J Med Biol Res*, **36**, 543-555.

Valle, G., Faulkner, G., De Antoni, A., Pacchioni, B., Pallavicini, A., Pandolfo, D., Tiso, N., Toppo, S., Trevisan, S. and Lanfranchi, G. (1997) Telethonin, a novel sarcomeric protein of heart and skeletal muscle. *FEBS Lett*, **415**, 163-168.

Vallenius, T., Luukko, K. and Makela, T.P. (2000) CLP-36 PDZ-LIM protein associates with nonmuscle alpha-actinin-1 and alpha-actinin-4. *J Biol Chem*, **275**, 11100-11105.

Vallenius, T., Scharm, B., Vesikansa, A., Luukko, K., Schafer, R. and Makela, T.P. (2004) The PDZ-LIM protein RIL modulates actin stress fiber turnover and enhances the association of alpha-actinin with F-actin. *Exp Cell Res*, **293**, 117-128.

van der Flier, A., Kuikman, I., Kramer, D., Geerts, D., Kreft, M., Takafuta, T., Shapiro, S.S. and Sonnenberg, A. (2002) Different splice variants of filamin-B affect myogenesis, subcellular distribution, and determine binding to integrin [beta] subunits. *J Cell Biol*, **156**, 361-376.

van der Flier, A. and Sonnenberg, A. (2001) Structural and functional aspects of filamins. *Biochim Biophys Acta*, **1538**, 99-117.

van der Ven, P.F., Wiesner, S., Salmikangas, P., Auerbach, D., Himmel, M., Kempa, S., Hayess, K., Pacholsky, D., Taivainen, A., Schroder, R., Carpen, O. and Furst, D.O. (2000) Indications for a novel muscular dystrophy pathway. gamma-filamin, the muscle-specific filamin isoform, interacts with myotilin. *J Cell Biol*, **151**, 235-248.

Vatta, M., Mohapatra, B., Jimenez, S., Sanchez, X., Faulkner, G., Perles, Z., Sinagra, G., Lin, J.H., Vu, T.M., Zhou, Q., Bowles, K.R., Di Lenarda, A., Schimmenti, L., Fox, M., Chrisco, M.A., Murphy, R.T., McKenna, W., Elliott, P., Bowles, N.E., Chen, J., Valle, G. and Towbin, J.A. (2003) Mutations in Cypher/ZASP in patients with dilated cardiomyopathy and left ventricular non-compaction. *J Am Coll Cardiol*, **42**, 2014-2027.

Venter, J.C., Adams, M.D., Myers, E.W., Li, P.W., Mural, R.J., Sutton, G.G., Smith, H.O., Yandell, M., Evans, C.A., Holt, R.A., Gocayne, J.D., Amanatides, P., Ballew, R.M., Huson, D.H., Wortman, J.R., Zhang, Q., Kodira, C.D., Zheng, X.H., Chen, L., Skupski, M., Subramanian, G., Thomas, P.D., Zhang, J., Gabor Miklos, G.L., Nelson, C., Broder, S., Clark, A.G., Nadeau, J., McKusick, V.A., Zinder, N., Levine, A.J., Roberts, R.J., Simon, M., Slayman, C., Hunkapiller, M., Bolanos, R., Delcher, A., Dew, I., Fasulo, D., Flanigan, M., Florea, L., Halpern, A., Hannenhalli, S., Kravitz, S., Levy, S., Mobarry, C., Reinert, K., Remington, K., Abu-Threideh, J., Beasley, E., Biddick, K., Bonazzi, V., Brandon, R., Cargill, M., Chandramouliswaran, I., Charlab, R., Chaturvedi, K., Deng, Z., Di Francesco, V., Dunn, P., Eilbeck, K., Evangelista, C., Gabrielian,

A.E., Gan, W., Ge, W., Gong, F., Gu, Z., Guan, P., Heiman, T.J., Higgins, M.E., Ji, R.R., Ke, Z., Ketchum, K.A., Lai, Z., Lei, Y., Li, Z., Li, J., Liang, Y., Lin, X., Lu, F., Merkulov, G.V., Milshina, N., Moore, H.M., Naik, A.K., Narayan, V.A., Neelam, B., Nusskern, D., Rusch, D.B., Salzberg, S., Shao, W., Shue, B., Sun, J., Wang, Z., Wang, A., Wang, X., Wang, J., Wei, M., Wides, R., Xiao, C., Yan, C., Yao, A., Ye, J., Zhan, M., Zhang, W., Zhang, H., Zhao, Q., Zheng, L., Zhong, F., Zhong, W., Zhu, S., Zhao, S., Gilbert, D., Baumhueter, S., Spier, G., Carter, C., Cravchik, A., Woodage, T., Ali, F., An, H., Awe, A., Baldwin, D., Baden, H., Barnstead, M., Barrow, I., Beeson, K., Busam, D., Carver, A., Center, A., Cheng, M.L., Curry, L., Danaher, S., Davenport, L., Desilets, R., Dietz, S., Dodson, K., Doup, L., Ferriera, S., Garg, N., Gluecksmann, A., Hart, B., Haynes, J., Haynes, C., Heiner, C., Hladun, S., Hostin, D., Houck, J., Howland, T., Ibegwam, C., Johnson, J., Kalush, F., Kline, L., Koduru, S., Love, A., Mann, F., May, D., McCawley, S., McIntosh, T., McMullen, I., Moy, M., Moy, L., Murphy, B., Nelson, K., Pfannkoch, C., Pratts, E., Puri, V., Qureshi, H., Reardon, M., Rodriguez, R., Rogers, Y.H., Romblad, D., Ruhfel, B., Scott, R., Sitter, C., Smallwood, M., Stewart, E., Strong, R., Suh, E., Thomas, R., Tint, N.N., Tse, S., Vech, C., Wang, G., Wetter, J., Williams, S., Williams, M., Windsor, S., Winn-Deen, E., Wolfe, K., Zaveri, J., Zaveri, K., Abril, J.F., Guigo, R., Campbell, M.J., Sjolander, K.V., Karlak, B., Kejariwal, A., Mi, H., Lazareva, B., Hatton, T., Narechania, A., Diemer, K., Muruganujan, A., Guo, N., Sato, S., Bafna, V., Istrail, S., Lippert, R., Schwartz, R., Walenz, B., Yooseph, S., Allen, D., Basu, A., Baxendale, J., Blick, L., Caminha, M., Carnes-Stine, J., Caulk, P., Chiang, Y.H., Coyne, M., Dahlke, C., Mays, A., Dombroski, M., Donnelly, M., Ely, D., Esparham, S., Fosler, C., Gire, H., Glanowski, S., Glasser, K., Glodek, A., Gorokhov, M., Graham, K., Gropman, B., Harris, M., Heil, J., Henderson, S., Hoover, J., Jennings, D., Jordan, C., Jordan, J., Kasha, J., Kagan, L., Kraft, C., Levitsky, A., Lewis, M., Liu, X., Lopez, J., Ma, D., Majoros, W., McDaniel, J., Murphy, S., Newman, M., Nguyen, T., Nguyen, N., Nodell, M., Pan, S., Peck, J., Peterson, M., Rowe, W., Sanders, R., Scott, J., Simpson, M., Smith, T., Sprague, A., Stockwell, T., Turner, R., Venter, E.,

Wang, M., Wen, M., Wu, D., Wu, M., Xia, A., Zandieh, A. and Zhu, X. (2001) The sequence of the human genome. *Science*, **291**, 1304-1351.

Verpy, E., Leibovici, M., Zwaenepoel, I., Liu, X.Z., Gal, A., Salem, N., Mansour, A., Blanchard, S., Kobayashi, I., Keats, B.J., Slim, R. and Petit, C. (2000) A defect in harmonin, a PDZ domain-containing protein expressed in the inner ear sensory hair cells, underlies Usher syndrome type 1C. *Nat Genet*, **26**, 51-55.

Vorgerd, M., van der Ven, P.F., Bruchertseifer, V., Lowe, T., Kley, R.A., Schroder, R., Lochmuller, H., Himmel, M., Koehler, K., Furst, D.O. and Huebner, A. (2005) A mutation in the dimerization domain of filamin c causes a novel type of autosomal dominant myofibrillar myopathy. *Am J Hum Genet*, **77**, 297-304.

Wang, H., Harrison-Shostak, D.C., Lemasters, J.J. and Herman, B. (1995) Cloning of a rat cDNA encoding a novel LIM domain protein with high homology to rat RIL. *Gene*, **165**, 267-271.

Wang, H., Yang, S., Yang, E., Zhu, Z., Mu, Y., Feng, S. and Li, K. (2007) NF-kappaB mediates the transcription of mouse calsarcin-1 gene, but not calsarcin-2, in C2C12 cells. *BMC Mol Biol*, **8**, 19.

Wang, H., Zhu, Z., Wang, H., Yang, S., Mo, D. and Li, K. (2006) Characterization of different expression patterns of calsarcin-1 and calsarcin-2 in porcine muscle. *Gene*, **374**, 104-111.

Wang, K., Ash, J.F. and Singer, S.J. (1975) Filamin, a new high-molecular-weight protein found in smooth muscle and non-muscle cells. *Proc Natl Acad Sci U S A*, **72**, 4483-4486.

Witt, S.H., Granzier, H., Witt, C.C. and Labeit, S. (2005) MURF-1 and MURF-2 target a specific subset of myofibrillar proteins redundantly: towards understanding MURF-dependent muscle ubiquitination. *J Mol Biol*, **350**, 713-722.

Woods, D.F. and Bryant, P.J. (1993) ZO-1, DlgA and PSD-95/SAP90: homologous proteins in tight, septate and synaptic cell junctions. *Mech Dev*, **44**, 85-89.

Wright, J., Huang, Q.Q. and Wang, K. (1993) Nebulin is a full-length template of actin filaments in the skeletal muscle sarcomere: an immunoelectron microscopic study of its orientation and span with site-specific monoclonal antibodies. *J Muscle Res Cell Motil*, **14**, 476-483.

Xia, H., Winokur, S.T., Kuo, W.L., Altherr, M.R. and Bredt, D.S. (1997) Actinin-associated LIM protein: identification of a domain interaction between PDZ and spectrin-like repeat motifs. *J Cell Biol*, **139**, 507-515.

Xie, Z., Xu, W., Davie, E.W. and Chung, D.W. (1998) Molecular cloning of human ABPL, an actin-binding protein homologue. *Biochem Biophys Res Commun*, **251**, 914-919.

Xu, X.Z., Choudhury, A., Li, X. and Montell, C. (1998) Coordination of an array of signaling proteins through homo- and heteromeric interactions between PDZ domains and target proteins. *J Cell Biol*, **142**, 545-555.

Yamaguchi, M., Izumimoto, M., Robson, R.M. and Stromer, M.H. (1985) Fine structure of wide and narrow vertebrate muscle Z-lines. A proposed model and computer simulation of Z-line architecture. *J Mol Biol*, **184**, 621-643.

Zhang, Q., Fan, J.S. and Zhang, M. (2001) Interdomain chaperoning between PSD-95, Dlg, and Zo-1 (PDZ) domains of glutamate receptor-interacting proteins. *J Biol Chem*, **276**, 43216-43220.

Zhou, Q., Chu, P.H., Huang, C., Cheng, C.F., Martone, M.E., Knoll, G., Shelton, G.D., Evans, S. and Chen, J. (2001) Ablation of Cypher, a PDZ-LIM domain Z-line protein, causes a severe form of congenital myopathy. *J Cell Biol*, **155**, 605-612.

Zhou, Q., Ruiz-Lozano, P., Martone, M.E. and Chen, J. (1999) Cypher, a striated muscle-restricted PDZ and LIM domain-containing protein, binds to alpha-actinin-2 and protein kinase C. *J Biol Chem*, **274**, 19807-19813.

Zou, P., Gautel, M., Geerlof, A., Wilmanns, M., Koch, M.H. and Svergun, D.I. (2003) Solution scattering suggests cross-linking function of telethonin in the complex with titin. *J Biol Chem*, **278**, 2636-2644.

Zou, Y., Evans, S., Chen, J., Kuo, H.C., Harvey, R.P. and Chien, K.R. (1997) CARP, a cardiac ankyrin repeat protein, is downstream in the Nkx2-5 homeobox gene pathway. *Development*, **124**, 793-804.